Technical Publication SJ2001-2

GEOSTATISTICAL ANALYSIS OF GEOLOGIC AND HYDROGEOLOGIC DATA FOR THE PALM COAST WELLFIELD, FLAGLER COUNTY, FLORIDA

by

David J. Toth, Ph.D., P.G.

David J. Toth

David J. Toth
Professional Geologist
License No. PG110
September 17, 2001

SEAL

St. Johns River Water Management District
Palatka, Florida

2001

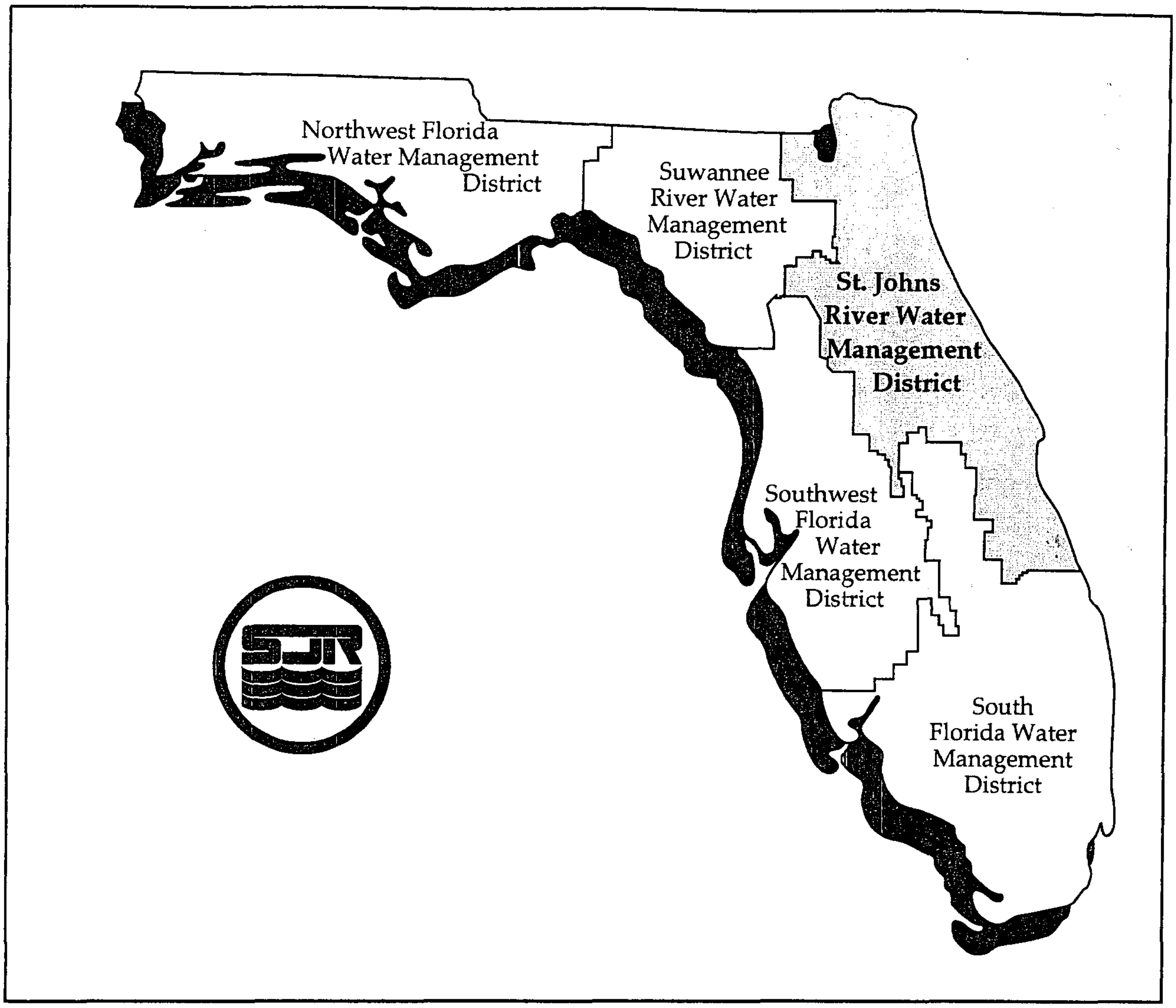

The St. Johns River Water Management District (SJRWMD) was created by the Florida Legislature in 1972 to be one of five water management districts in Florida. It includes all or part of 19 counties in northeast Florida. The mission of SJRWMD is to manage water resources to ensure their continued availability while maximizing environmental and economic benefits. SJRWMD accomplishes its mission through regulation; applied research; assistance to federal, state, and local governments; operation and maintenance of water control works; and land acquisition and management.

This document is published to disseminate information collected by SJRWMD in pursuit of its mission. Copies of this document can be obtained from:

Library
St. Johns River Water Management District
P.O. Box 1429
Palatka, FL 32178-1429

Phone: (386) 329-4132

EXECUTIVE SUMMARY

Geostatistics provides a framework for the analysis, characterization, and estimation of spatial data. A geostatistical analysis was undertaken of hydrogeologic data in the Palm Coast area of Flagler County, Florida. The elevations of the top and bottom of the intermediate aquifer, the elevation of the top of the confining unit for the intermediate aquifer, and the land surface elevation were kriged to determine their areal distribution. In addition, the leakance for the confining unit of the intermediate aquifer and the natural logarithm of hydraulic conductivity of the intermediate aquifer were simulated. Grid files of these parameters were created. These files can be input into MODFLOW. The St. Johns River Water Management District (SJRWMD) plans to develop a MODFLOW model for the Palm Coast area. This MODFLOW model will be used to determine the effects, if any, of groundwater withdrawals on wetlands and the groundwater flow system in the vicinity of Palm Coast, Florida. This model will be used in support of SJRWMD's water supply planning and consumptive use permitting programs and is expected to be used by Florida Water Services to assist in wellfield management.

CONTENTS

FIGURES

TABLES

INTRODUCTION

The purpose of this study is to use geostatistical analysis of the geologic and hydrogeologic data collected at the Palm Coast wellfield in Flagler County, Florida, to develop input files for MODFLOW. The St. Johns River Water Management District (SJRWMD) plans to develop a MODFLOW model of the Palm Coast area to determine the effects, if any, of groundwater withdrawals on wetlands and the groundwater flow system in the vicinity of Palm Coast, Florida.

The Palm Coast wellfield in Flagler County, Florida, withdraws water from both the intermediate and Floridan aquifers. The intermediate aquifer provides a substantial amount of water for Florida Water Services (FWS) at Palm Coast, but because of its hydraulic connection to the overlying surficial aquifer system, impacts may occur to existing wetlands as a result of increased pumpage from FWS and other users. Withdrawals from the Floridan aquifer currently complement water being produced from the intermediate aquifer to supply water for use by FWS customers. Increased withdrawals from the Floridan aquifer are being considered as a potential source to meet future demand for Palm Coast and other potential users. However, the Floridan aquifer in the Palm Coast area has a relatively thin layer of naturally occurring water which meets drinking water standards.

The MODFLOW model that will be developed will be used as a wellfield management tool as well as a predictive tool. It will also be used to assist SJRWMD in determining potential long-term monitoring sites for the surficial, intermediate, and Floridan aquifers for the purposes of SJRWMD's water supply planning and consumptive use permitting programs for Palm Coast and other users in the area.

The parameters of interest for this geostatistical analysis are the elevation of the top of the intermediate aquifer, the elevation of the bottom of the intermediate aquifer, the elevation of the top of the confining unit for the intermediate aquifer, the leakance for the confining unit for the intermediate aquifer, the hydraulic conductivity of the intermediate aquifer, and land surface elevation. The source of water for Palm Coast is the intermediate and Upper Floridan aquifers (Navoy and Bradner 1987).

STUDY AREA

The study area is in southeast St. Johns, east Flagler, and northeast Volusia counties (Figure 1). The UTM and latitude-longitude coordinates of the lower left (northing: 3250904, easting: 464842; 292318.63, 812144.38) and upper right (northing: 3282908, easting: 484654; 294039.93, 810930.99) of the MODFLOW model area for Palm Coast were determined by SJRWMD staff. A larger area was used to obtain geologic and hydrologic data for the geostatistical analysis. The UTM and latitude-longitude coordinates of the lower left (northing: 3248899, easting: 461260; 292213.00, 812356.99) and upper right (northing: 3288549, easting: 494210; 294343.41, 810335.53) of the geostatistical data area for Palm Coast were also determined by SJRWMD staff.

GEOLOGIC AND HYDROLOGIC DATA

Data used in the geostatistical analysis came from two sources. Data for 89 wells (57 SW or intermediate aquifer wells, and 32 LW or Floridan aquifer wells) came from FWS. Data for 54 wells (52 geophysical logs and two geologic logs) came from SJRWMD files. The data included elevation of the top of the intermediate aquifer, elevation of the bottom of the intermediate aquifer, elevation of the top of the confining unit, leakance of the confining unit, and transmissivity of the intermediate aquifer (Appendix A). The elevation data for the intermediate aquifer were used to calculate a thickness for that aquifer. Hydraulic conductivity for the intermediate aquifer was calculated by dividing the transmissivity for the aquifer by its thickness. The data for the 143 wells were supplied to SJRWMD by Gary E. Eichler, vice president of Connect Consulting and a consultant for FWS. All of the geologic and hydrologic data were inferred from geophysical logs. Transmissivity (T) and leakance (L) were determined from either pump or specific-capacity tests at 52 (T) and 29 (L) of the FWS wells.

Topographic elevation data were taken from the U.S. Geological Survey's topographic maps of the study area. Point elevations were extracted every 200 meters (m) from the vertices of the digitized contour lines. The elevations for the 143 wells were also added to the elevation file; the resulting file contained 17,143 records.

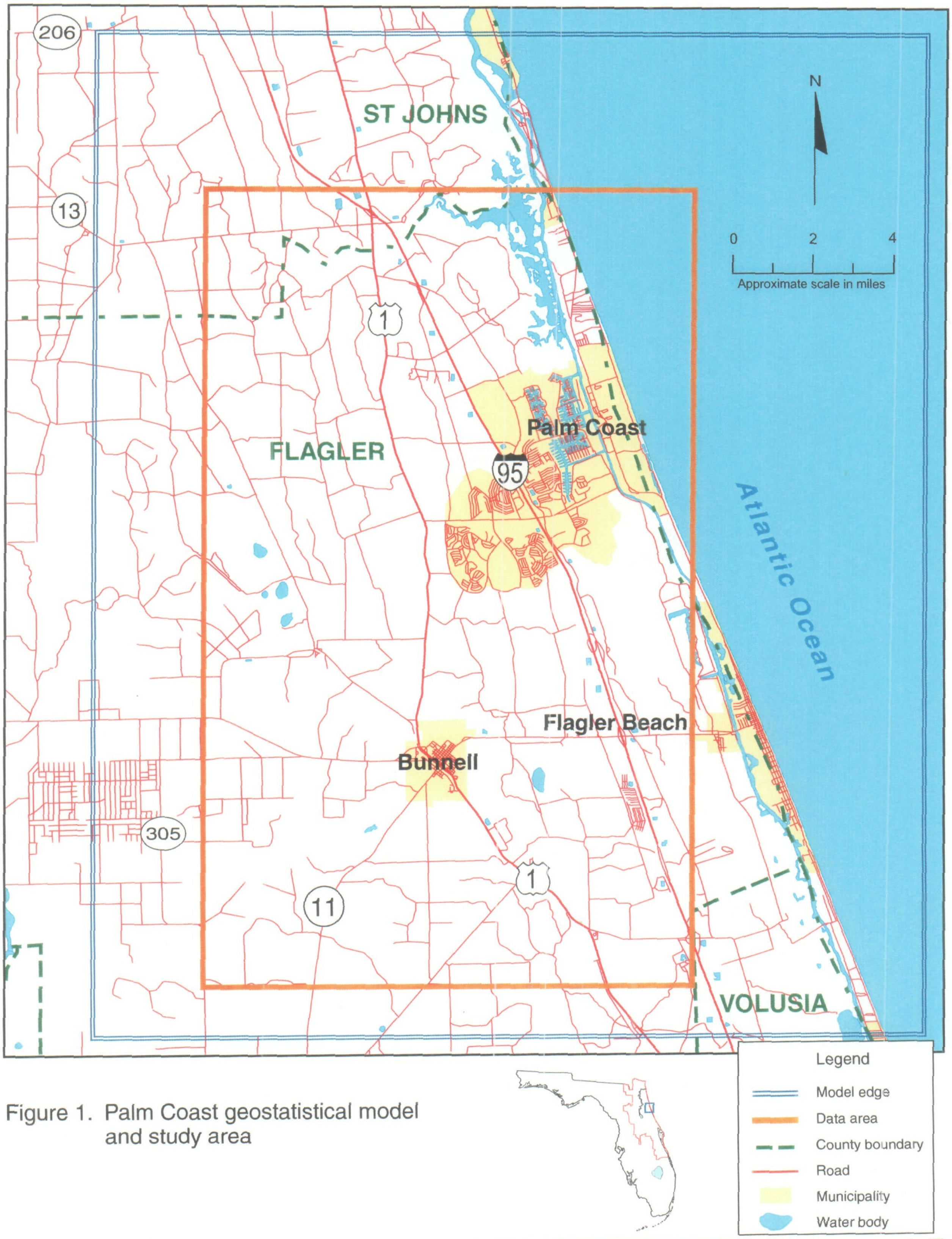

Figure 1. Palm Coast geostatistical model and study area

GEOSTATISTICAL ANALYSIS

Geostatistics is a collection of statistical methods for the analysis and estimation of spatial data. These methods incorporate the spatial characteristics of actual data into statistical estimation processes. Geostatistics recognizes that data are often biased and clustered and uses well-defined criteria to provide statistical tools for (1) calculating the most accurate estimations, based on sample results and (2) quantifying the accuracy of these estimations. As a result of the successful application of geostatistical tools, the U.S. Environmental Protection Agency (1990) has recommended use of these tools in spatial environmental data analysis. The procedures followed in this study are those recommended by Shahrokh Rouhani, P.E., Ph.D., New Fields, Inc., Atlanta, Ga., personal communication 1999.

GEOSTATISTICAL SOFTWARE

ISATIS software was used to perform this geostatistical analysis. ISATIS was developed by Geovariances and the Center of Geostatistics at the Paris School of Mines (Geovariances 1997). This program includes extensive estimation and simulation options combined with an efficient data management system. ISATIS results have been extensively validated by research work and practical applications in an increasing variety of new fields.

The geostatistical procedures used in this study conform to the American Society for Testing and Materials (ASTM) standard guides. The following ASTM standard guides were used:

- D 5549-94 for reporting geostatistical site investigations (ASTM 1994)
- D 5922-96 for analyzing spatial variation in geostatistical site investigations (ASTM 1996a)
- D 5923-96 for selecting kriging for use in geostatistical site investigations (ASTM 1996b)

ELEVATION OF THE TOP OF THE INTERMEDIATE AQUIFER

The elevation of the top of the intermediate aquifer was estimated from 143 data points (Appendix B). The minimum elevation is –77 feet mean sea level (ft msl) and the maximum elevation is 10 ft msl. The mean and median elevations are –32.23 and –32 ft msl, respectively. A histogram and a probability plot of the elevation of the top of the intermediate aquifer are shown in Figures 2 and 3, respectively. The histogram plot approximates a bell shape, and the probability plot lies close to a straight line. Both figures indicate the data approximate a normal distribution.

STRUCTURAL ANALYSIS OF THE DATA

A structural analysis was conducted to determine the spatial correlation of the investigated data. The process was accomplished through the computation and modeling of the variogram function. A variogram is a graph that depicts the average of one-half of the squared differences between data values as a function of the separation distance (ASTM 1996a). The use of a variogram allows an assessment of how well a sample measurement at one location can represent the elevation at another location a certain distance and direction away. In this analysis, the elevations of the top of the intermediate aquifer were used to calculate the experimental variogram and to select an appropriate model. The model was used to estimate elevations and the standard deviations of the estimated elevations.

Experimental Variograms

For modeling purposes, the pair results in the variogram analysis are grouped into a number of distance groups, or lags. The lag is the distance at which sample differences are compared. In each lag, the average of one-half the squared difference is computed and plotted against its corresponding separation distance. The resulting plot is referred to as the experimental variogram (ASTM 1996a).

Omnidirectional and directional experimental variograms with lag distances ranging from 400 to 30,000 m and lag counts of 9 were examined. An omnidirectional or isotropic variogram is one in which the spatial correlation structure of the data set depends only on the variability of the separation distance between data values and not on the direction. A

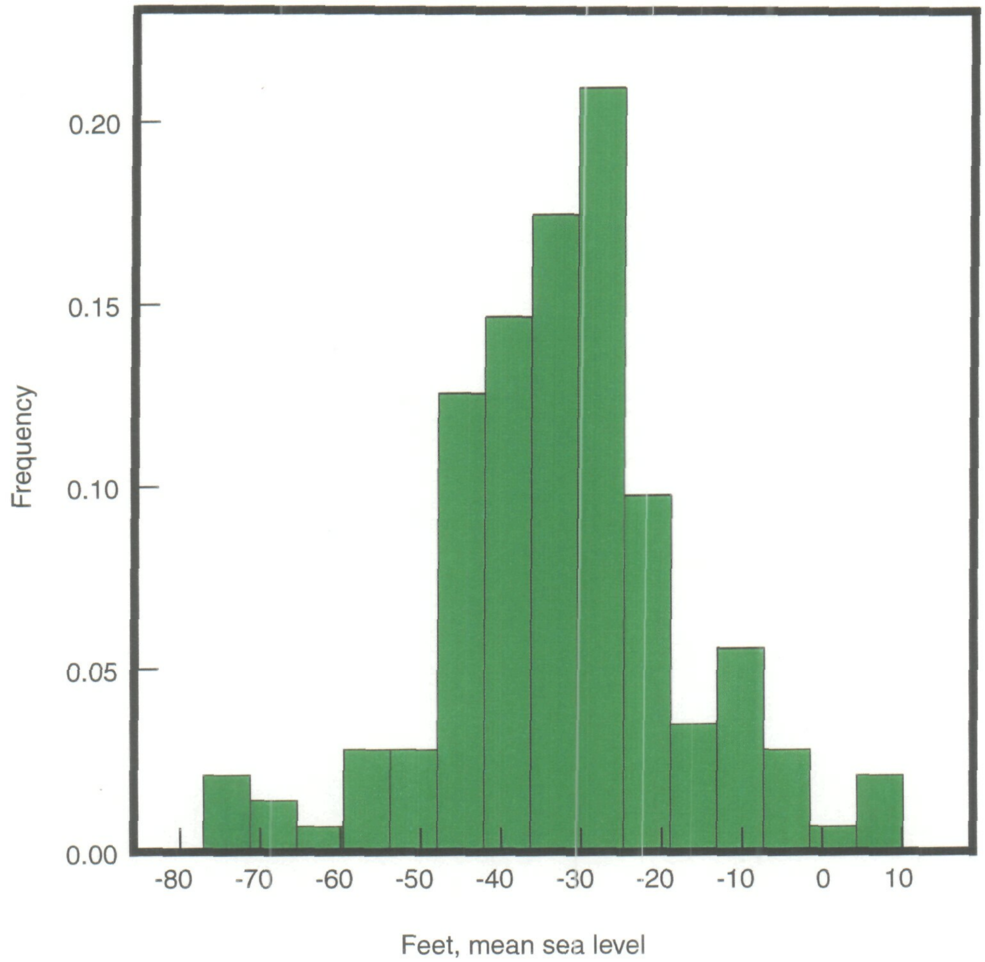

Figure 2. Histogram of the elevation of the top of the intermediate aquifer in the study area

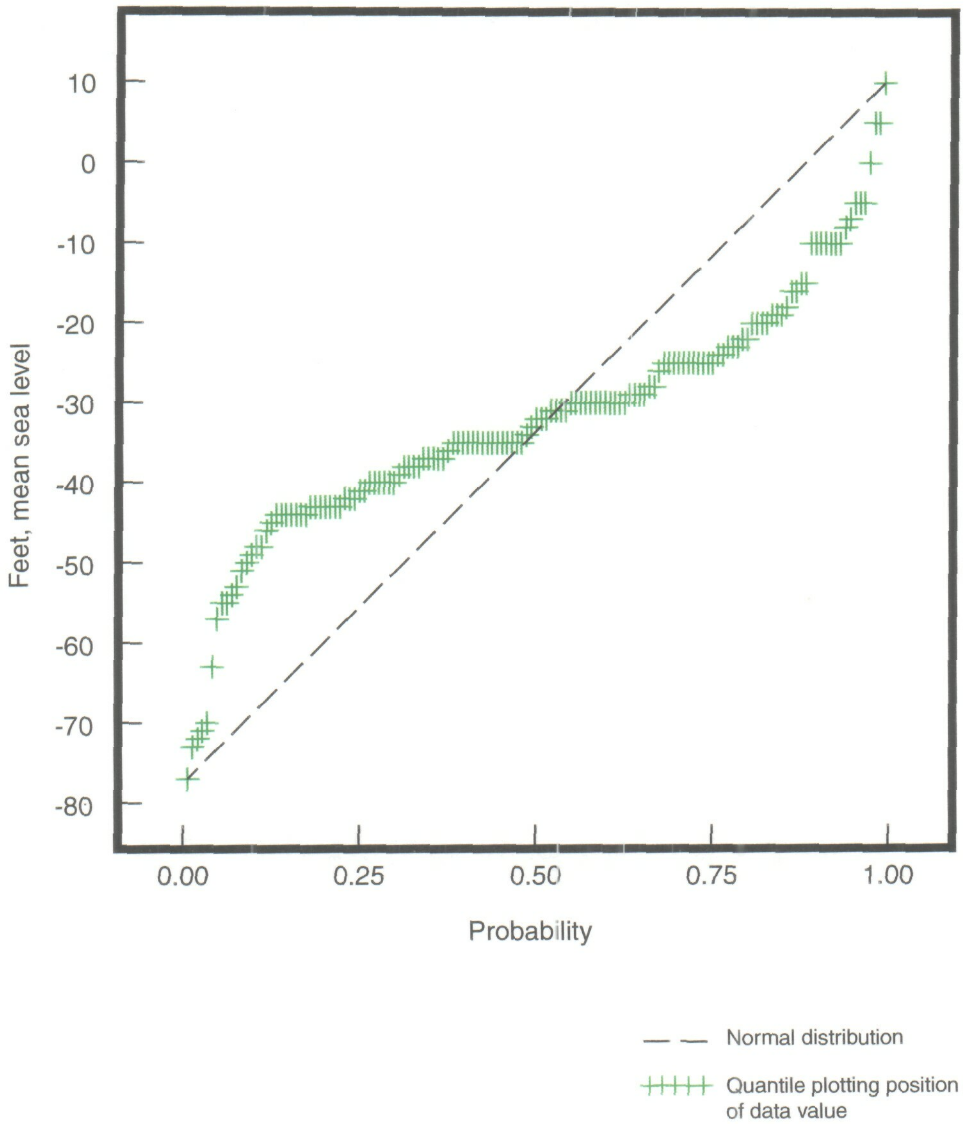

Figure 3. Probability plot of the elevation of the top of the intermediate aquifer in the study area

directional variogram has a structure dependent on both distance and direction.

A lag value of 1,625 m and a lag count of 9 were selected as input values to the omnidirectional experimental variogram of the elevation of the top of the intermediate aquifer (Figure 4). The number of data pairs for a lag interval ranged from 113 to 933. Generally, a variogram is considered reliable if the number of pairs in each lag exceeds 20 (S. Rouhani, NewFields, Atlanta, pers. com. 1998).

Variogram Model—Isotropic

An isotropic model was fitted to the omnidirectional experimental variogram (Figure 4). The model-fitting procedure was performed graphically in order to find a structure that would be as close as possible to the experimental variogram curve. The final isotropic model of the experimental variogram was configured with a nugget and one spherical structure.

Sill, nugget, and range are parameters that describe the variogram model. The variogram is said to have reached a sill where the variogram plot levels off. The sill represents the population variance of the investigated data (ASTM 1996a).

A jump up the y axis from the origin of the variogram plot is called a nugget. The nugget represents micro-scale variations and/or measurement errors. The ratio of the nugget to the sill represents the level of unexplained variations (ASTM 1996a). A nugget-to-sill ratio of less than 0.3 indicates a well-structured variogram, while a nugget-to-sill ratio over 0.7 indicates a poorly structured variogram (S. Rouhani, pers. com. 1998). For the omnidirectional variogram model, the nugget was 122.09 and the sill was 203.25, with a nugget-to-sill ratio of 0.60. The range was 23,855.71 m.

The range is the distance (in meters) from the origin to a point where the variogram model reaches the sill. When a variogram is well structured (i.e., has a low nugget-to-sill ratio), the range is a measure of the extent of the spatial correlation exhibited by the investigated data, or the maximum distance over which the data exhibit spatial correlation (ASTM 1996a).

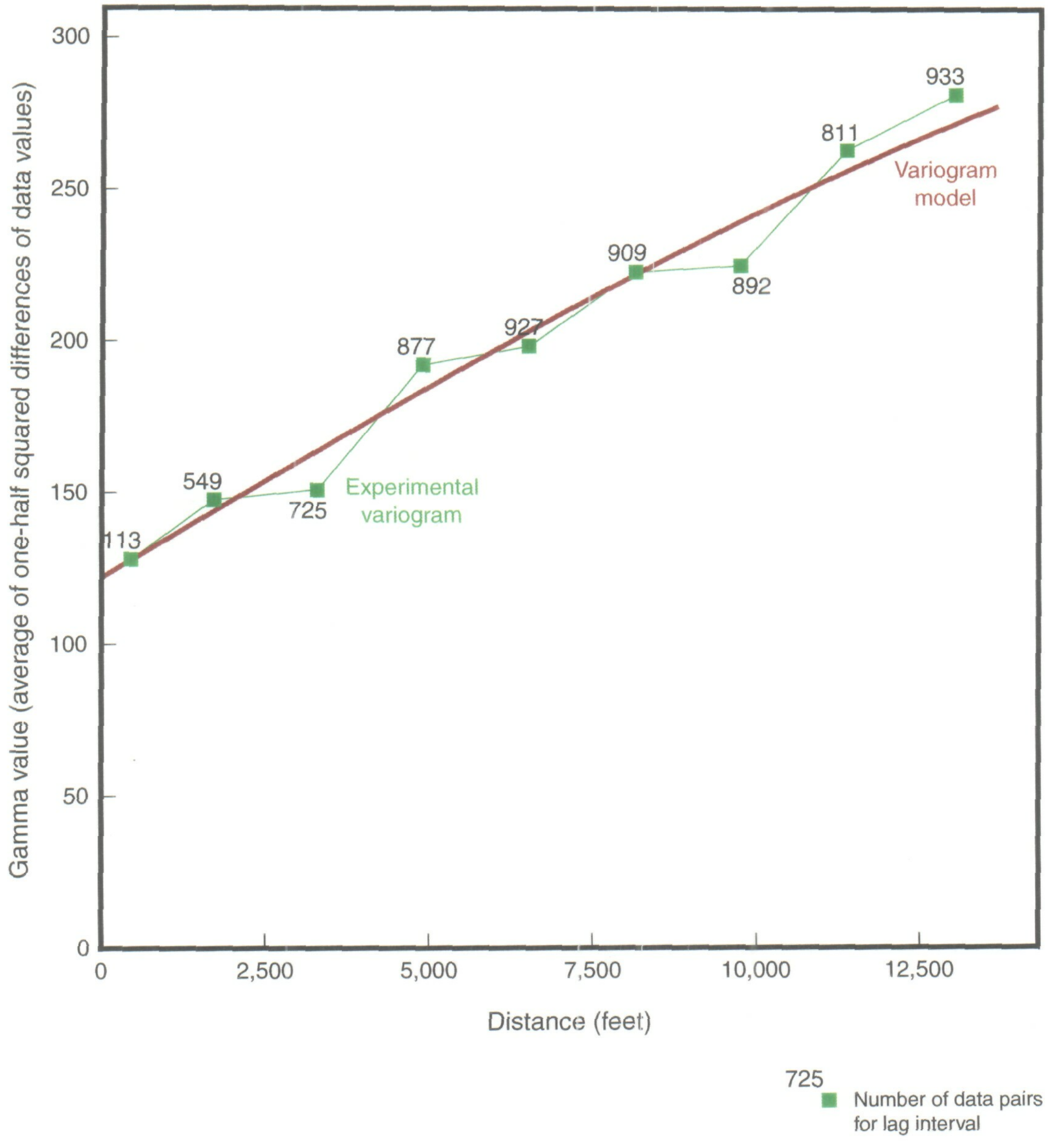

Figure 4. Isotropic (omnidirectional) variogram model of the elevation of the top of the intermediate aquifer

Variogram Map

A variogram map was used to determine if the spatial correlation structure of the data is dependent upon direction (Figure 5). A variogram map is calculated by laying the center of a grid over each data location one at a time. For each cell where data exist, the squared difference of the values between the center and the cell are accumulated. The average of the accumulated differences is the value for that cell of the variogram map (Chu et al. 1994). For the elevation of the top of the intermediate aquifer, the variogram map suggested a slight anisotropy in a northwest-southeast direction.

Variogram Model—Anisotropic

Based on the results of the variogram map, an anisotropic model was fitted to an anisotropic experimental variogram (Figure 6). The anisotropic model consists of two directions perpendicular to one another. The primary direction is northwest-southeast, and the secondary direction is northeast-southwest. First, the model was adjusted to obtain the best fit to the experimental variogram in the primary direction, then the model was adjusted to obtain the best fit in the secondary direction. The number of data pairs for a lag interval of the anisotropic experimental variogram ranged from 52 to 360 in the primary northwest-southeast direction (D1 on Figure 6) and from 61 to 630 in the northeast-southwest direction (D2 on Figure 6).

The lag value and the number of lags used in the isotropic variogram model were also used for the anisotropic variogram model. In addition, nugget, sill, azimuth (i.e., direction of trend), and range values were used as parameters for the anisotropic model (Table 1).

Because the variograms for the primary and secondary directions are so close to one another for a distance up to 8,000 m, an isotropic variogram model was used for cross-validation and estimation procedures.

Neighborhood

A neighborhood must be defined in order to cross-validate the data values and to estimate elevation values in areas where the data have not been collected. Due to the observed weak anisotropy of the variogram model, a circular search neighborhood was selected. The radius for the neighborhood was set at 8,000 m, the distance at which the variograms in

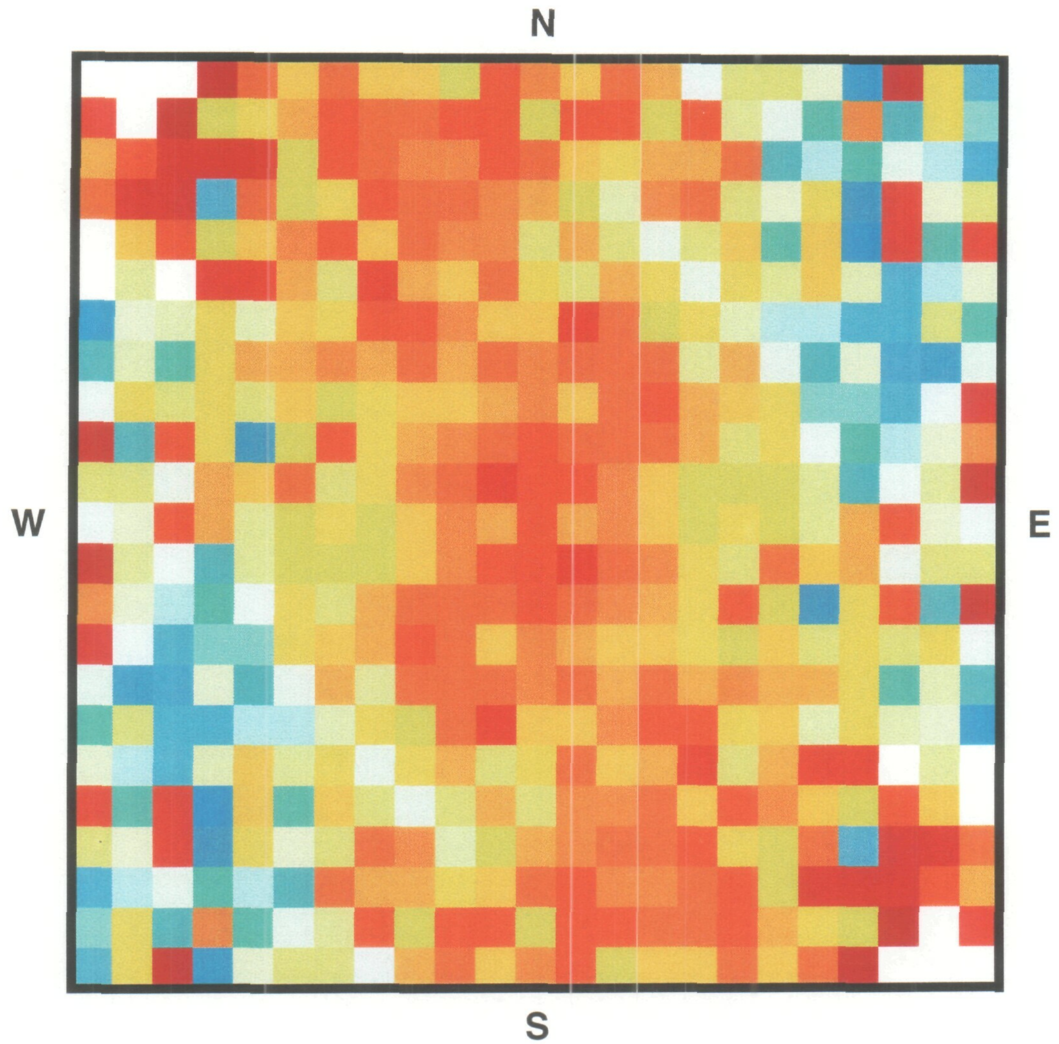

Figure 5. Variogram map of the elevation of the top of the intermediate aquifer. *Alignment of colors in a northwest-southeast direction suggests slight anisotropy in that direction.*

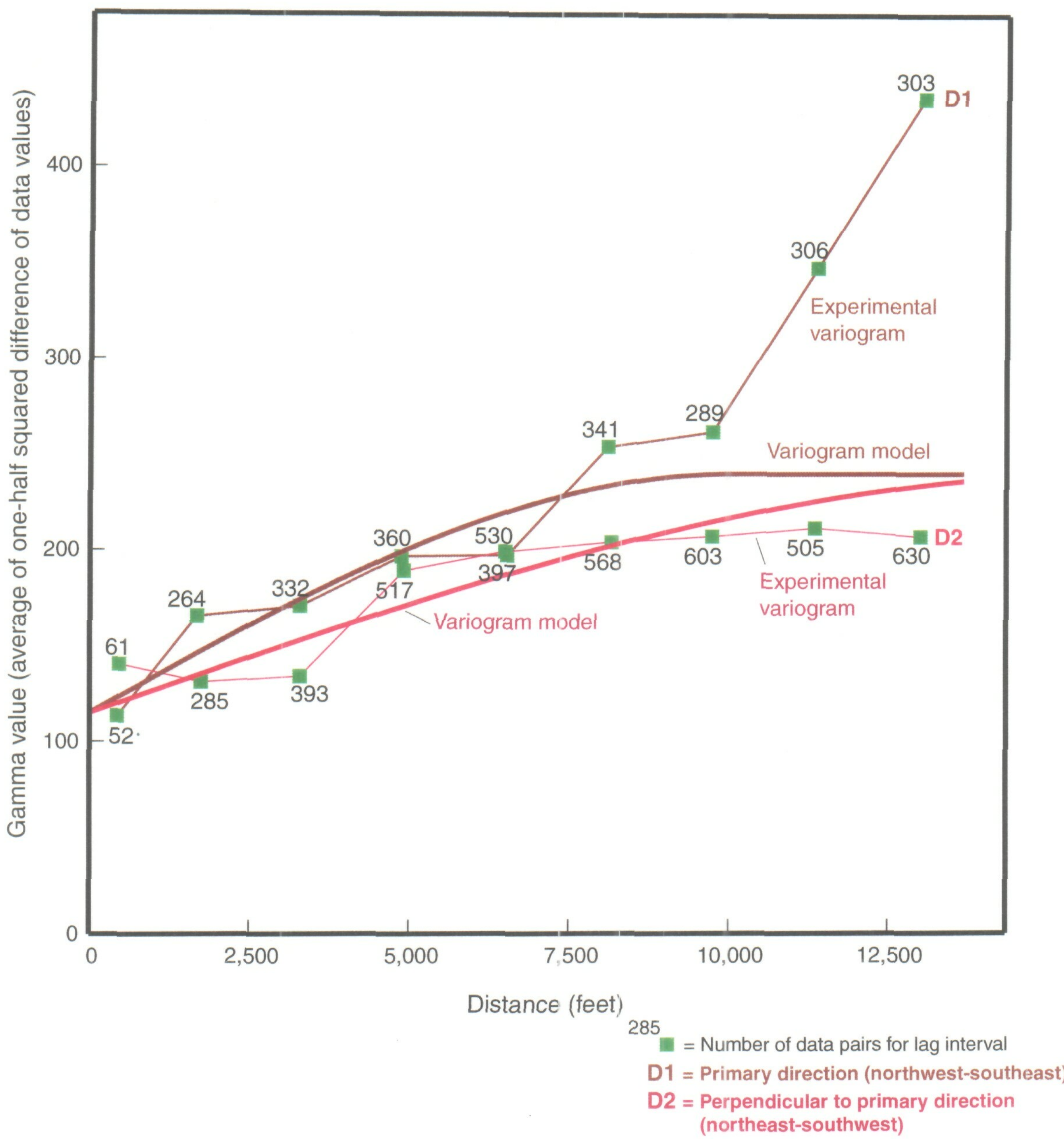

Figure 6. Anisotropic (directional) variogram model of the elevation of the top of the intermediate aquifer

Table 1. Parameters for the anisotropic variogram model of the top of the intermediate aquifer

Parameter	Numerical Value
Lag value	1,625 meters
Number of lags	9
Spherical Structure	
Azimuth	−120 degrees (northwest-southeast direction)
Range, principal direction	10,000 meters
Range, secondary direction	16,000 meters
Sill	125
Nugget Structure	
Sill	115

the anisotropic variogram model diverge. The minimum number of samples used in the calculations for each neighborhood was one, and the maximum number was ten.

Cross-validation

Cross-validation assesses the overall quality of the spatial analysis and estimation procedures. Validation involves sequentially removing each data value, estimating the value using the variogram model and the neighborhood information, and then comparing the resulting pairs of estimated and actual values (ASTM 1994).

The difference between the cross-validation estimated value (Z^*) and the true value (Z) is the estimation error ($Z^* - Z$). The standard deviation of the estimation (S^*) was also computed. The estimation error divided by the standard deviation of the estimation is the cross-validation standardized estimation error $(Z^* - Z)/(S^*)$, also known as the Z score (Geovariances 1997; Englund and Sparks 1988). Standardized estimation errors between −2.5 and 2.5 represent robust data, signifying a model that can yield correct predictions in spite of errors in data collection or model parameters (Olea 1991). Standardized estimation errors less than −2.5 or greater than 2.5 represent nonrobust data, or values that lie outside the 95% confidence limit of a normal distribution.

A base map showing the standardized estimation errors, a histogram of the standardized estimation errors, a scatter diagram of the true data value (Z on the *y* axis) versus the estimated value (Z^* on the *x* axis), and a scatter diagram of the standardized estimation error versus the estimated value were used to display the cross-validation results (Figure 7). Based on the distribution of the standardized estimation error, the data were spatially unbiased. The normally distributed histogram of the standardized estimation errors supports the assumption that the elevation data approximated a normal distribution as well as the validity of the variogram model that was used. Based on the scatter diagrams, the data were numerically unbiased.

The cross-validation procedure for elevation of the top of the intermediate aquifer resulted in only seven nonrobust data points. So few nonrobust data points imply that the estimates for the elevation of the top of the intermediate aquifer were reliable.

Estimation

Estimation is a procedure by which the value of the investigated variable at an unsampled location is predicted using sample values from the neighborhood of that location. Kriging is a collection of linear estimation methods in which sample values are weighted using a linear least-squares optimization procedure based on the variogram model and the neighborhood data (ASTM 1996b).

Point kriging was used to estimate the elevation of the top of the intermediate aquifer on the nodes of the estimation grid. Each grid cell represents a distance of 50 by 50 m on the earth's surface. To encompass the entire Palm Coast study area, the grid had 660 nodes extending in an east-west direction and 794 nodes extending in a north-south direction.

In this study, point kriging was utilized on a 50 by 50 m spacing to estimate the various geohydrologic variable. This spacing is acceptable because of the small distances (50 by 50 m) with the Palm Coast kriging grid (S. Rouhani, pers. com. 1999). However, should another model with larger grids be used, it may be necessary to estimate the variables for input into a hydrologic model with block kriging. Block kriging would give the block estimate, which would be a better match for what goes into a model.

A contour map of the estimated elevation of the top of the intermediate aquifer was produced using kriging (Figure 8). This map portrays the estimated elevation of the top of the intermediate aquifer in the Palm Coast study area. Generally, the estimated elevation to the top of the

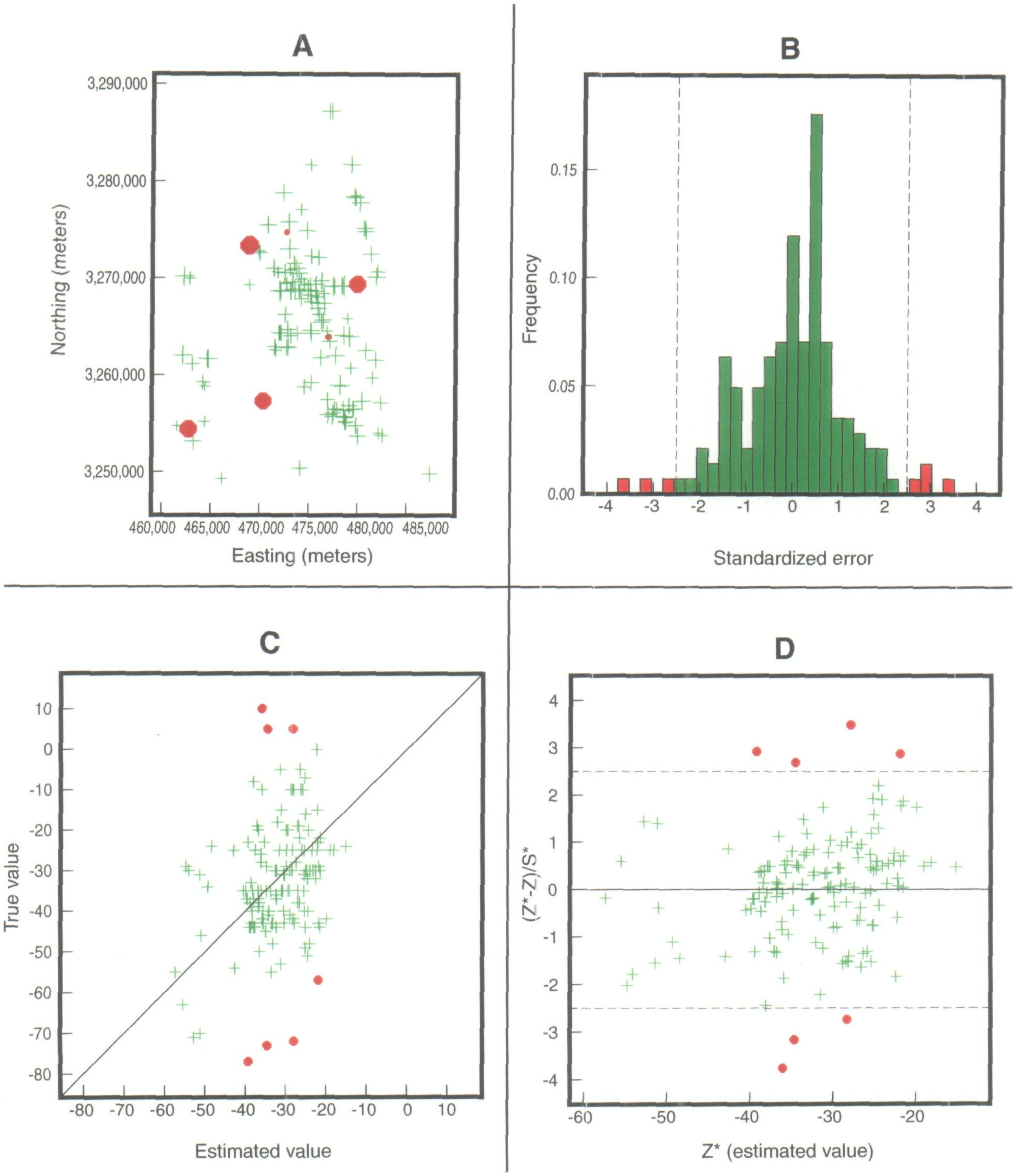

Figure 7. (A) Base map, (B) histogram, and (C, D) scatter diagrams for the cross-validation procedure for the elevation of the top of the intermediate aquifer. *Red denotes nonrobust data; green denotes data values where the standardized error lies between –2.5 and +2.5.*

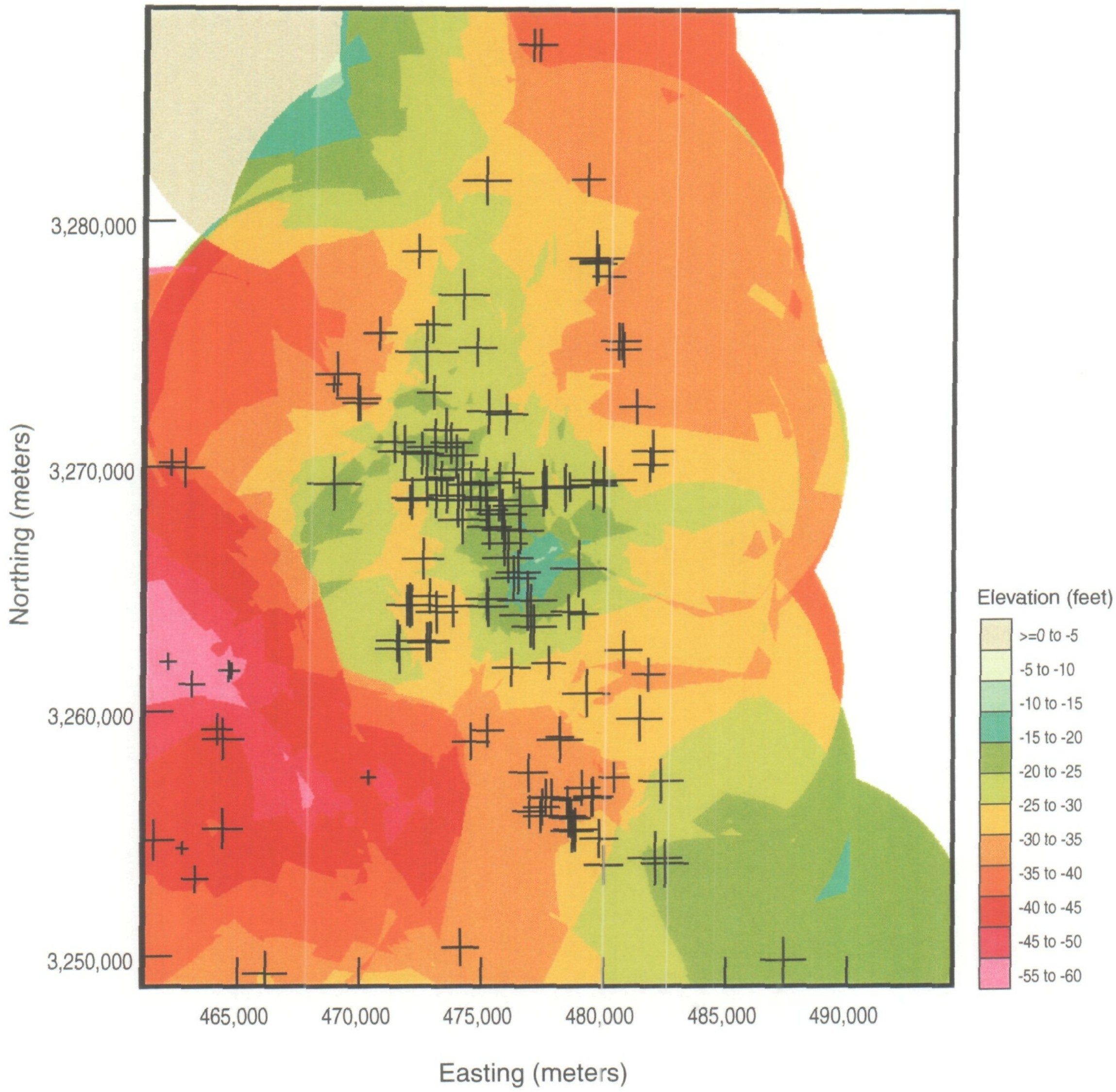

Figure 8. Estimated elevation of the top of the intermediate aquifer in the study area. *Pluses denote location of data points and are drawn at a size that is proportional to data values.*

intermediate aquifer decreases to the west. Well locations are superimposed on the map to indicate where the data values are located.

A map of the relative standard deviations of the elevation data (Figure 9) depicts the relative accuracy of the estimated values. In the eastern and northwestern part of the study area, data are insufficient to estimate elevations of the top of the intermediate aquifer with a high degree of certainty.

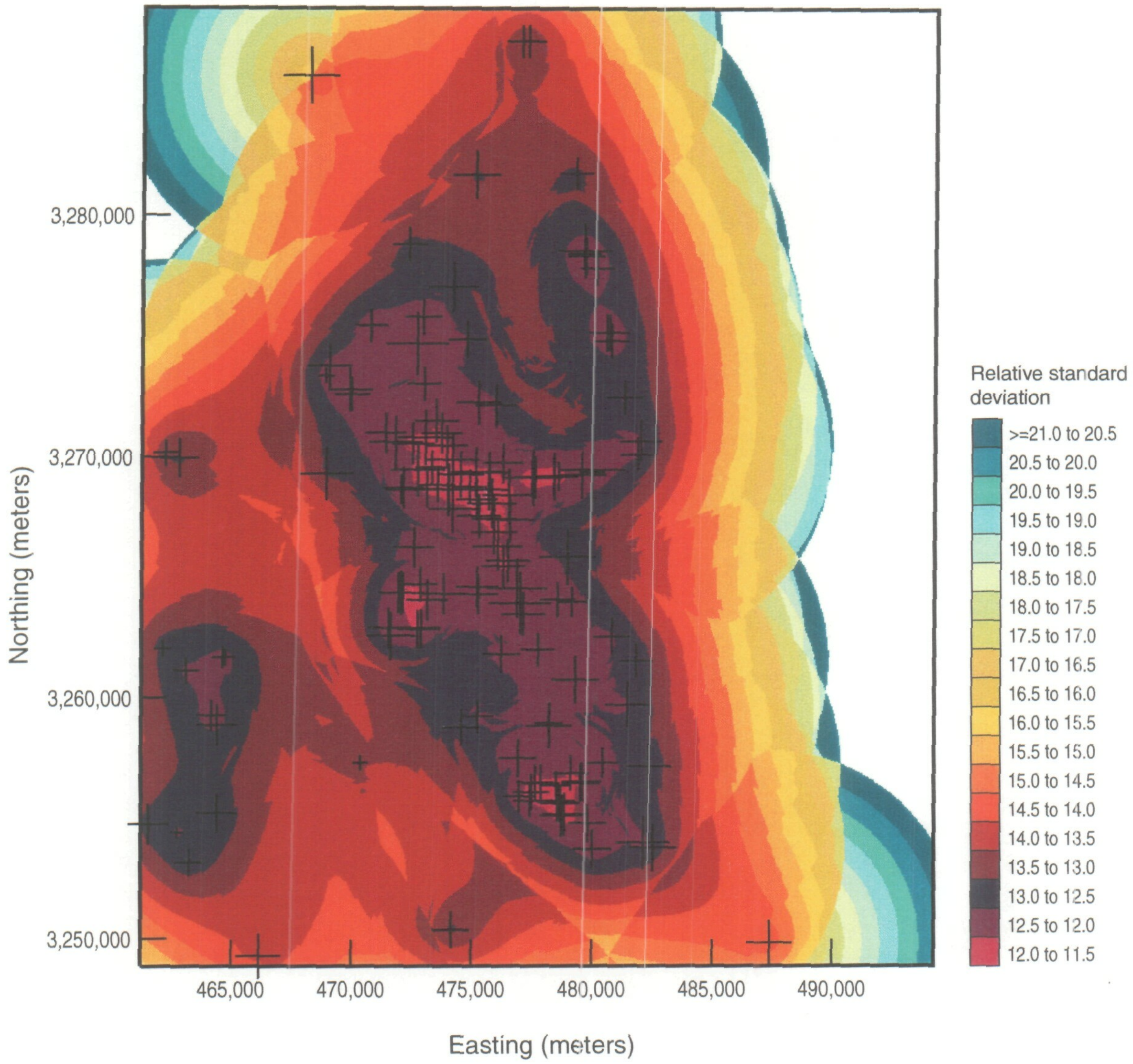

Figure 9. Relative standard deviations of the estimated elevation of the top of the intermediate aquifer. *Pluses denote location of data points and are drawn at a size that is proportional to data values.*

ELEVATION OF THE BOTTOM OF THE INTERMEDIATE AQUIFER

The elevation of the bottom of the intermediate aquifer was estimated from 138 data points. The minimum elevation is –100 ft msl and the maximum elevation is at 0 ft msl. The mean and median elevations are –53.91 and –53 ft msl, respectively. A histogram and a probability plot of the elevation of the bottom of the intermediate aquifer are shown in Figures 10 and 11, respectively. The histogram plot approximates a bell shape, and the probability plot lies close to a straight line. Both figures indicate the data approximate a normal distribution.

There are five fewer data points for the elevation of the bottom of the intermediate aquifer than there are for the top of this aquifer. The elevations of the bottom of the intermediate aquifer for these five points was estimated by point kriging. The estimated elevations were used to compute thicknesses for the intermediate aquifer at these five points. The thicknesses were used in the calculation of hydraulic conductivities.

STRUCTURAL ANALYSIS OF THE DATA

A structural analysis was conducted to determine the spatial correlation of the investigated data. The process was accomplished through the computation and modeling of the variogram function.

Experimental Variogram

A lag value of 3,250 m and a lag count of 7 were selected as input values to the omnidirectional experimental variogram of the elevation of the bottom of the intermediate aquifer (Figure 12). The number of data pairs for a lag interval ranged from 322 to 1,645.

Variogram Model—Isotropic

An isotropic model was fitted to the omnidirectional experimental variogram (Figure 12). The final isotropic model of the experimental variogram was configured with a nugget and one spherical structure.

For the omnidirectional variogram model, the nugget was 163.73 and the sill was 71.72, with a nugget-to-sill ratio of 2.28. The range was 15,204.62 m.

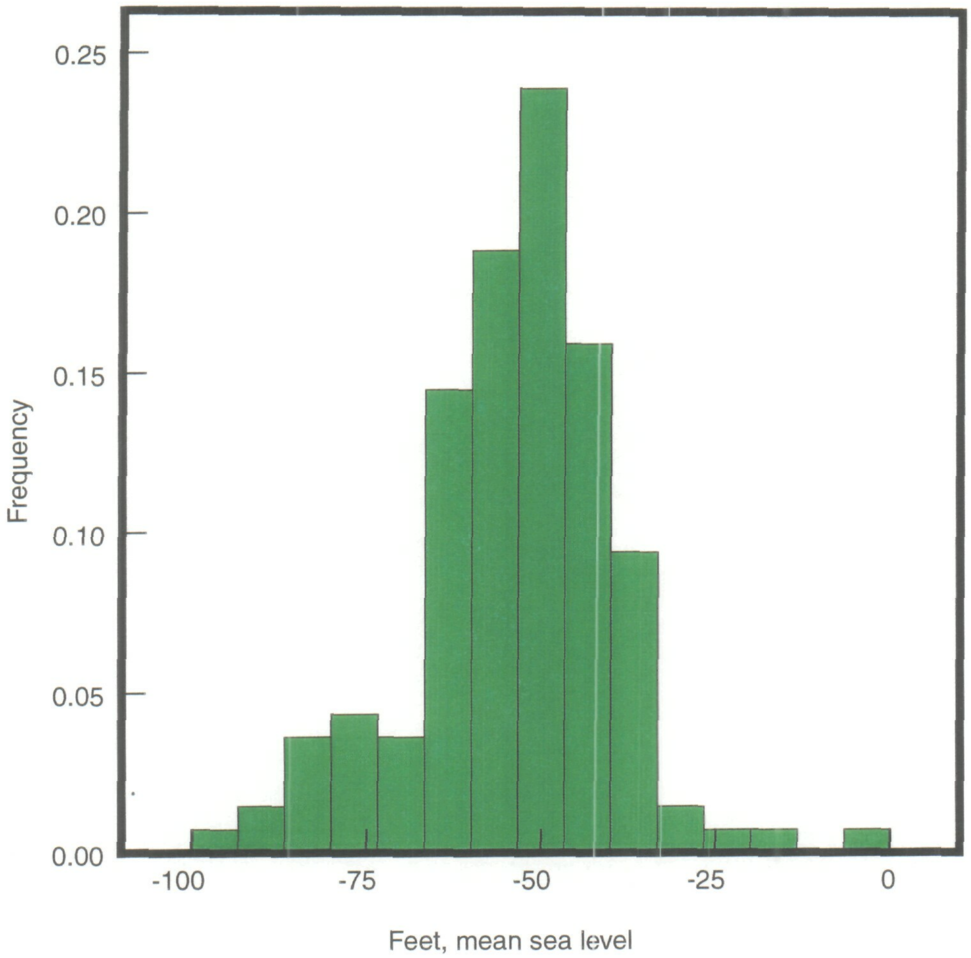

Figure 10. Histogram of the elevation of the bottom of the intermediate aquifer in the study area

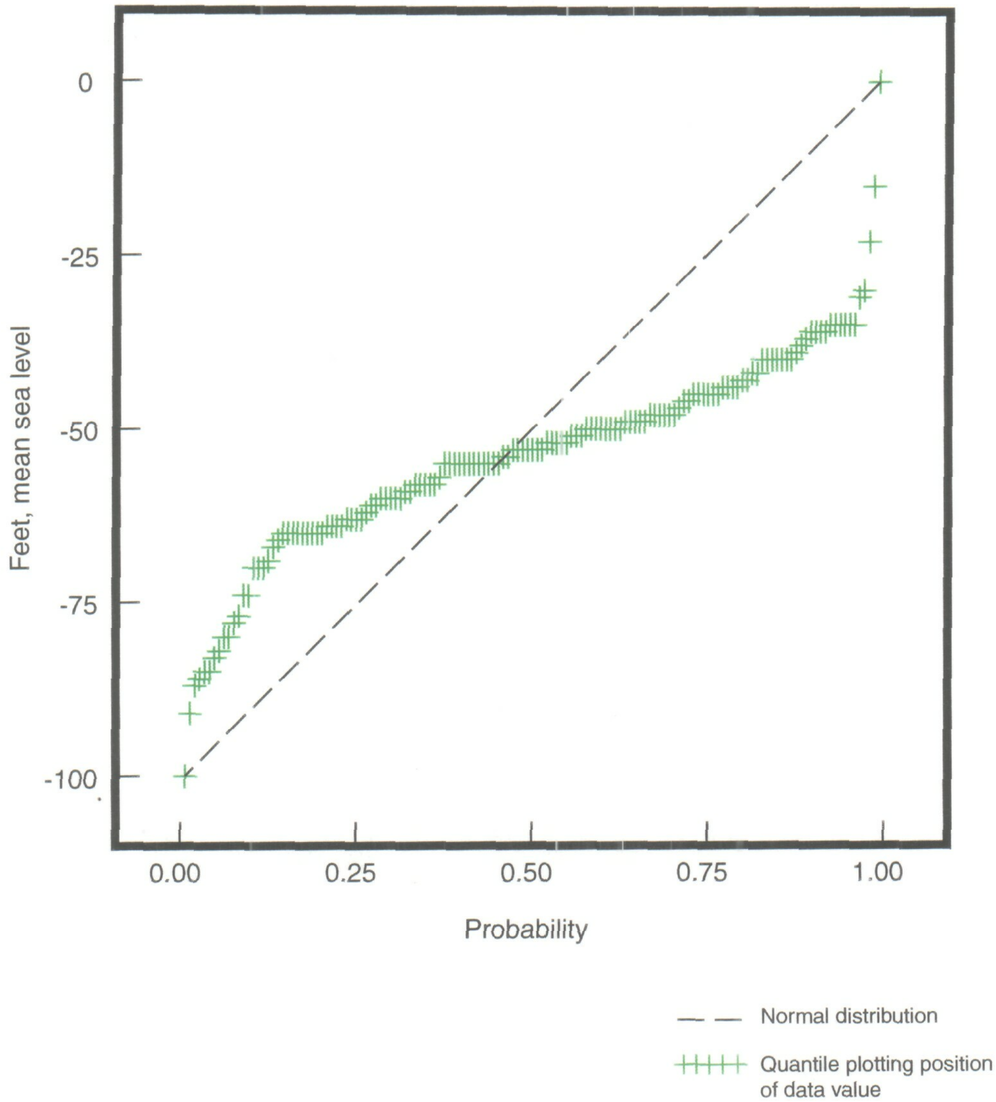

Figure 11. Probability plot of the elevation of the bottom of the intermediate aquifer in the study area

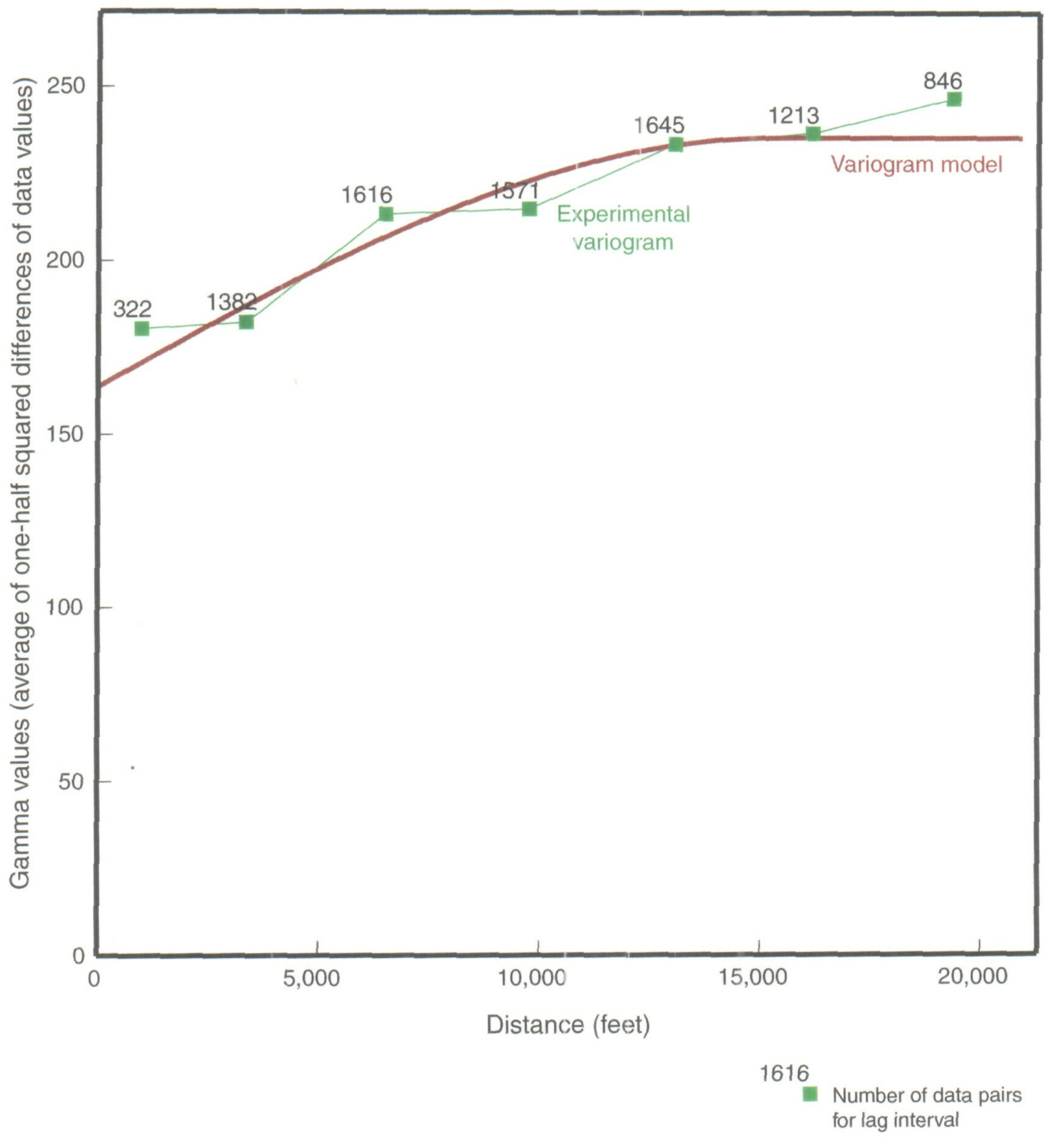

Figure 12. Isotropic (omnidirectional) variogram model of the elevation of the bottom of the intermediate aquifer

Variogram Map

A variogram map was used to determine if the spatial correlation structure of the data is dependent upon direction (Figure 13). For the elevation of the bottom of the intermediate aquifer, the variogram map suggested a strong anisotropy in a northwest-southeast direction.

Variogram Model—Anisotropic

Based on the results of the variogram map, an anisotropic model was fitted to an anisotropic experimental variogram (Figure 14). The anisotropic model consists of two directions perpendicular to one another. The number of data pairs for a lag interval of the anisotropic experimental variogram ranged from 168 to 645 in the primary northwest-southeast direction (D1 on Figure 14) and from 154 to 1,066 in the northeast-southwest direction (D2 on Figure 14).

The lag value and the number of lags used in the isotropic variogram model were also used for the anisotropic variogram model. In addition, nugget, sill, azimuth (i.e., direction of trend), and range values were used as parameters for the anisotropic model (Table 2).

An anisotropic variogram model was used for cross-validation and estimation procedures.

Neighborhood

A circular search neighborhood was selected. The radius of the neighborhood was set at 8,000 m, a distance near where the variograms in the anisotropic variogram model diverge. The minimum number of samples used in the calculation for each neighborhood was one, and the maximum number was ten.

Cross-validation

A base map showing the standardized estimation errors, a histogram of the standardized estimation errors, a scatter diagram of the true data value (Z on the y axis) versus the estimated value (Z^* on the x axis), and a scatter diagram of the standardized estimation error versus the estimated value were used to display the cross-validation results (Figure 15). Based on the distribution of the standardized estimation error, the data were spatially unbiased. The normally distributed histogram of the

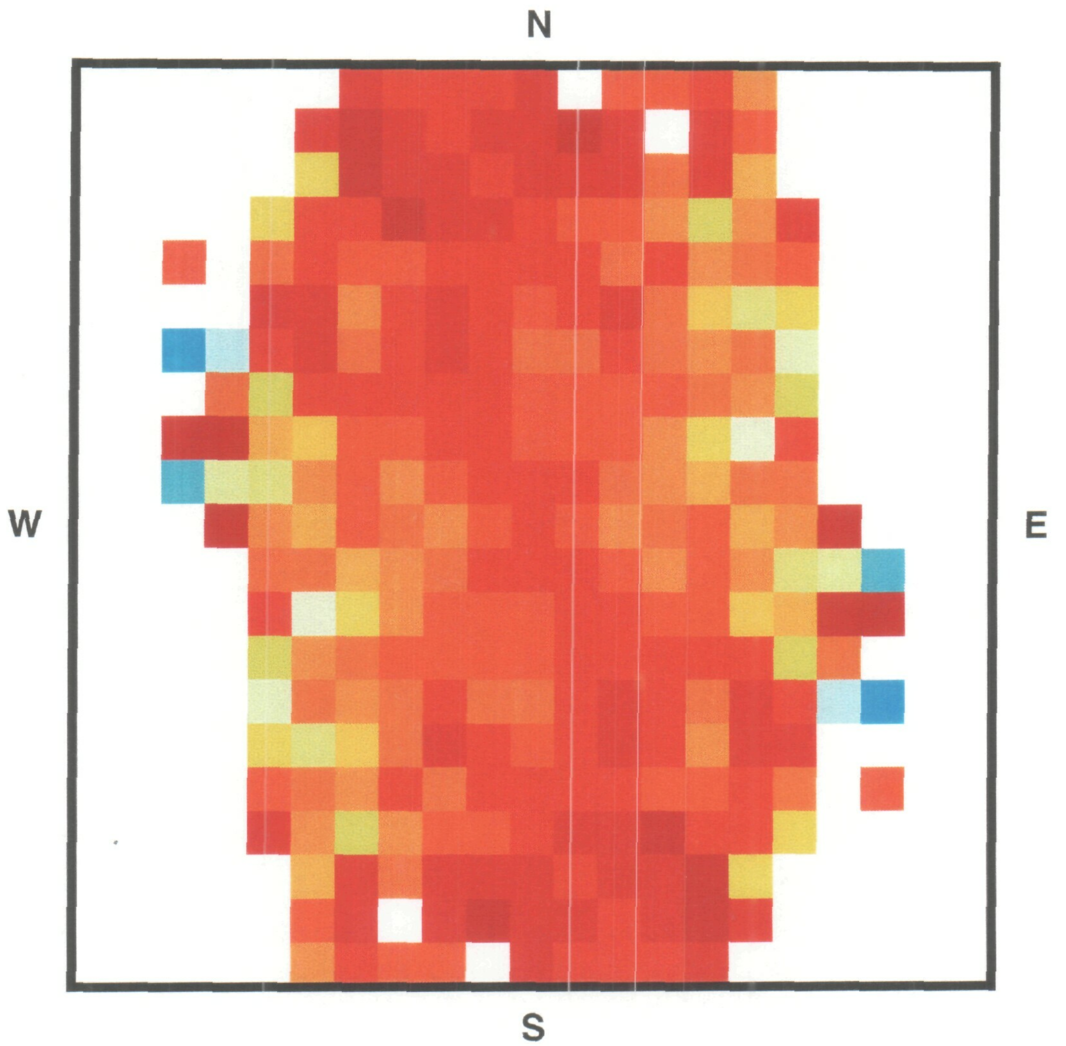

Figure 13. Variogram map of the elevation of the bottom of the intermediate aquifer. *Alignment of darker colors in a northwest-southeast direction indicates primary direction of anisotropy.*

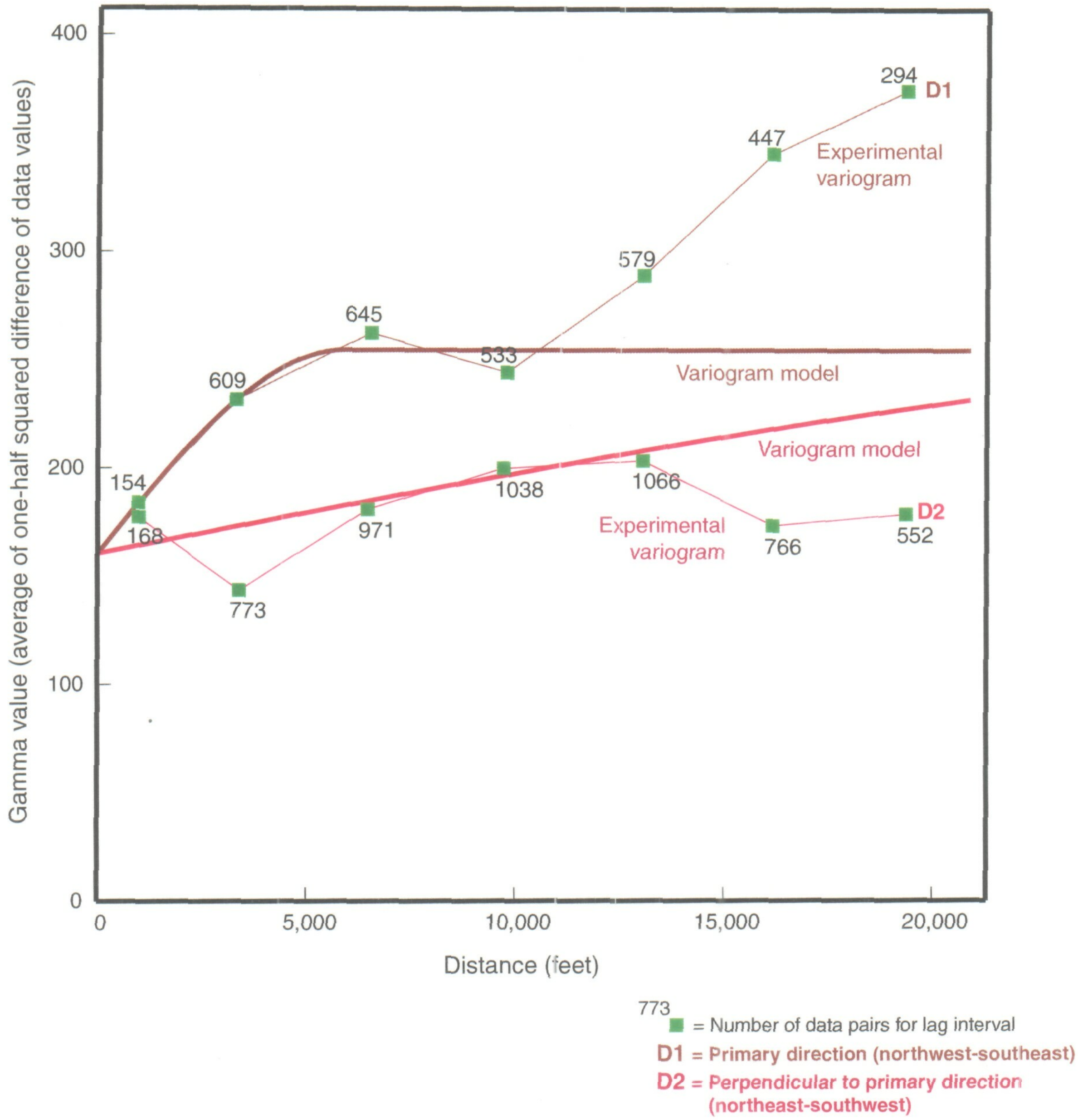

Figure 14. Anisotropic (directional) variogram model of the elevation of the bottom of the intermediate aquifer

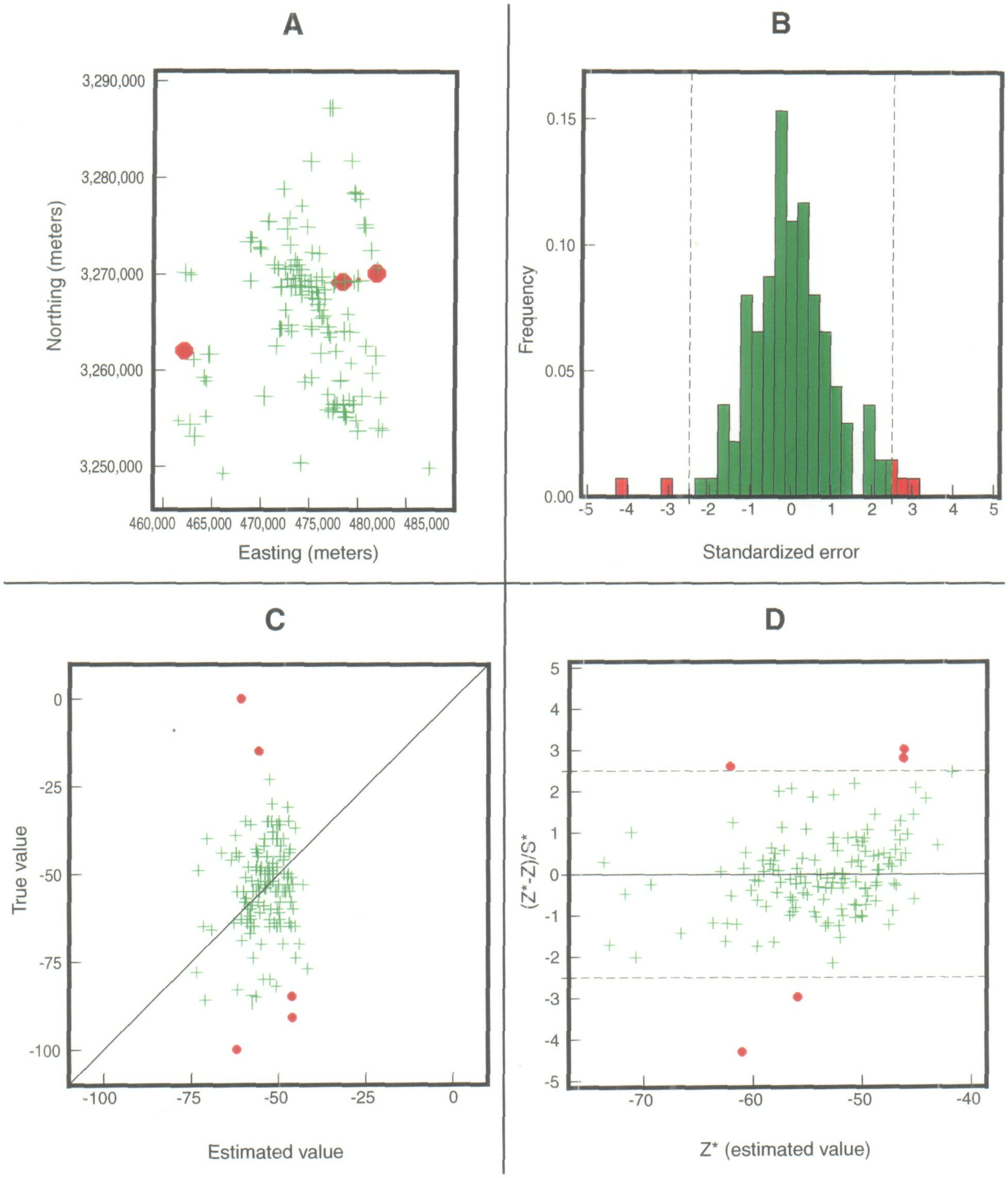

Figure 15. (A) Base map, (B) histogram, and (C, D) scatter diagrams for the cross-validation procedure for the elevation of the bottom of the intermediate aquifer. *Red denotes nonrobust data; green denotes data values where the standardized error lies between –2.5 and +2.5.*

Table 2. Parameters for the anisotropic variogram model of the bottom of the intermediate aquifer

Parameter	Numerical Value
Lag value	3,250 meters
Number of lags	7
Spherical Structure	
Azimuth	−120 degrees (northwest-southeast direction)
Range, principal direction	5,900 meters
Range, secondary direction	37,000 meters
Sill	94.33
Nugget Structure	
Sill	160.29

standardized estimation errors supports the assumption that the elevation data approximated a normal distribution as well as the validity of the variogram model that was used. Based on the scatter diagrams, the data were numerically unbiased.

The cross-validation procedure for elevation of the bottom of the intermediate aquifer resulted in only five nonrobust data points. So few nonrobust data points imply that the estimates for the elevation of the bottom of the intermediate aquifer were reliable.

Estimation

Point kriging was used to estimate the elevation of the bottom of the intermediate aquifer on the nodes of the estimation grid. Each grid cell represents a distance of 50 by 50 m on the earth's surface. To encompass the entire Palm Coast study area, the grid had 660 nodes extending in an east-west direction and 794 nodes extending in a north-south direction.

A contour map of the estimated elevation of the bottom of the intermediate aquifer was produced using kriging (Figure 16). This map portrays the estimated elevation of the bottom of the intermediate aquifer in the Palm Coast study area. Generally, the estimated elevation of the bottom of the intermediate aquifer decreases to the west. Well locations are superimposed on the map to indicate where the data values are located.

A map of the relative standard deviations of the elevation data (Figure 17) depicts the relative accuracy of the estimated values. In the eastern and

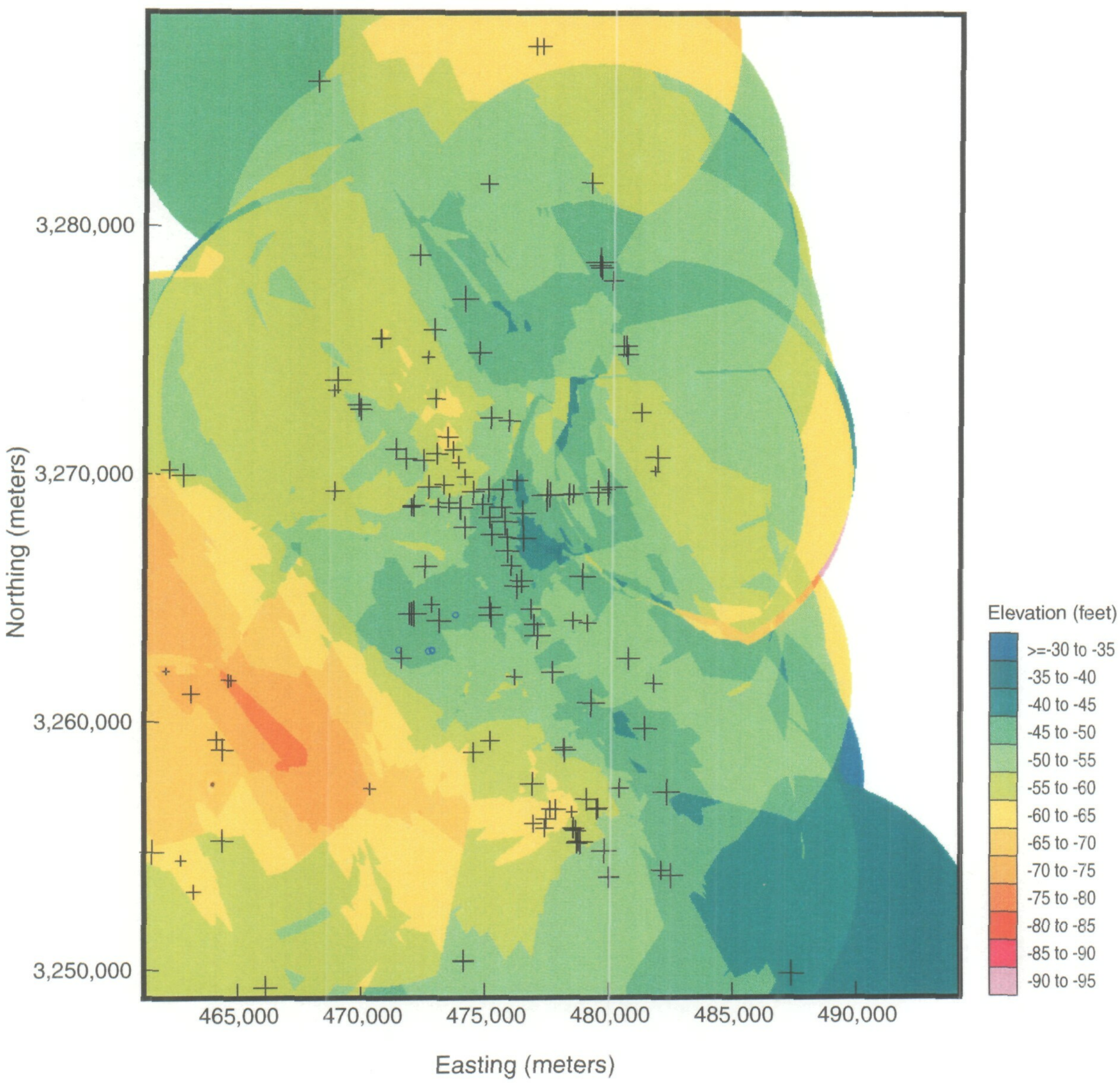

Figure 16. Estimated elevation of the bottom of the intermediate aquifer in the study area. *Pluses denote location of data points and are drawn at a size that is proportional to data values.*

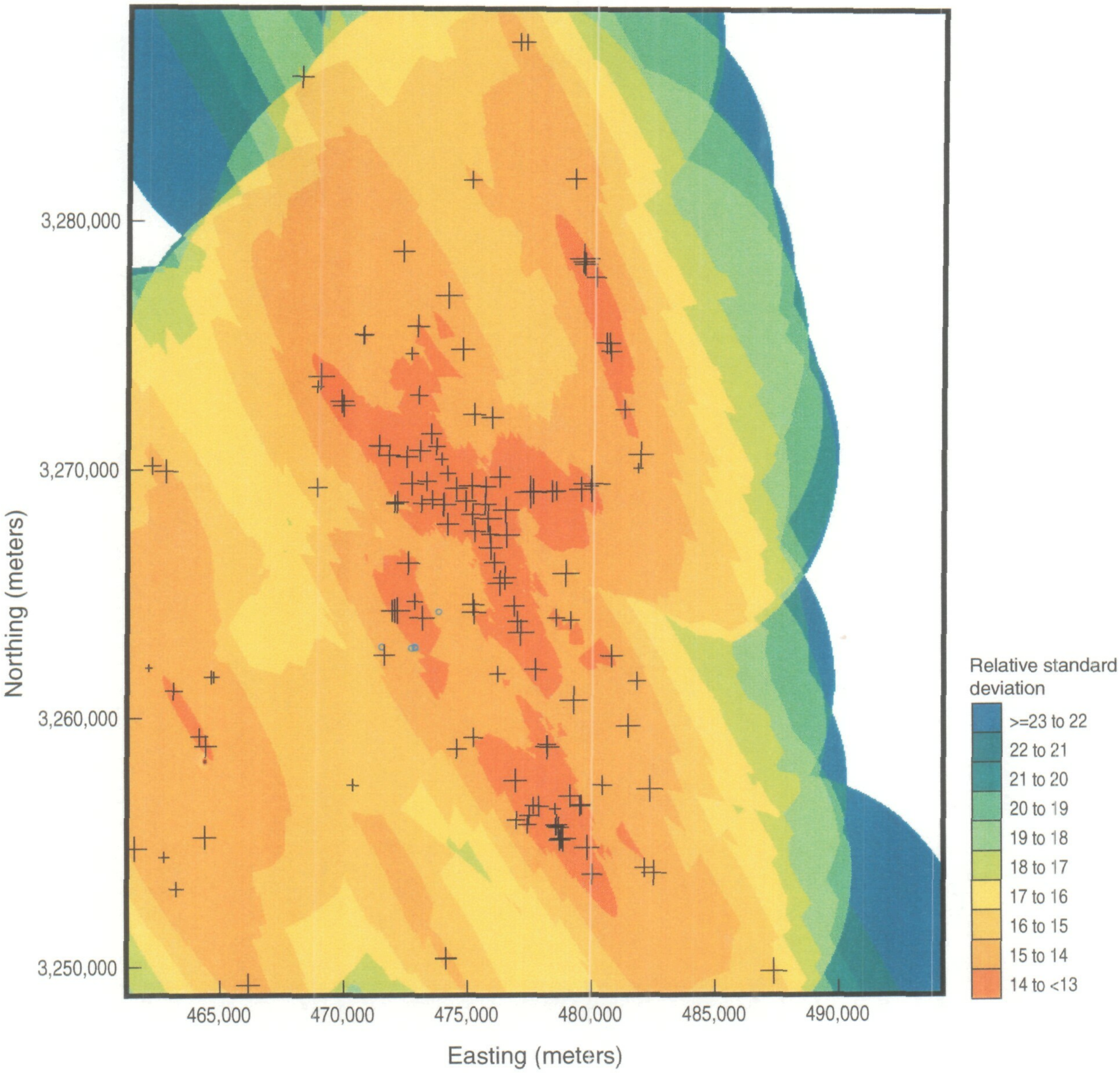

Figure 17. Relative standard deviations of the estimated elevation of the bottom of the intermediate aquifer. *Pluses denote location of data points and are drawn at a size that is proportional to data values.*

northwestern part of the study area, data are insufficient to estimate elevations of the bottom of the intermediate aquifer with a high degree of certainty.

ELEVATION OF THE TOP OF THE CONFINING UNIT

The elevation of the top of the confining unit was estimated from 143 data points. The minimum elevation is –57 ft msl and the maximum elevation is 17 ft msl. The mean and median elevations are –20.68 and –20 ft msl, respectively. A histogram and a probability plot of the elevation of the top of the confining unit are shown in Figures 18 and 19, respectively. The histogram plot approximates a bell shape, and the probability plot lies close to a straight line. Both figures indicate the data approximate a normal distribution.

STRUCTURAL ANALYSIS OF THE DATA

A structural analysis was conducted to determine the spatial correlation of the investigated data. The process was accomplished through the computation and modeling of the variogram function.

Experimental Variogram

A lag value of 2,275 m and a lag count of 9 were selected as input values to the omnidirectional experimental variogram of the elevation of the top of the confining unit (Figure 20). The number of data pairs for a lag interval ranged from 180 to 1,285.

Variogram Model—Isotropic

An isotropic model was fitted to the omnidirectional experimental variogram (Figure 20). The final isotropic model of the experimental variogram was configured with a nugget and one spherical structure.

For the omnidirectional variogram model, the nugget was 133.16 and the sill was 114.67, with a nugget-to-sill ratio of 1.16. The range was 26,463.94 m.

Variogram Map

A variogram map was used to determine if the spatial correlation structure of the data is dependent upon direction (Figure 21). For the elevation of the top of the confining unit, the variogram map suggested a weak anisotropy in a northwest-southeast direction.

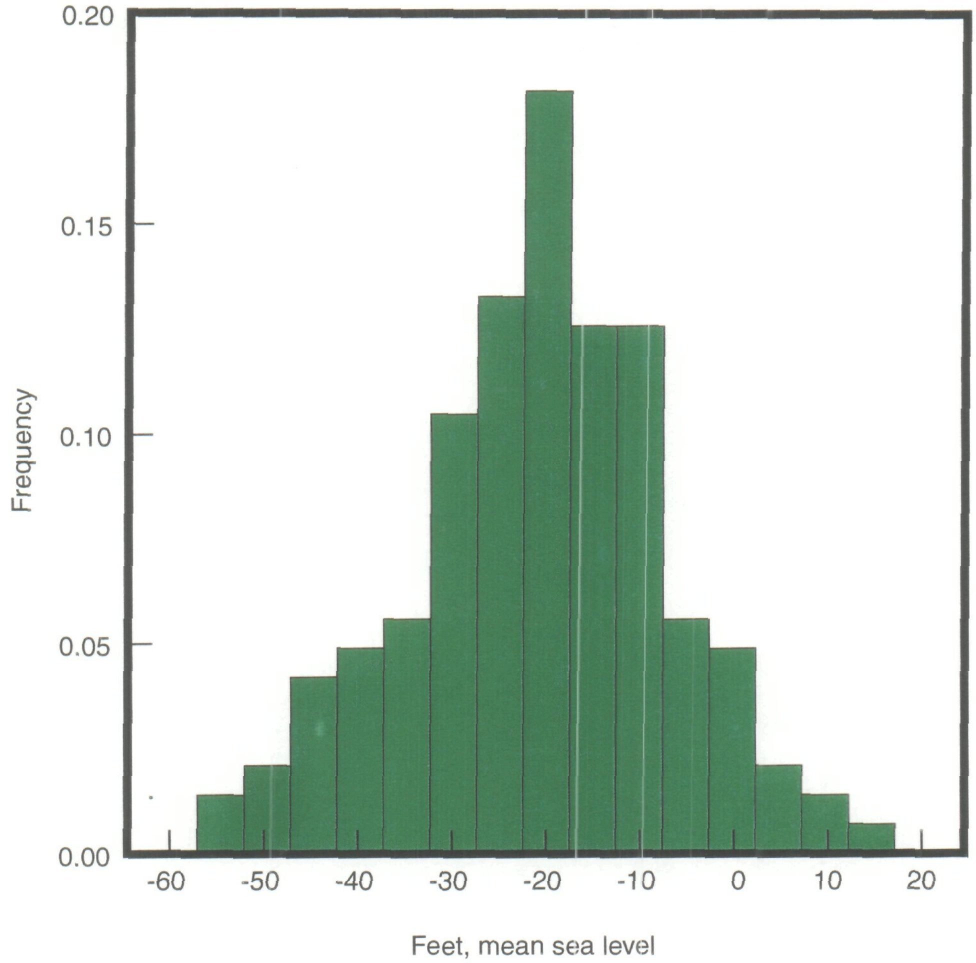

Figure 18. Histogram of the elevation of the top of the confining unit in the study area

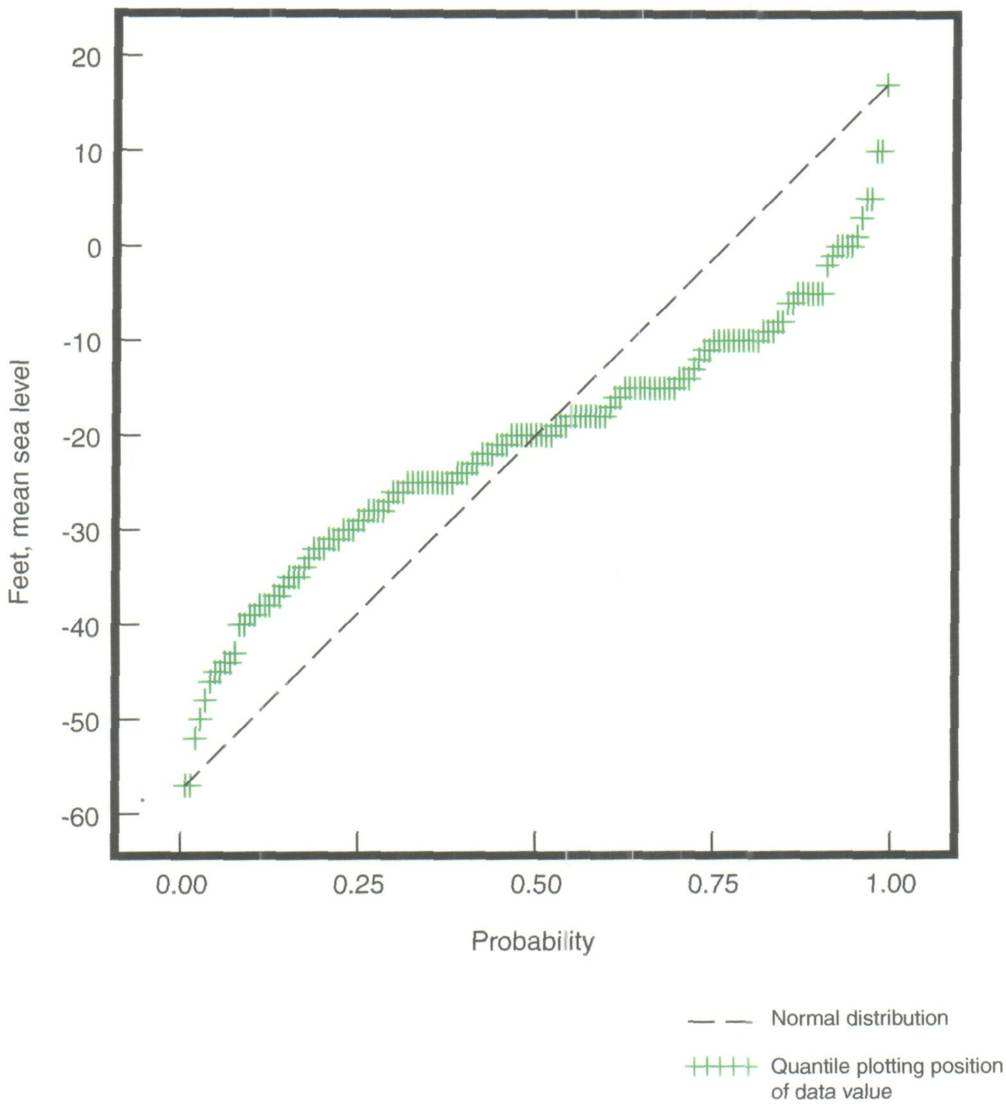

Figure 19. Probability plot of the elevation of the top of the confining unit in the study area

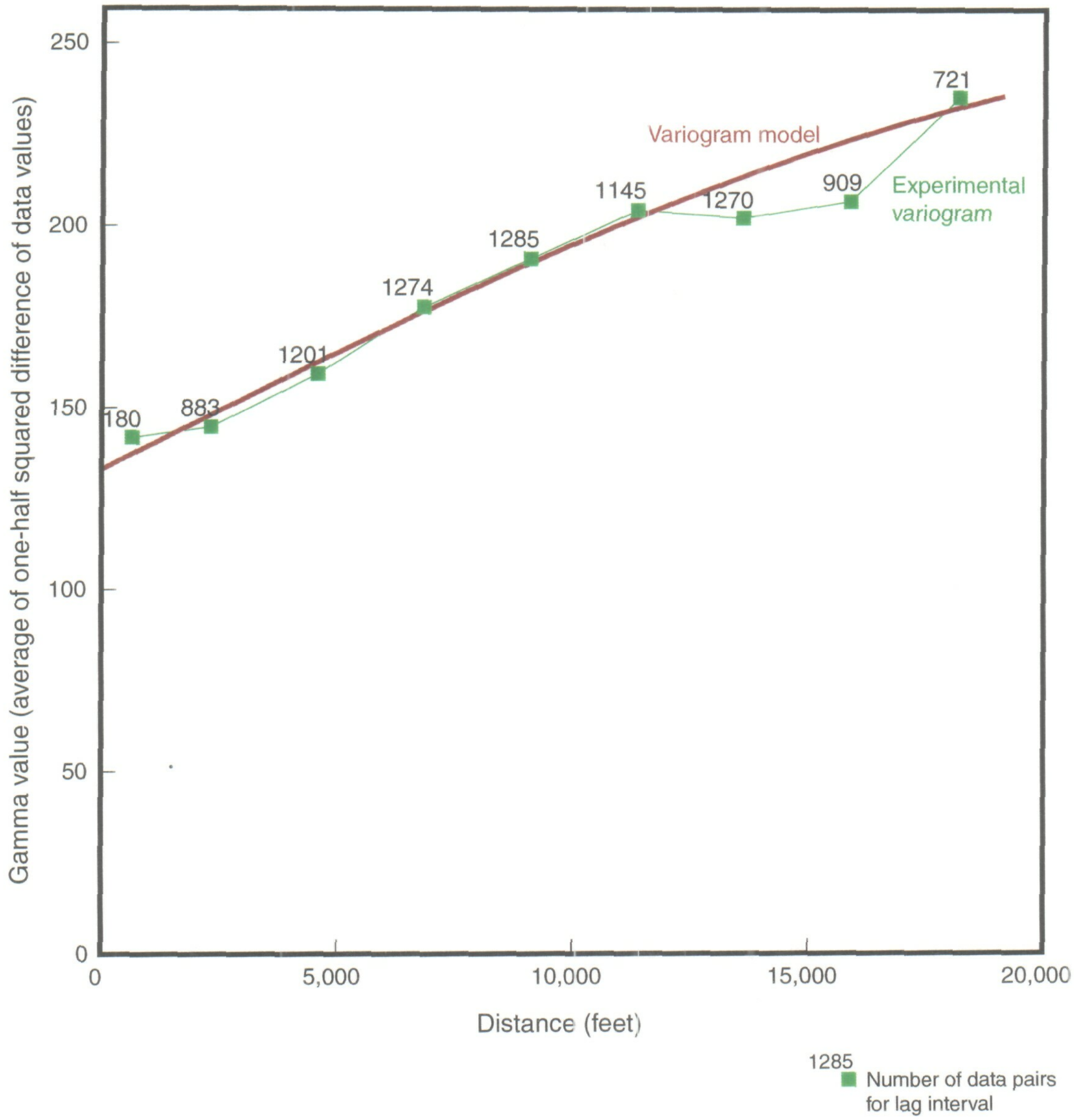

Figure 20. Isotropic (omnidirectional) variogram model of the elevation of the top of the confining unit

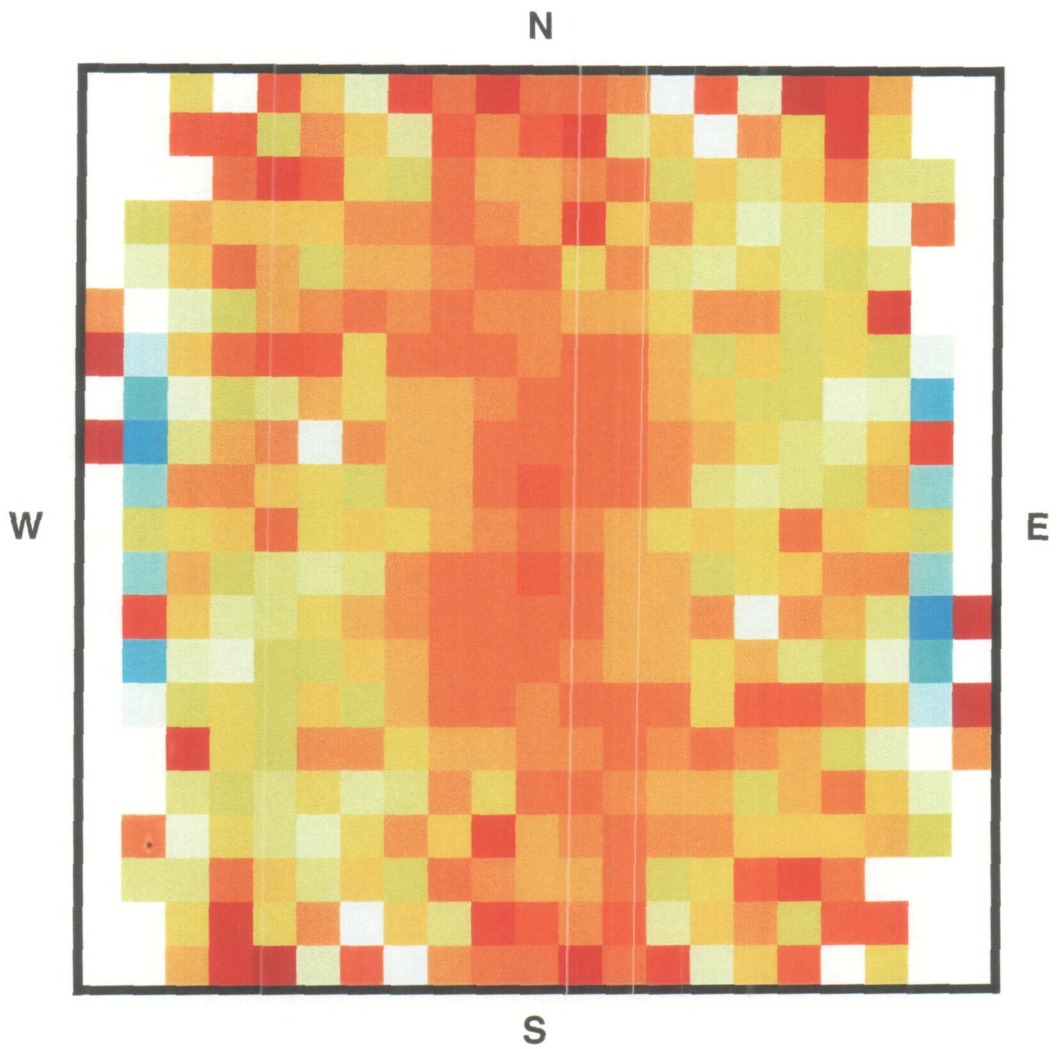

Figure 21. Variogram map of the elevation of the top of the confining unit. *Alignment of colors in a northwest-southeast direction suggests a weak anisotropy in this direction.*

Variogram Model—Anisotropic

Based on the results of the variogram map, an anisotropic model was fitted to an anisotropic experimental variogram (Figure 22). The anisotropic model consists of two directions perpendicular to one another. The number of data pairs for each lag interval of the anisotropic experimental variogram ranged from 89 to 535 in the primary northwest-southeast direction (D1 on Figure 22) and from 91 to 842 in the northeast-southwest direction (D2 on Figure 22).

The lag value and the number of lags used in the isotropic variogram model were also used for the anisotropic variogram model. In addition, nugget, sill, azimuth (i.e., direction of trend), and range values were used as parameters for the anisotropic model (Table 3).

Because the variograms for the primary and secondary directions are so close to one another for a distance up to 8,000 m, an isotropic variogram model was used for cross-validation and estimation procedures.

Neighborhood

A circular search neighborhood was selected. The radius of the neighborhood was set at 8,000 m, a distance where the variograms in the anisotropic variogram model diverge. The minimum number of samples used in the calculation for each neighborhood was one, and the maximum number was ten.

Cross-validation

A base map showing the standardized estimation errors, a histogram of the standardized estimation errors, a scatter diagram of the true data value (Z on the y axis) versus the estimated value (Z^* on the x axis), and a scatter diagram of the standardized estimation error versus the estimated value were used to display the cross-validation results (Figure 23). Based on the distribution of the standardized estimation error, the data were spatially unbiased. The normally distributed histogram of the standardized estimation errors supports the assumption that the elevation data approximated a normal distribution as well as the validity of the variogram model that was used. Based on the scatter diagrams, the data were numerically unbiased.

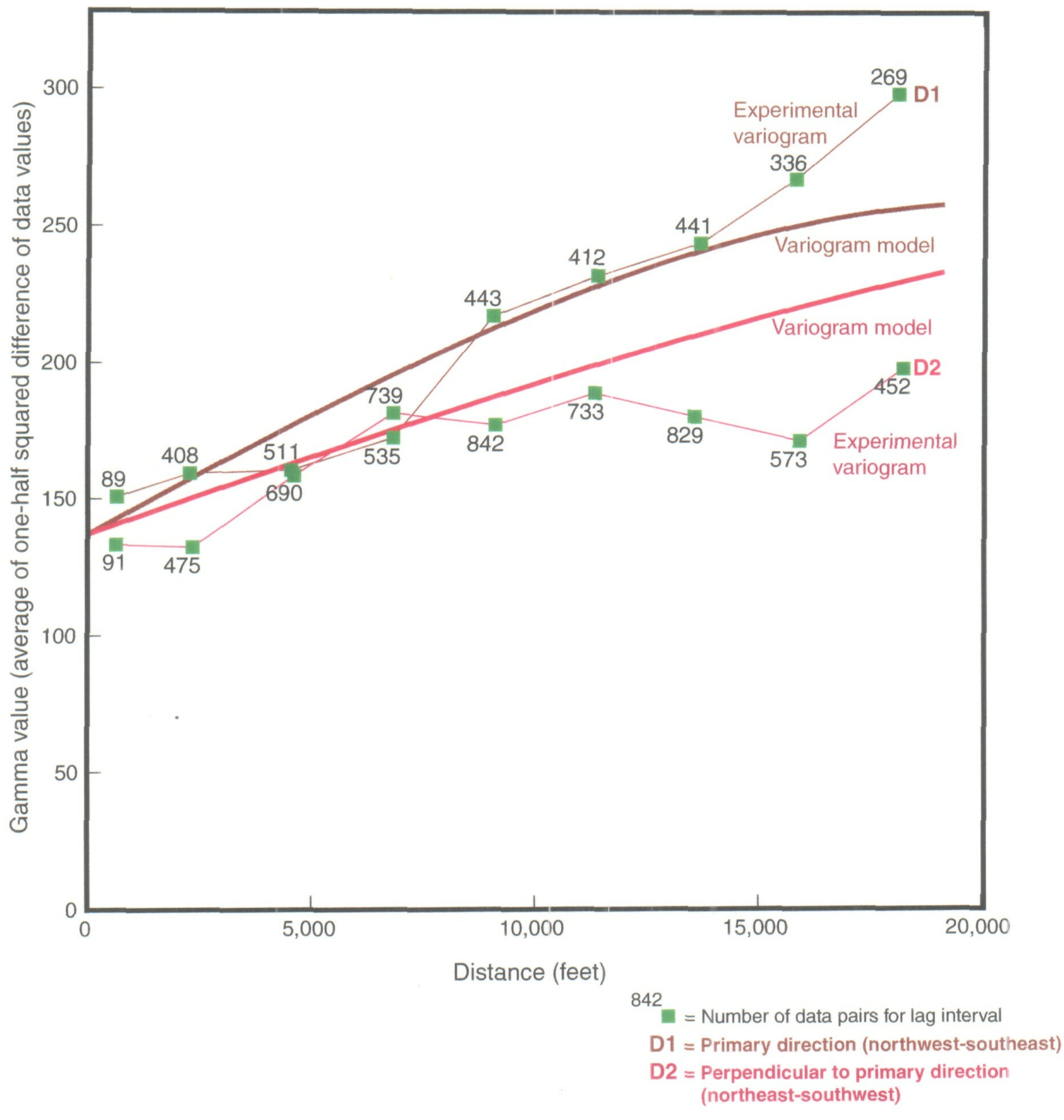

Figure 22. Anisotropic (directional) variogram model of the elevation of the top of the confining unit

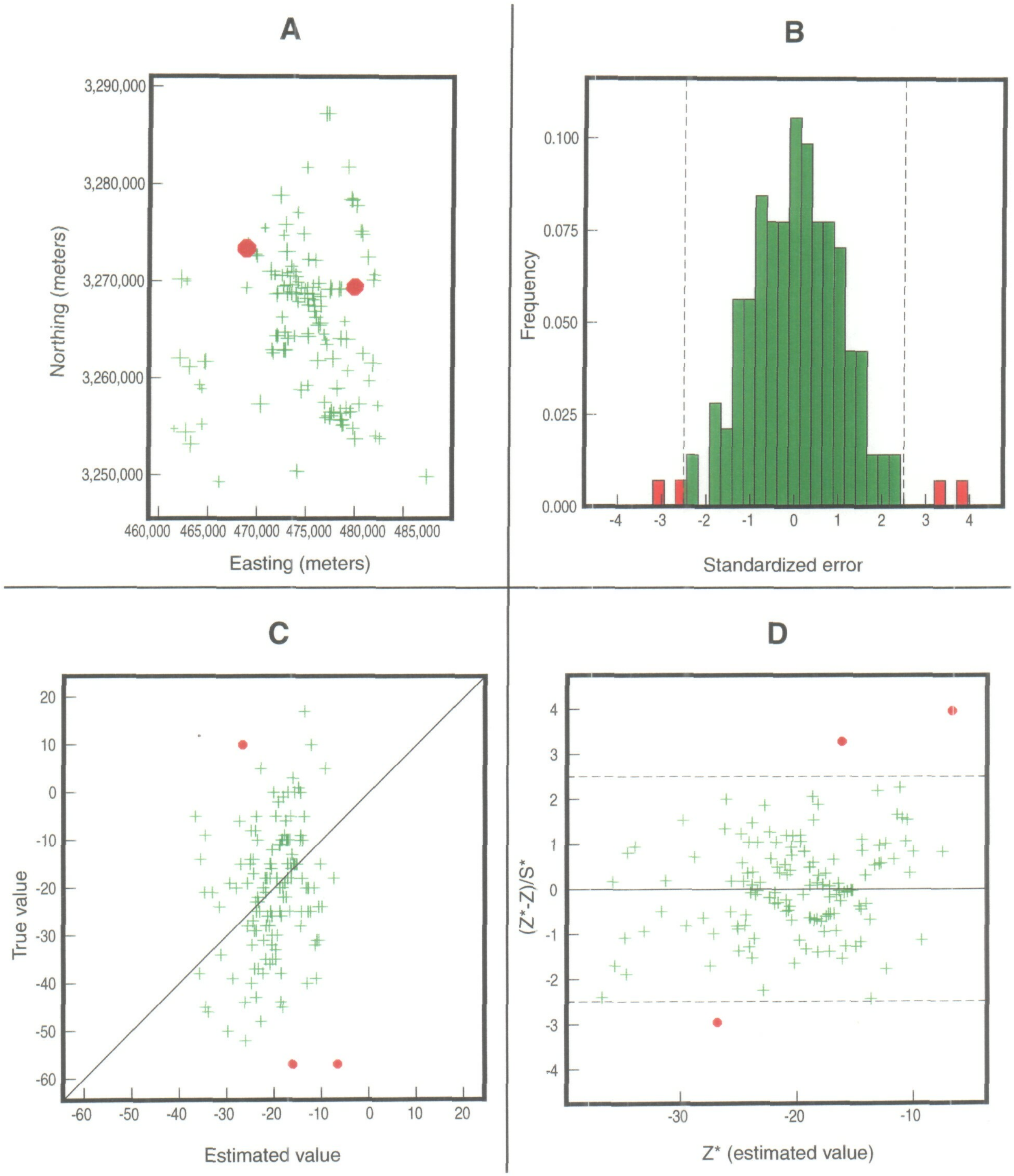

Figure 23. (A) Base map, (B) histogram, and (C, D) scatter diagrams for the cross-validation procedure for the elevation of the top of the confining unit. *Red denotes nonrobust data; green denotes data values where the standardized error lies between –2.5 and +2.5.*

Table 3. Parameters for the anisotropic variogram model of the top of the confining unit

Parameter	Numerical Value
Lag value	2,275 meters
Number of lags	9
Spherical Structure	
Azimuth	−120 degrees (northwest-southeast direction)
Range, principal direction	18,000 meters
Range, secondary direction	60,000 meters
Sill	121.81
Nugget Structure	
Sill	137.08

The cross-validation procedure for elevation of the top of the confining unit resulted in only three nonrobust data points. So few nonrobust data points imply that the estimates for the elevation of the top of the confining unit were reliable.

Estimation

Point kriging was used to estimate the elevation of the top of the confining unit on the nodes of the estimation grid. Each grid cell represents a distance of 50 by 50 m on the earth's surface. To encompass the entire Palm Coast study area, the grid had 660 nodes extending in an east-west direction and 794 nodes extending in a north-south direction.

A contour map of the estimated elevation of the top of the confining unit was produced using kriging (Figure 24). This map portrays the estimated elevation of the top of the confining unit in the Palm Coast study area. Generally, the estimated elevation of the top of the confining unit decreases to the west. Well locations are superimposed on the map to indicate where the data values are located.

A map of the relative standard deviations of the elevation data (Figure 25) depicts the relative accuracy of the estimated values. In the eastern and northwestern part of the study area, data are insufficient to estimate elevations of the top of the confining unit with a high degree of certainty.

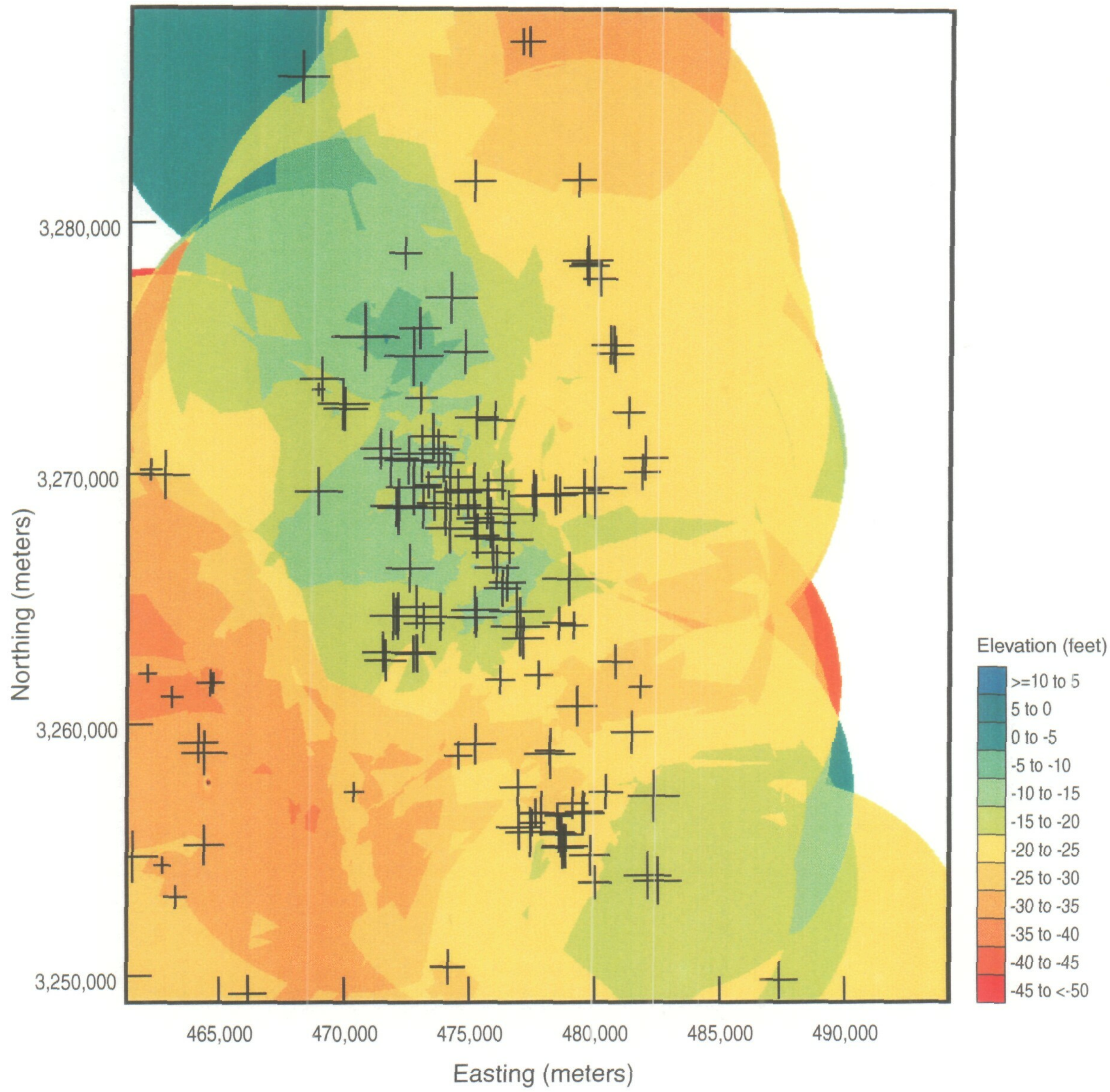

Figure 24. Estimated elevation of the top of the confining unit in the study area. *Pluses denote location of data points and are drawn at a size that is proportional to data values.*

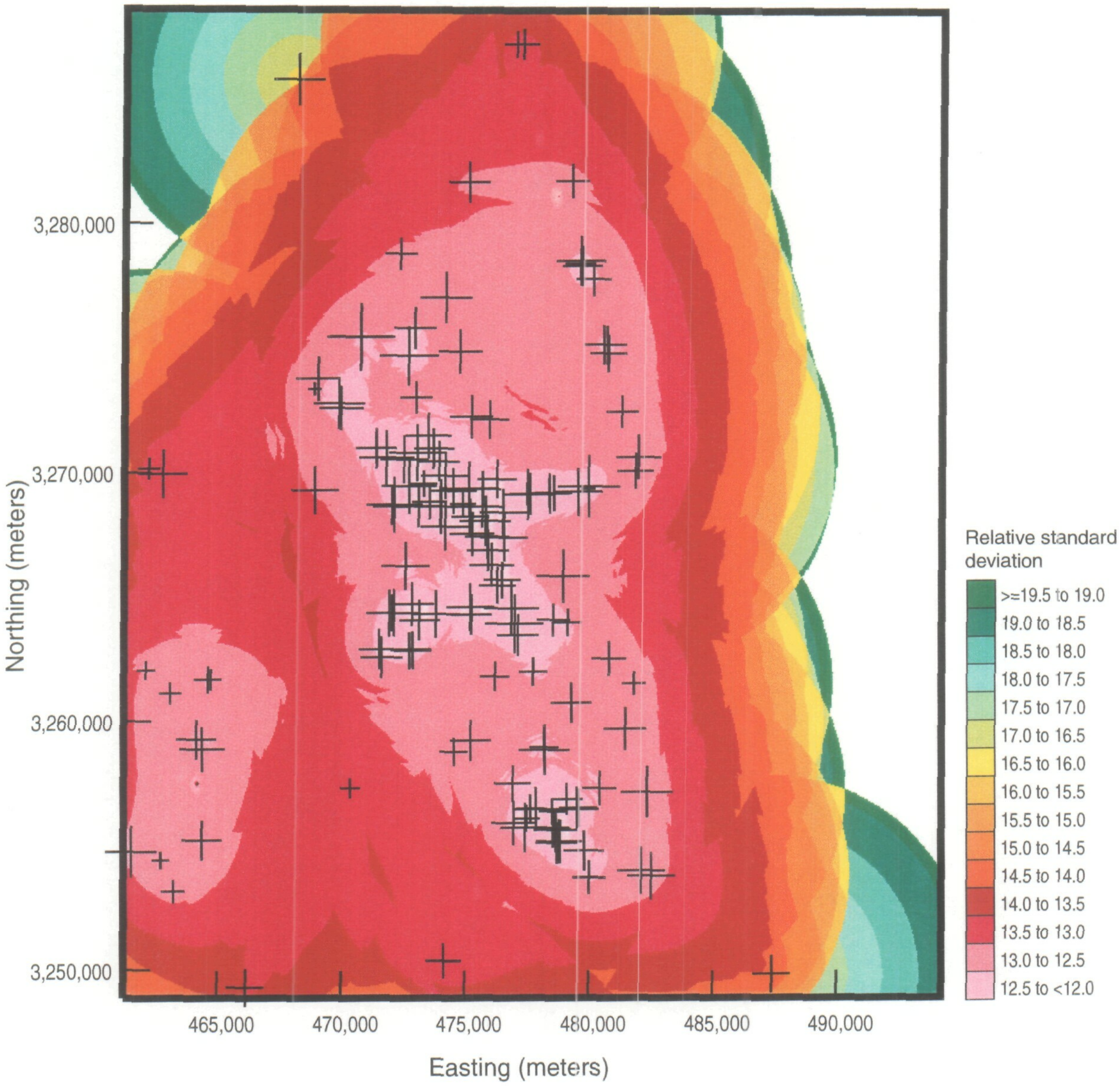

Figure 25. Relative standard deviations of the estimated elevation of the top of the confining unit. *Pluses denote location of data points and are drawn at a size that is proportional to data values.*

LEAKANCE OF THE CONFINING UNIT FOR THE INTERMEDIATE AQUIFER

Leakance of the confining unit for the intermediate aquifer was estimated from 143 data points. Leakance values at the data points were estimated by Gary Eichler, FWS consultant, from geophysical logs, based on leakance determinations from pump tests at 29 points. All leakance values in this report were multiplied by 10^5 to facilitate their entry into ISATIS. All mention of leakance values in this report is based on the value multiplied by 10^5.

The minimum and maximum values for leakance are 3 and 100 day^{-1}, respectively. The mean and median leakance values are 18.56 and 10 day^{-1}, respectively. Most leakance values are clustered between 0 and 50 day^{-1}, with less than 5% occurring at 100 day^{-1} (Figure 26). Taking the natural log of the leakance values more closely approximates a normal distribution (Figure 27). Therefore, geostatistics was performed on the natural log of the leakance values.

STRUCTURAL ANALYSIS OF THE DATA

A structural analysis was conducted to determine the spatial correlation of the investigated data. The process was accomplished through the computation and modeling of the variogram function.

Experimental Variogram

A lag value of 500 m and a lag count of 7 were selected as input values to the omnidirectional experimental variogram of the natural log of leakance (Figure 28). The number of data pairs for each lag interval ranged from 34 to 205.

Variogram Model—Isotropic

An isotropic model was fitted to the omnidirectional experimental variogram (Figure 28). The final isotropic model of the experimental variogram was configured with a nugget and one spherical structure.

For the omnidirectional variogram model, the nugget was 0.34 and the sill was 0.65, with a nugget-to-sill ratio of 0.52. The range was 1,969.8 m.

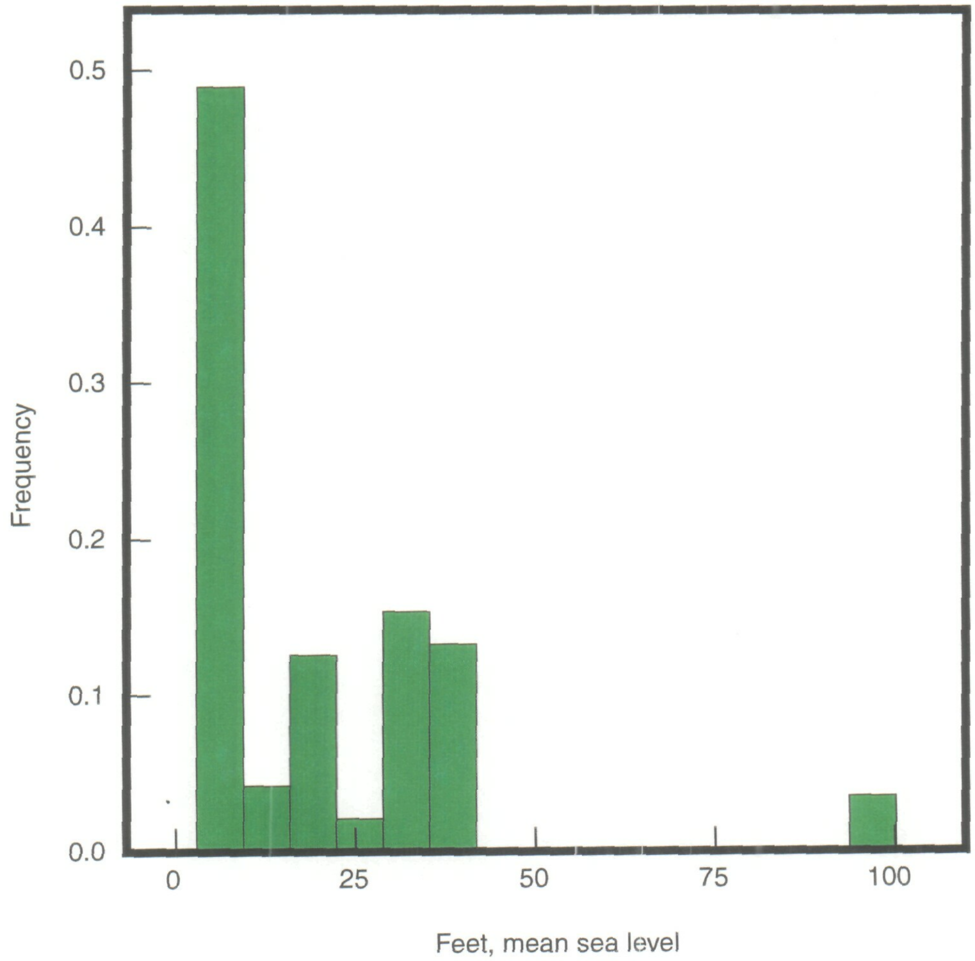

Figure 26. Histogram of leakance of the confining unit for the intermediate aquifer (Note: Leakance values were multiplied by 10^5)

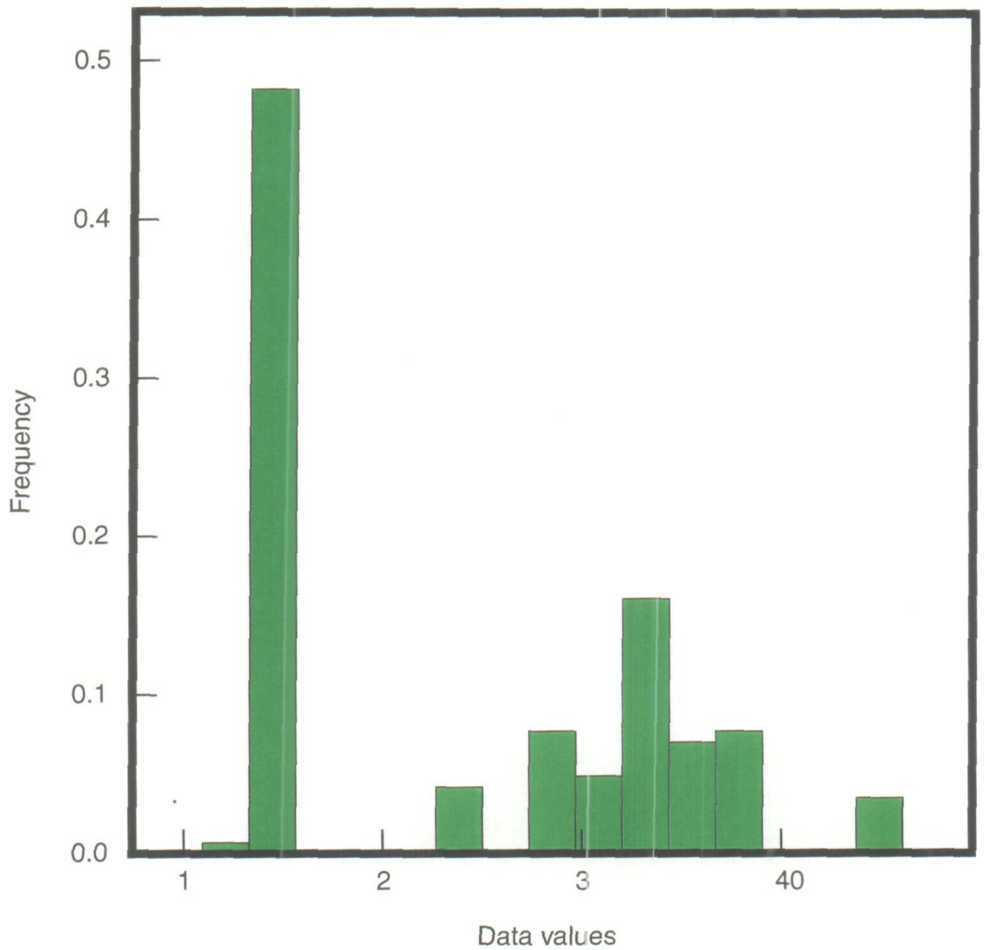

Figure 27. Histogram of the natural log of leakance (Note: Leakance values were multiplied by 10^5)

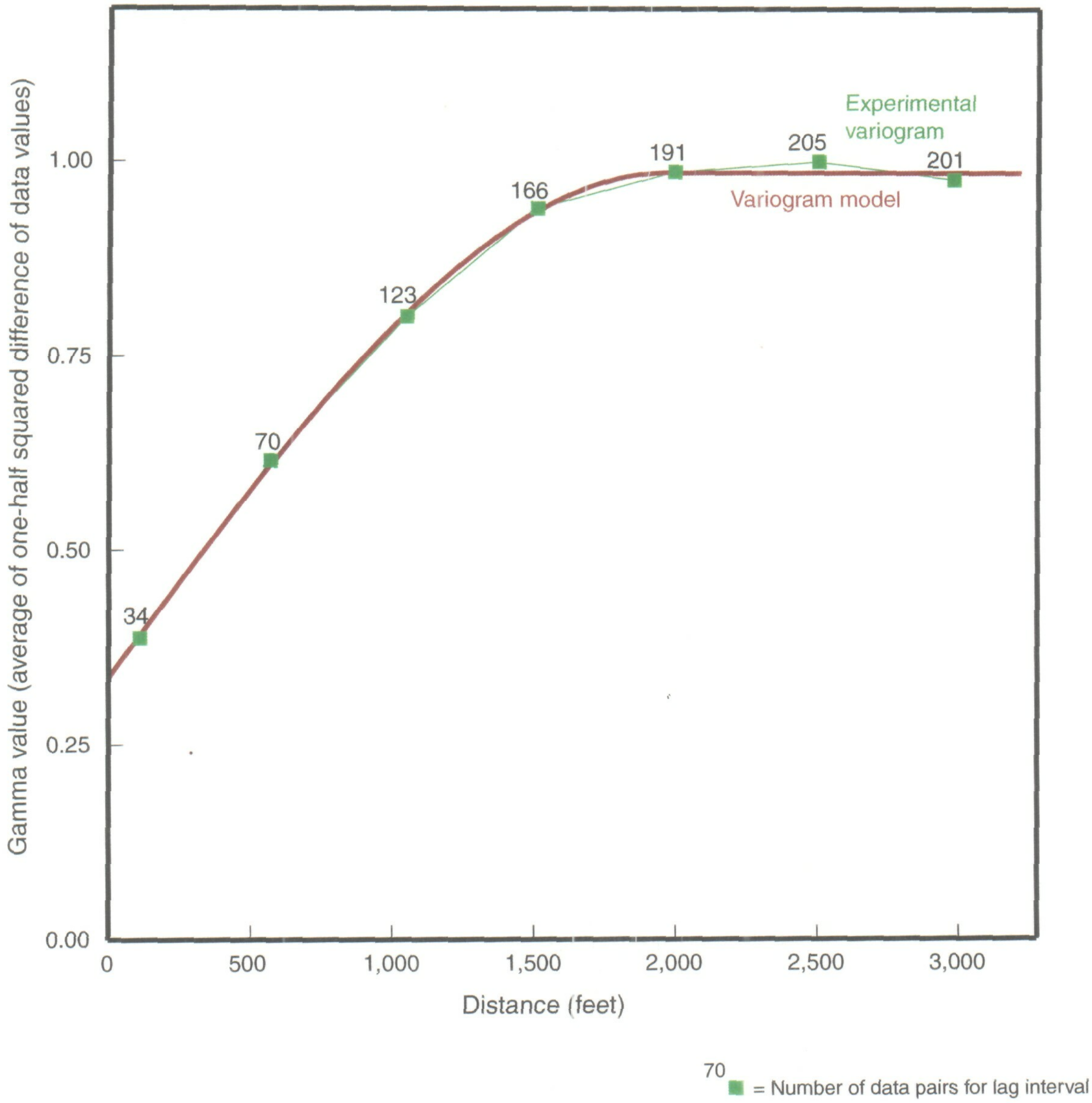

Figure 28. Isotropic (omnidirectional) variogram model of the natural log of leakance

Variogram Map

A variogram map was used to determine if the spatial correlation structure of the data is dependent upon direction (Figure 29). For the leakance of the confining unit, the variogram map did not suggest any anisotropy. Therefore, an isotropic model was used for cross-validation and estimation procedures.

Neighborhood

A circular search neighborhood was selected. The radius of the neighborhood was set at 1,970 m, a distance beyond which the variogram model is invalid. The minimum number of samples used in the calculation for each neighborhood was one, and the maximum number was ten.

Cross-validation

A base map showing the standardized estimation errors, a histogram of the standardized estimation errors, a scatter diagram of the true data value (Z on the y axis) versus the estimated value (Z^* on the x axis), and a scatter diagram of the standardized estimation error versus the estimated value were used to display the cross-validation results (Figure 30). Based on the distribution of the standardized estimation error, the data were spatially unbiased. The normally distributed histogram of the standardized estimation errors supports the assumption that the natural log of leakance data approximated a normal distribution as well as the validity of the variogram model that was used. Based on the scatter diagrams, the data were numerically unbiased.

The cross-validation procedure for the natural log of leakance of the confining unit resulted in only four nonrobust data points. So few nonrobust data points imply that the estimates for the natural log of leakance of the confining unit were reliable.

Estimation

Simulation was used to estimate the natural log of leakance of the confining unit on the nodes of the estimation grid. Each grid cell represents a distance of 50 by 50 m on the earth's surface. To encompass the entire Palm Coast study area, the grid had 660 nodes extending in an east-west direction and 794 nodes extending in a north-south direction. Fifty simulations were performed.

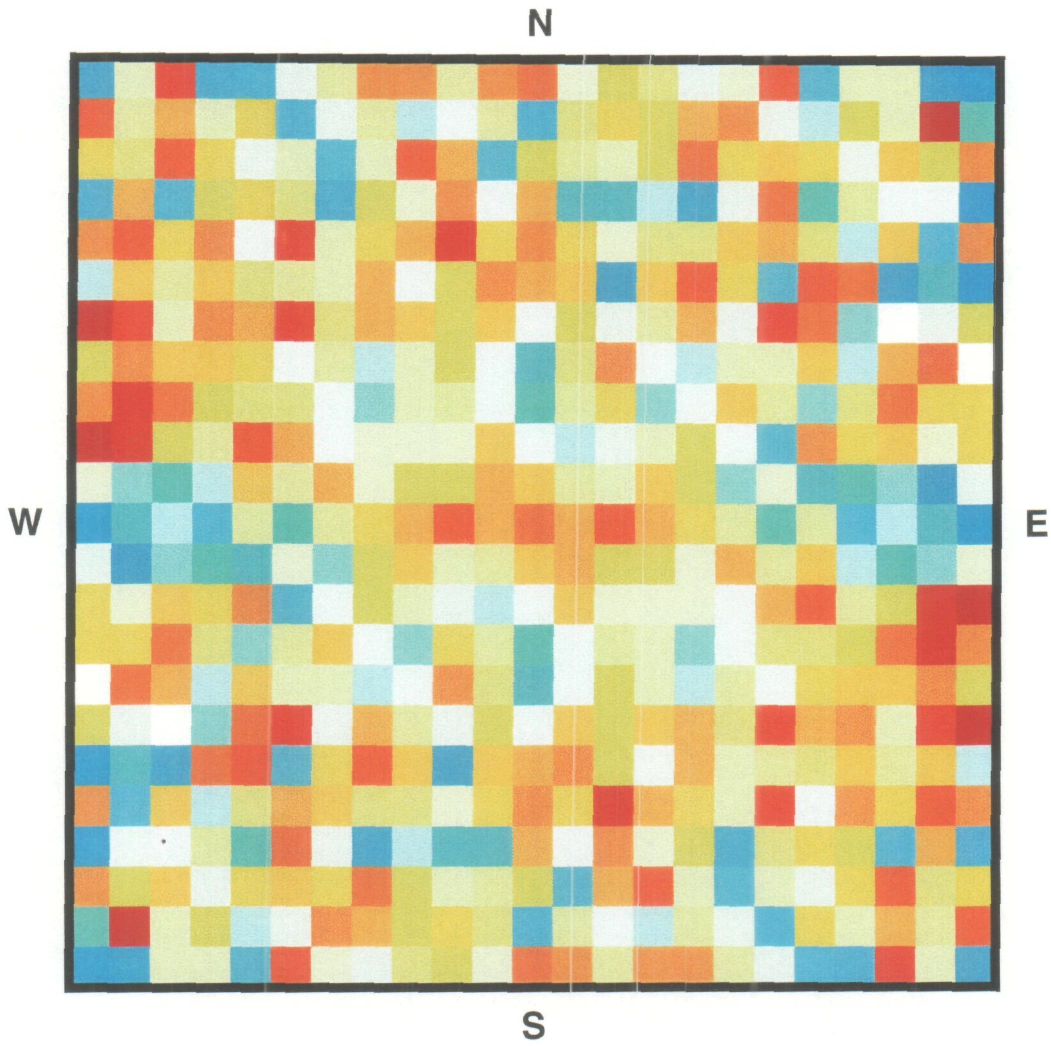

Figure 29. Variogram map of the natural log of leakance. *Lack of alignment of the colors suggests that there is no anisotropy.*

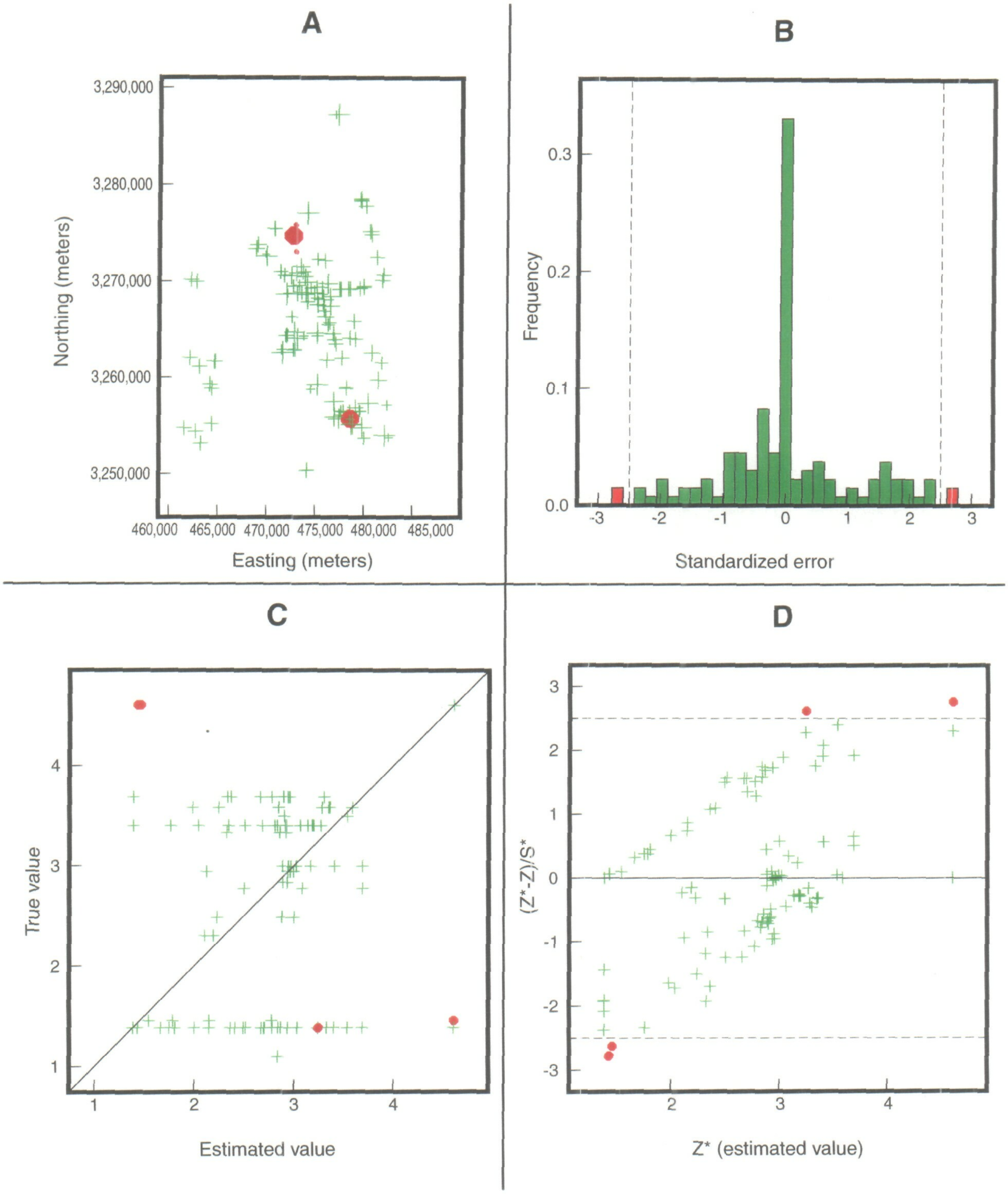

Figure 30. (A) Base map, (B) histogram, and (C, D) scatter diagrams for the cross-validation procedure for the natural log of leakance. *Red denotes nonrobust data; green denotes data values where the standardized error lies between –2.5 and +2.5.*

Simulation is a procedure by which the value of the investigated variable at an unsampled location is predicted using sample values from the neighborhood of that location and the variogram model. Simulation is the only method which reproduces the variability of the real phenomenon (i.e., the natural log of leakance or the natural log of hydraulic conductivity).

One contour map of the natural log of leakance of the confining unit produced by simulation is shown in Figure 31. This map portrays the natural log of leakance of the confining unit in the Palm Coast study area. Generally, the natural log of leakance of the confining unit decreases to the west. Well locations are superimposed on the map to indicate where the data values are located. There was insufficient data to completely fill the model area. White areas on the map indicate where data are missing.

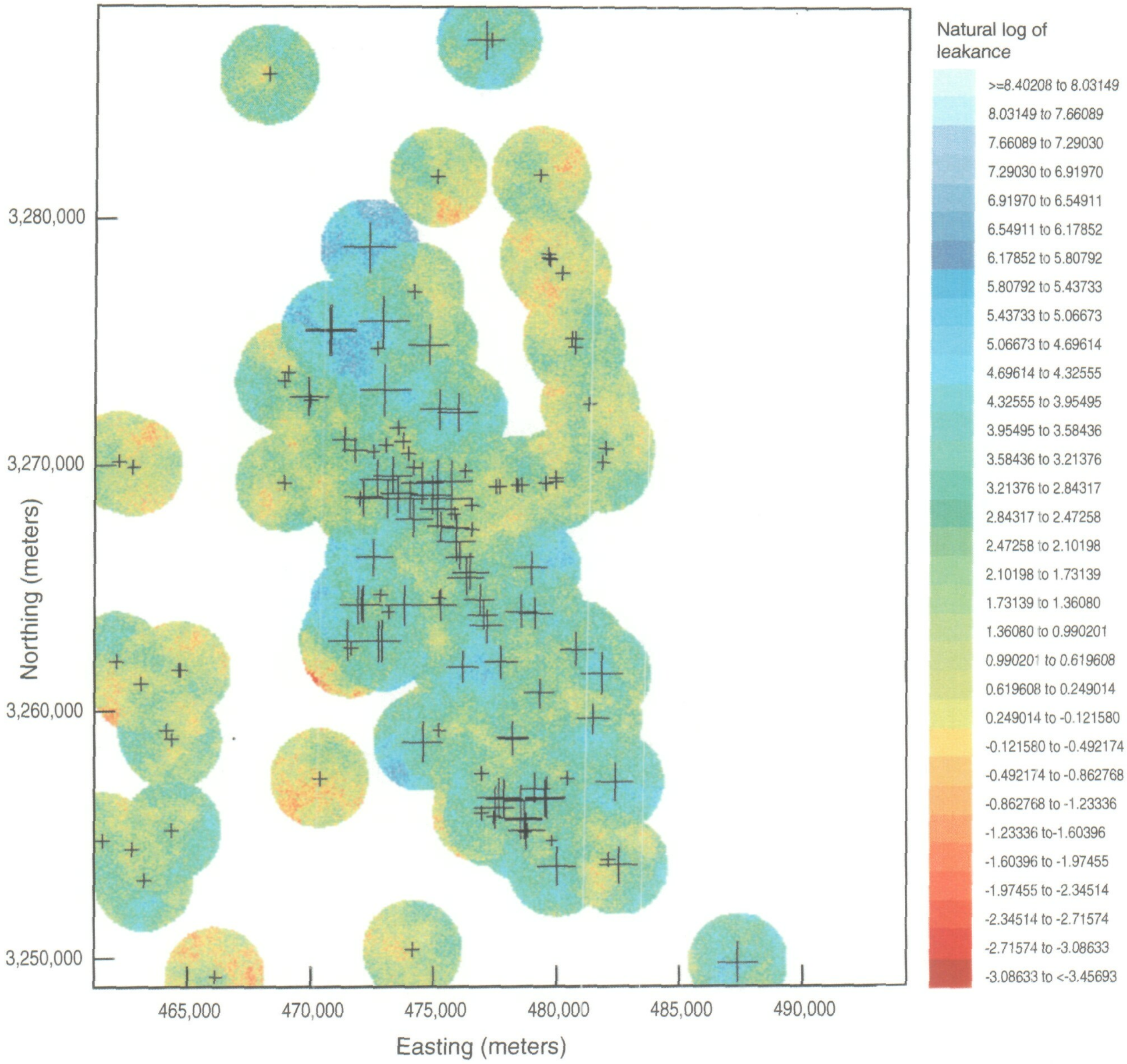

Figure 31. Simulation of the natural log of leakance of the confining unit for the intermediate aquifer. *Pluses denote location of data points and are drawn at a size that is proportional to the natural log of data values.*

HYDRAULIC CONDUCTIVITY OF THE INTERMEDIATE AQUIFER

Hydraulic conductivity of the intermediate aquifer was estimated from 143 data points. Hydraulic conductivity was calculated by dividing the transmissivity of the intermediate aquifer by its thickness. Most values for transmissivity at the data points were estimated by Gary Eichler, FWS consultant, from geophysical logs, based on transmissivity determinations from pump and specific-capacity tests at 52 well points.

The minimum and maximum values for hydraulic conductivity are 6.7 and 404.8 feet per day, respectively. The mean and median hydraulic conductivity values are 101.24 and 100 feet per day, respectively. The distribution of hydraulic conductivity has a tail toward the high end (Figure 32). To make the distribution approximate a bell shape or normal distribution, the natural log was taken (Figure 33). Therefore, geostatistics was performed on the natural log of hydraulic conductivity.

STRUCTURAL ANALYSIS OF THE DATA

A structural analysis was conducted to determine the spatial correlation of the investigated data. The process was accomplished through the computation and modeling of the variogram function.

Experimental Variogram

A lag value of 850 m and a lag count of 6 were selected as input values to the omnidirectional experimental variogram of the natural log of hydraulic conductivity (Figure 34). The number of data pairs for each lag interval ranged from 42 to 444.

Variogram Model—Isotropic

An isotropic model was fitted to the omnidirectional experimental variogram (Figure 34). The final isotropic model of the experimental variogram was configured with a nugget and one spherical structure.

For the omnidirectional variogram model, the nugget was 0.075 and the sill was 0.405, with a nugget-to-sill ratio of 0.18. The range was 5,503.24 m.

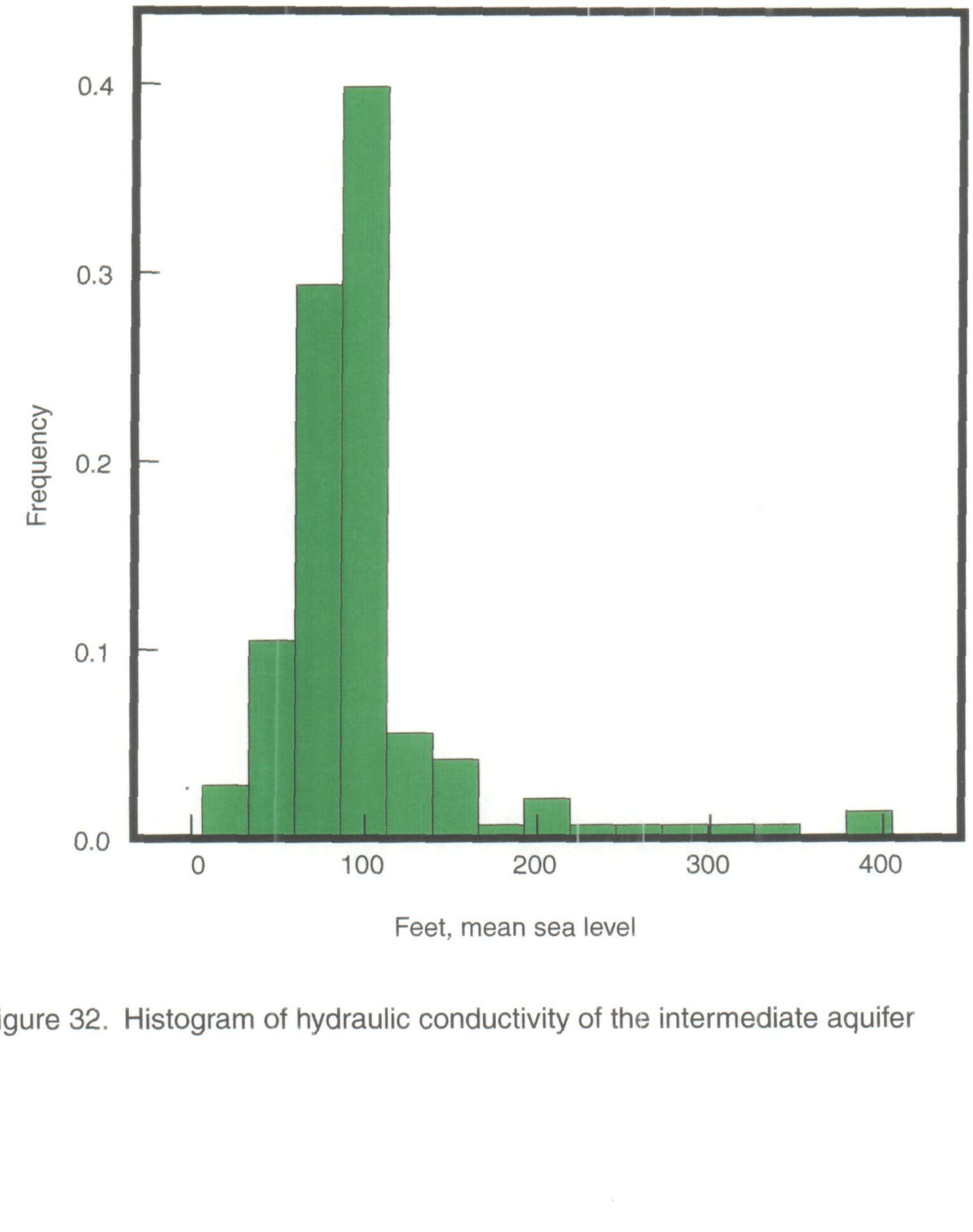

Figure 32. Histogram of hydraulic conductivity of the intermediate aquifer

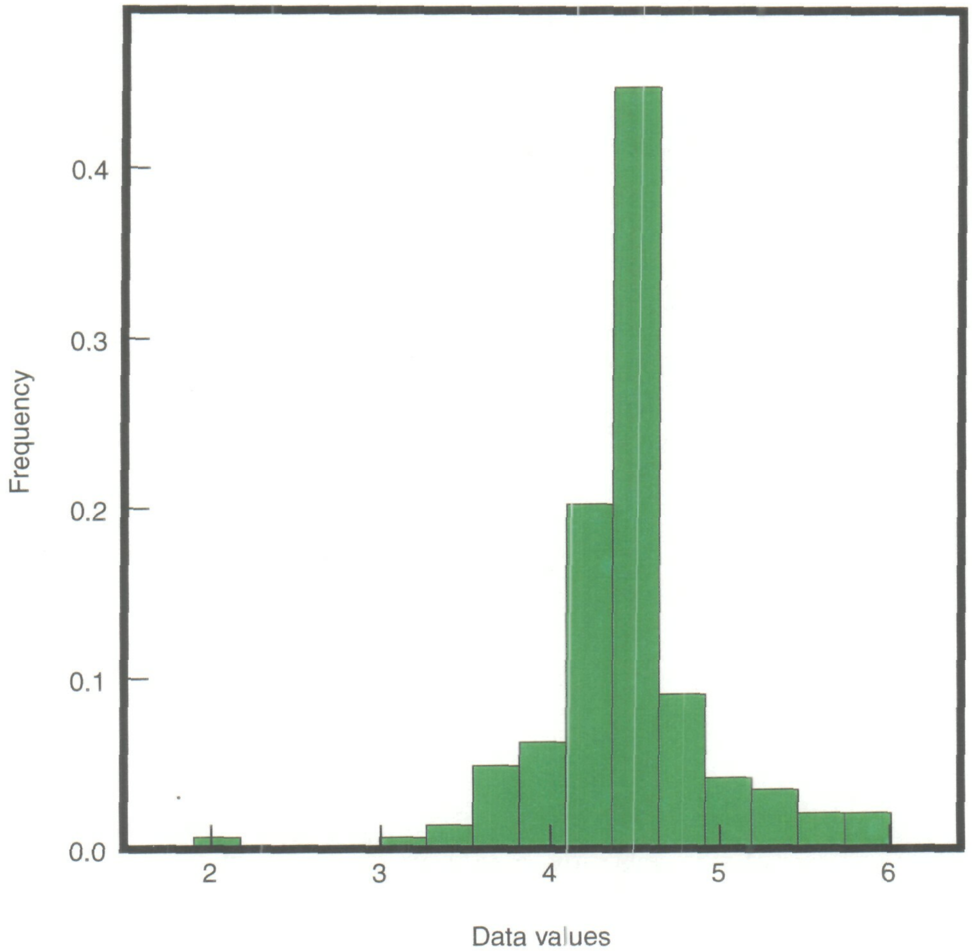

Figure 33. Histogram of the natural log of hydraulic conductivity

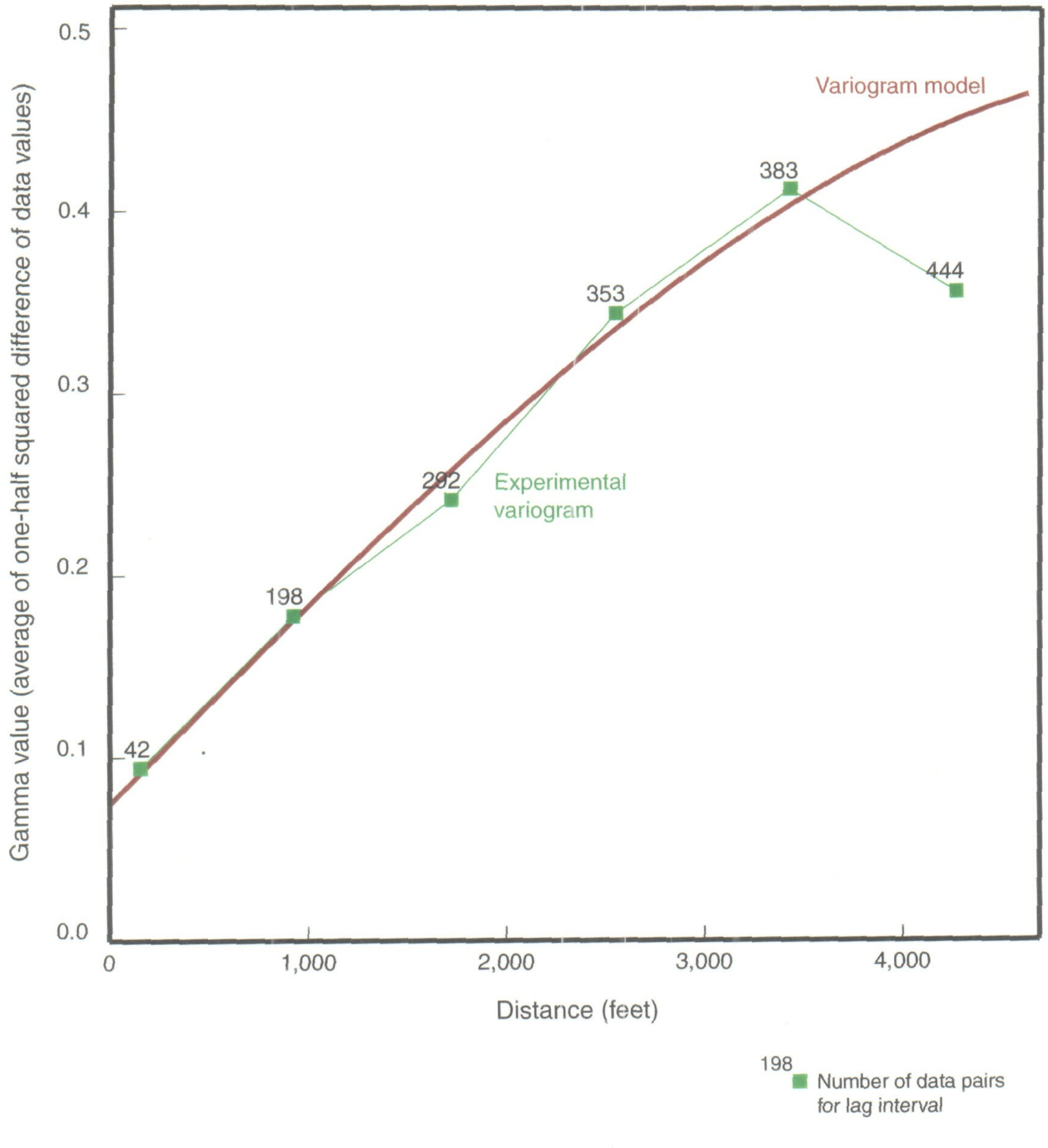

Figure 34. Isotropic (omnidirectional) variogram model of the natural log of hydraulic conductivity

Variogram Map

A variogram map was used to determine if the spatial correlation structure of the data is dependent upon direction (Figure 35). For the natural log of hydraulic conductivity, the variogram map did not suggest any anisotropy. Therefore, an isotropic model was used for cross-validation and estimation procedures.

Neighborhood

A circular search neighborhood was selected. The radius of the neighborhood was set at 3,500 m, a distance beyond which the variogram model is invalid. The minimum number of samples used in the calculation for each neighborhood was one, and the maximum number was ten.

Cross-validation

A base map showing the standardized estimation errors, a histogram of the standardized estimation errors, a scatter diagram of the true data value (Z on the y axis) versus the estimated value (Z^* on the x axis), and a scatter diagram of the standardized estimation error versus the estimated value were used to display the cross-validation results (Figure 36). Based on the distribution of the standardized estimation error, the data were spatially unbiased. The normally distributed histogram of the standardized estimation errors supports the assumption that the natural log of hydraulic conductivity data approximated a normal distribution as well as the validity of the variogram model that was used. Based on the scatter diagrams, the data were numerically unbiased.

The cross-validation procedure for natural log of hydraulic conductivity resulted in only seven nonrobust data points. So few nonrobust data points imply that the estimates for the natural log of hydraulic conductivity were reliable.

Estimation

Simulation was used to estimate the natural log of hydraulic conductivity on the nodes of the estimation grid. Each grid cell represents a distance of 50 by 50 m on the earth's surface. To encompass the entire Palm Coast study area, the grid had 660 nodes extending in an east-west direction and 794 nodes extending in a north-south direction. Fifty simulations were performed.

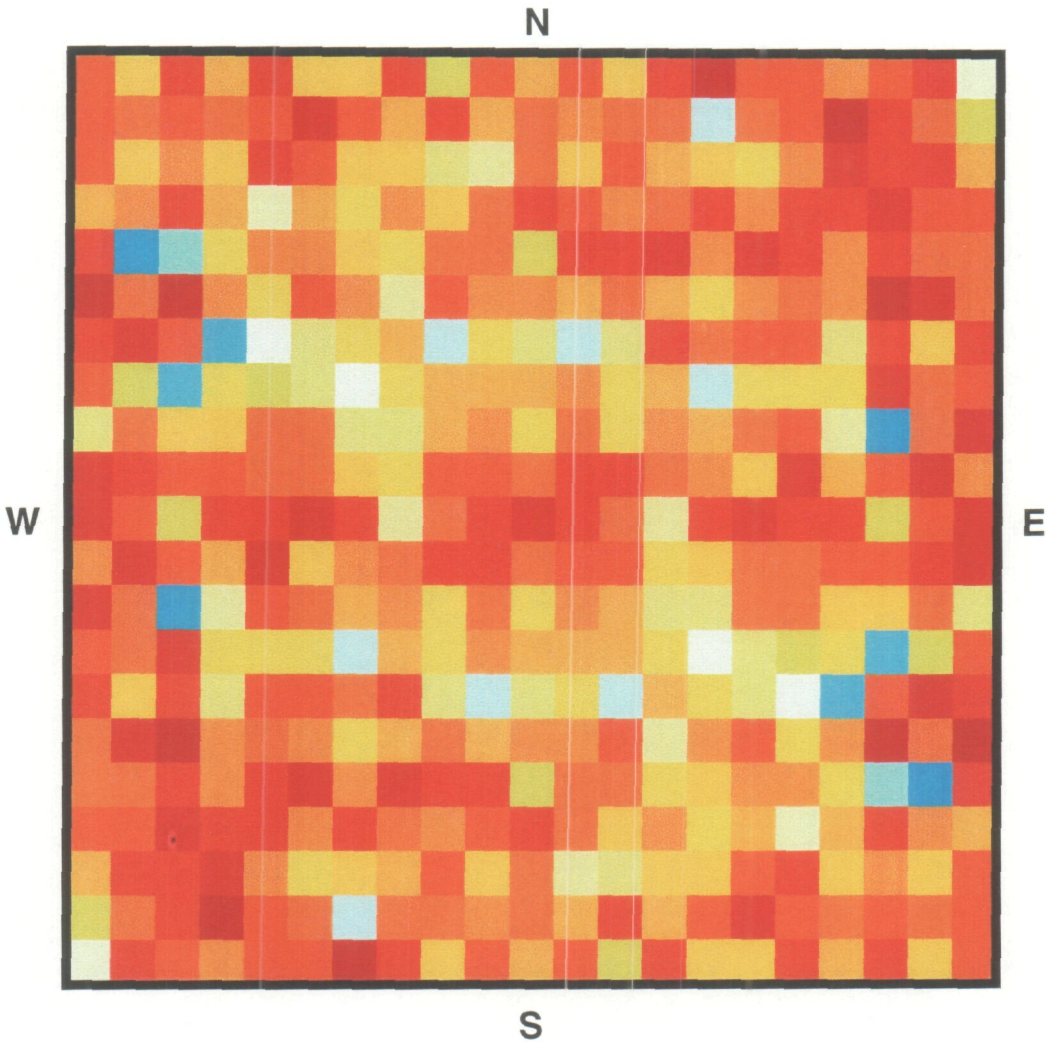

Figure 35. Variogram map of the natural log of hydraulic conductivity. *Lack of alignment of the colors suggests that there is no anisotropy.*

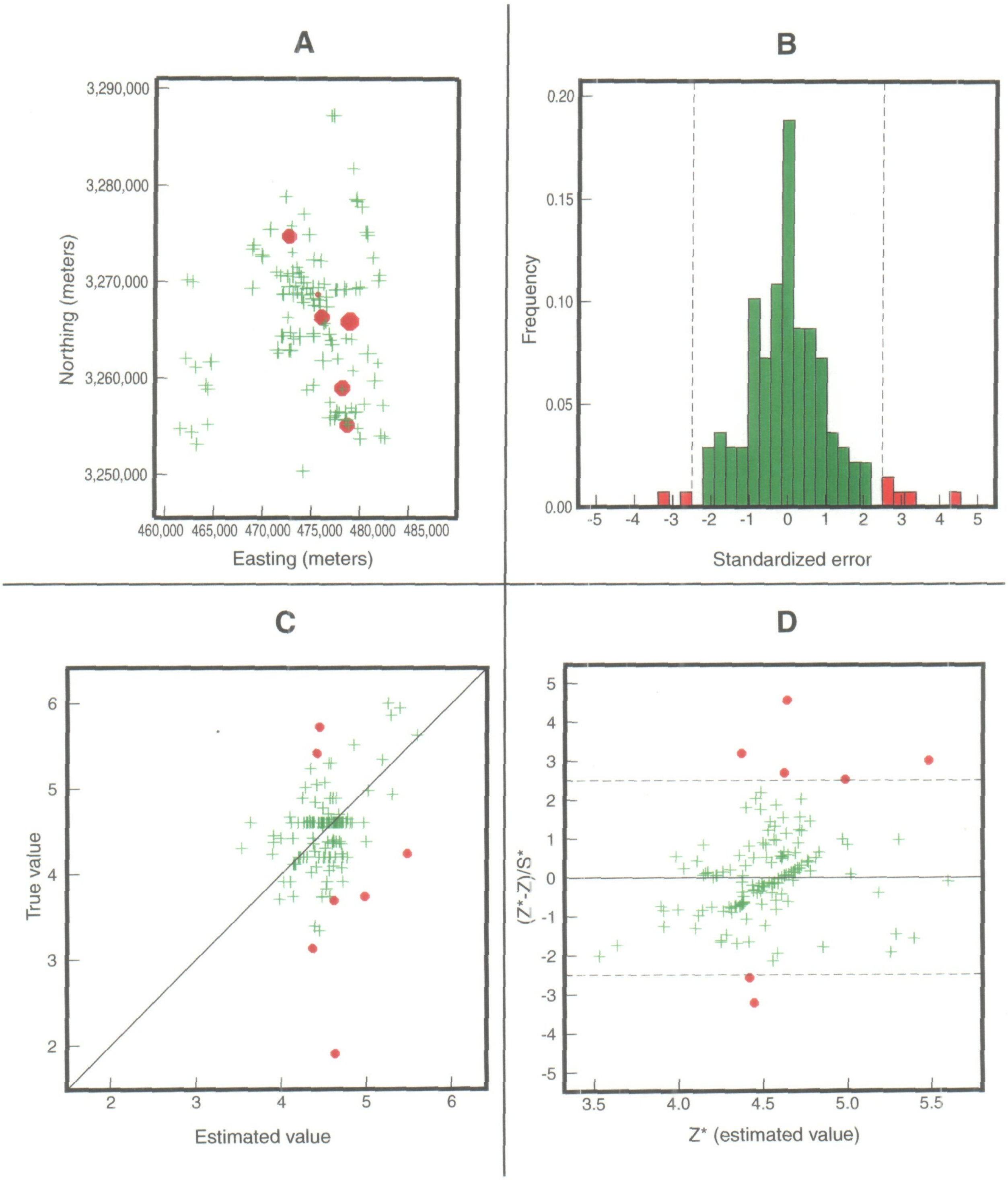

Figure 36. (A) Base map, (B) histogram, and (C, D) scatter diagrams for the cross-validation procedure for the natural log of hydraulic conductivity. *Red denotes nonrobust data; green denotes data values where the standardized error lies between –2.5 and +2.5.*

One contour map of the natural log of hydraulic conductivity produced by simulation is shown in Figure 37. This map portrays the natural log of hydraulic conductivity in the Palm Coast study area. Generally, the natural log of hydraulic conductivity decreases to the west. Well locations are superimposed on the map to indicate where the data values are located. There was insufficient data to completely fill the model area. White areas on the map indicate where data are missing.

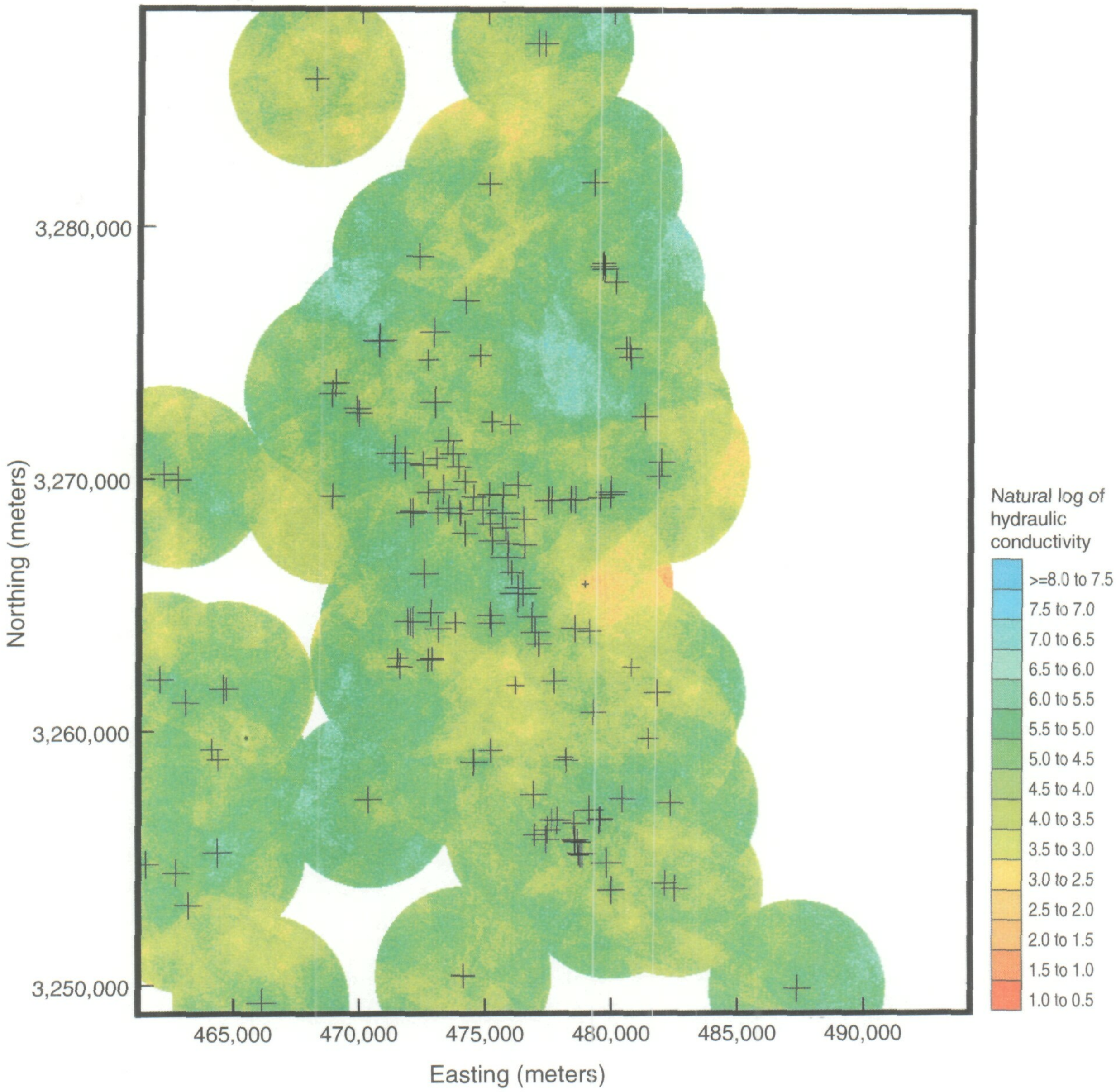

Figure 37. Simulation of the natural log of hydraulic conductivity

LAND SURFACE ELEVATION

Land surface elevation data were taken from the U.S. Geological Survey's topographic maps of the study area. Point elevations were devolved every 200 m from the vertices of the digitized contour lines. The elevations for the 143 wells were also added to the elevation file; the resulting file contained 17,143 records. The minimum land surface elevation is 4 ft msl and the maximum elevation is 55 ft msl. The mean and median elevations are 20.22 and 20 ft msl, respectively. The histogram plot of land surface elevation (Figure 38) approximates a bell shape, and the probability plot (Figure 39) lies close to a straight line. Both figures indicate the data approximate a normal distribution.

STRUCTURAL ANALYSIS OF THE DATA

A structural analysis was conducted to determine the spatial correlation of the investigated data. The process was accomplished through the computation and modeling of the variogram function.

Experimental Variogram

A lag value of 750 m and a lag count of 9 were selected as input values to the omnidirectional experimental variogram of land surface elevation (Figure 40). The number of data pairs for each lag interval were too numerous to show on Figure 40.

Variogram Model—Isotropic

An isotropic model was fitted to the omnidirectional experimental variogram (Figure 40). The final isotropic model of the experimental variogram was configured with a nugget and one spherical structure.

For the omnidirectional variogram model, the nugget was 20.47 and the sill was 26.08, with a nugget-to-sill ratio of 0.78. The range was 4,989.37 m.

Variogram Map

A variogram map was used to determine if the spatial correlation structure of the data is dependent upon direction (Figure 41). For land surface elevation, the variogram map suggested a strong anisotropy in a northwest-southeast direction.

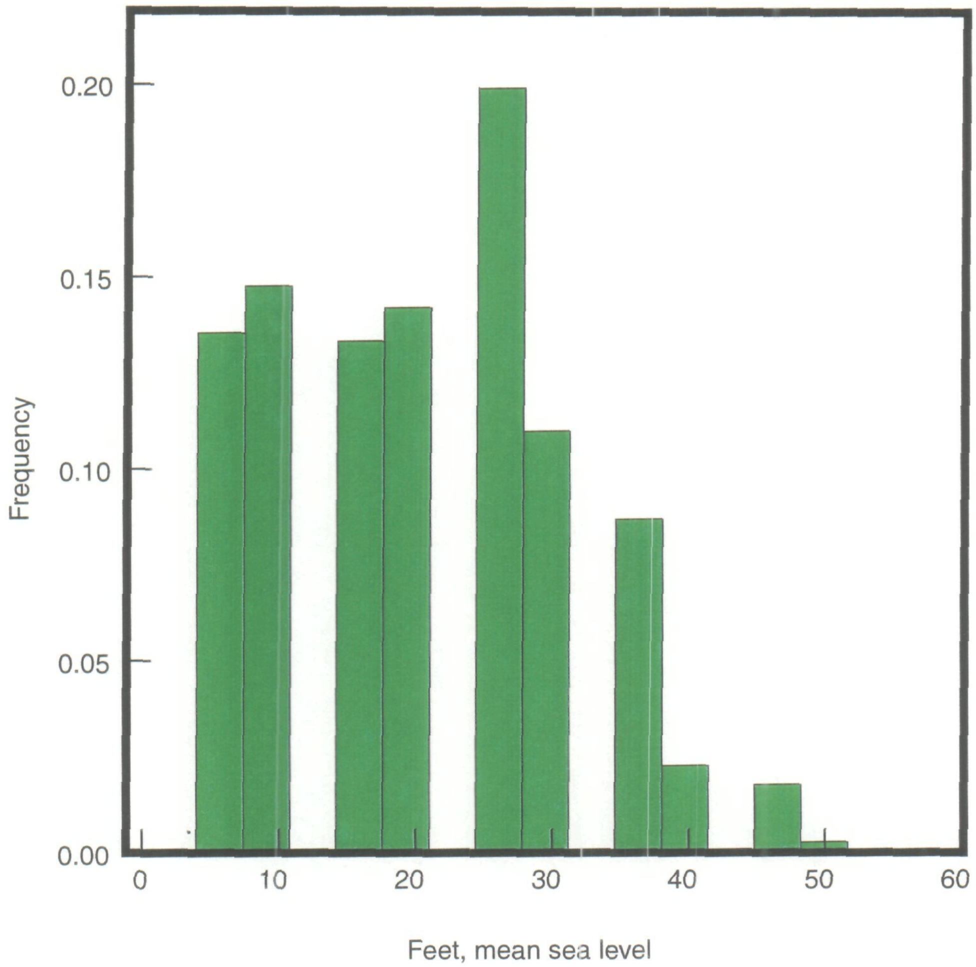

Figure 38. Histogram of land surface elevation

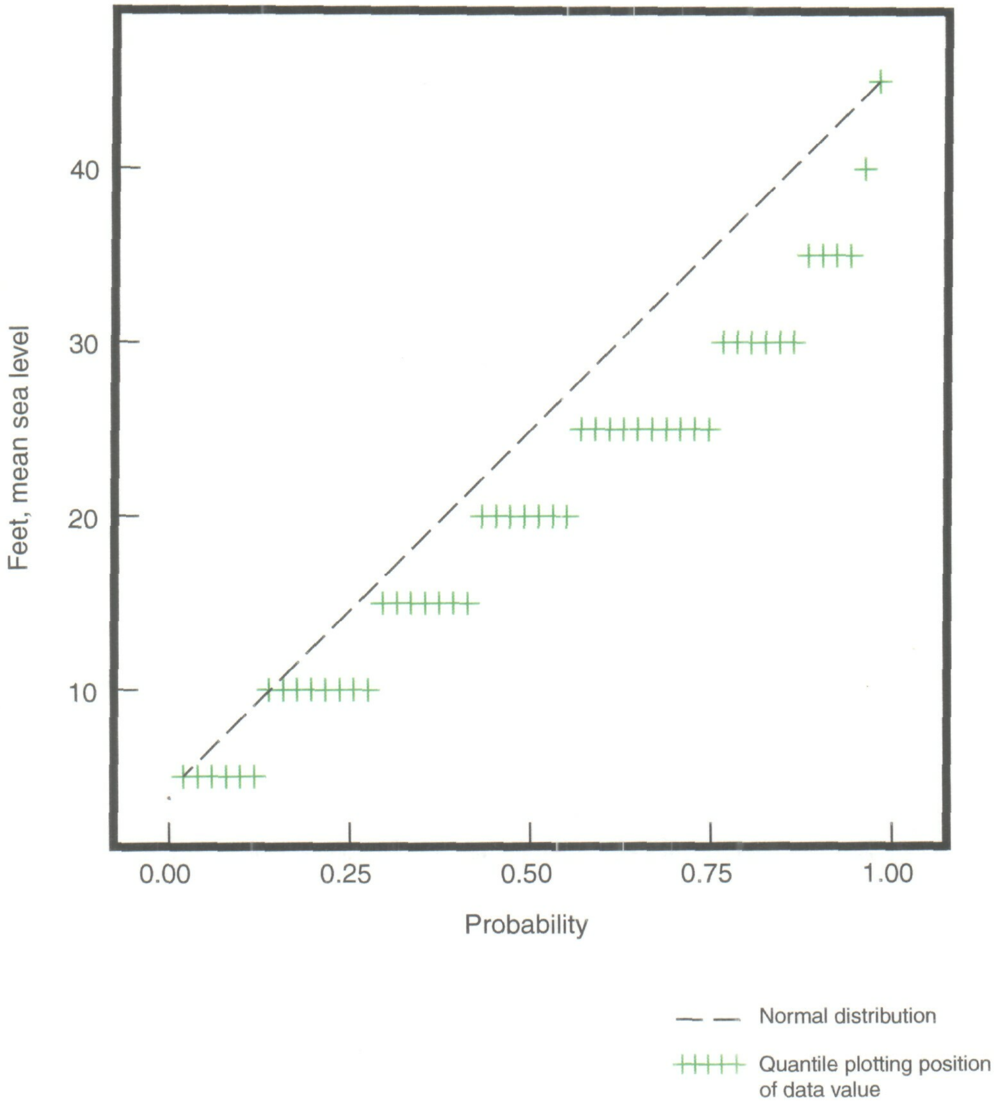

Figure 39. Probability plot of land surface elevation

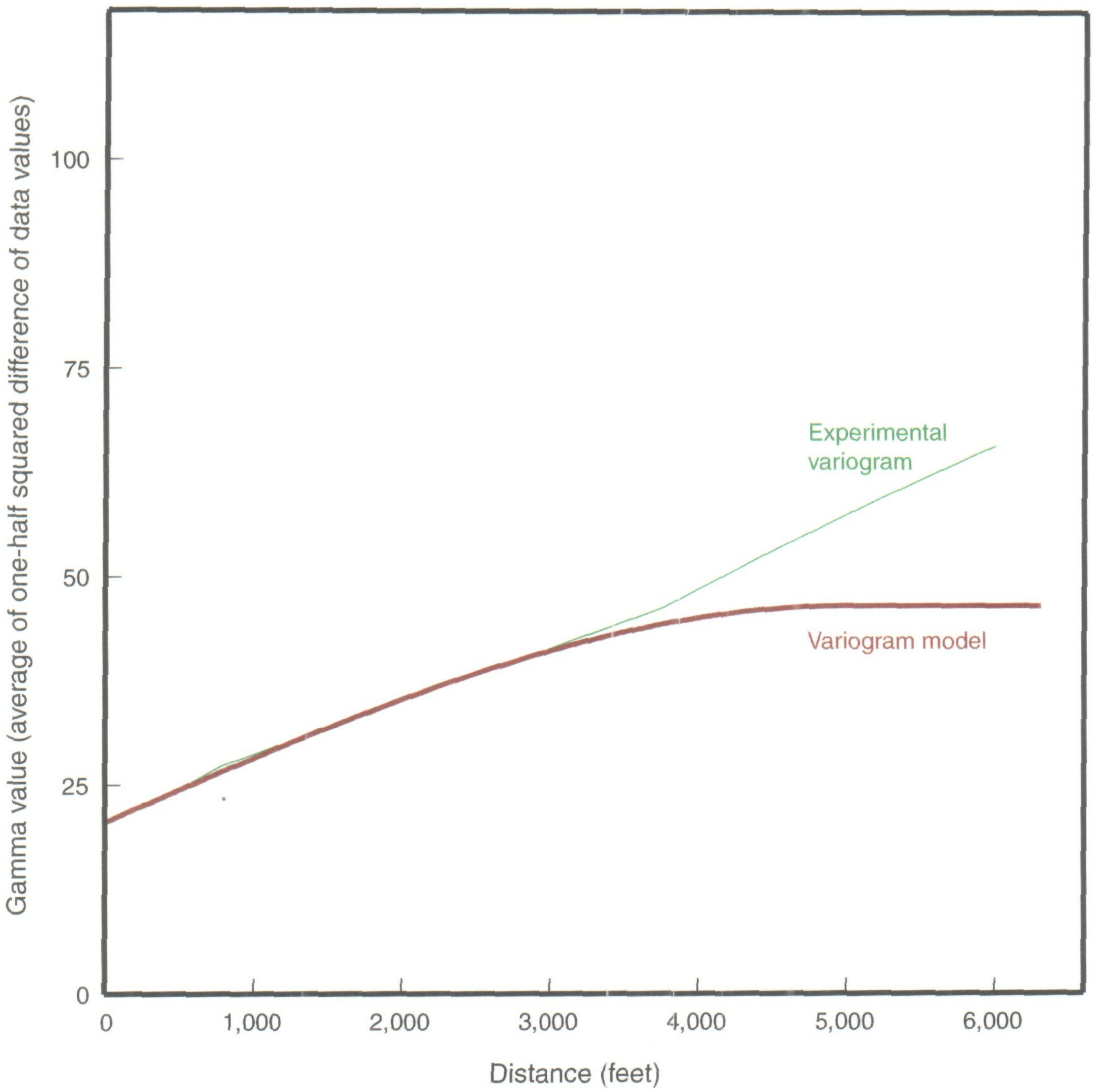

Figure 40. Isotropic (omnidirectional) variogram model of land surface elevation

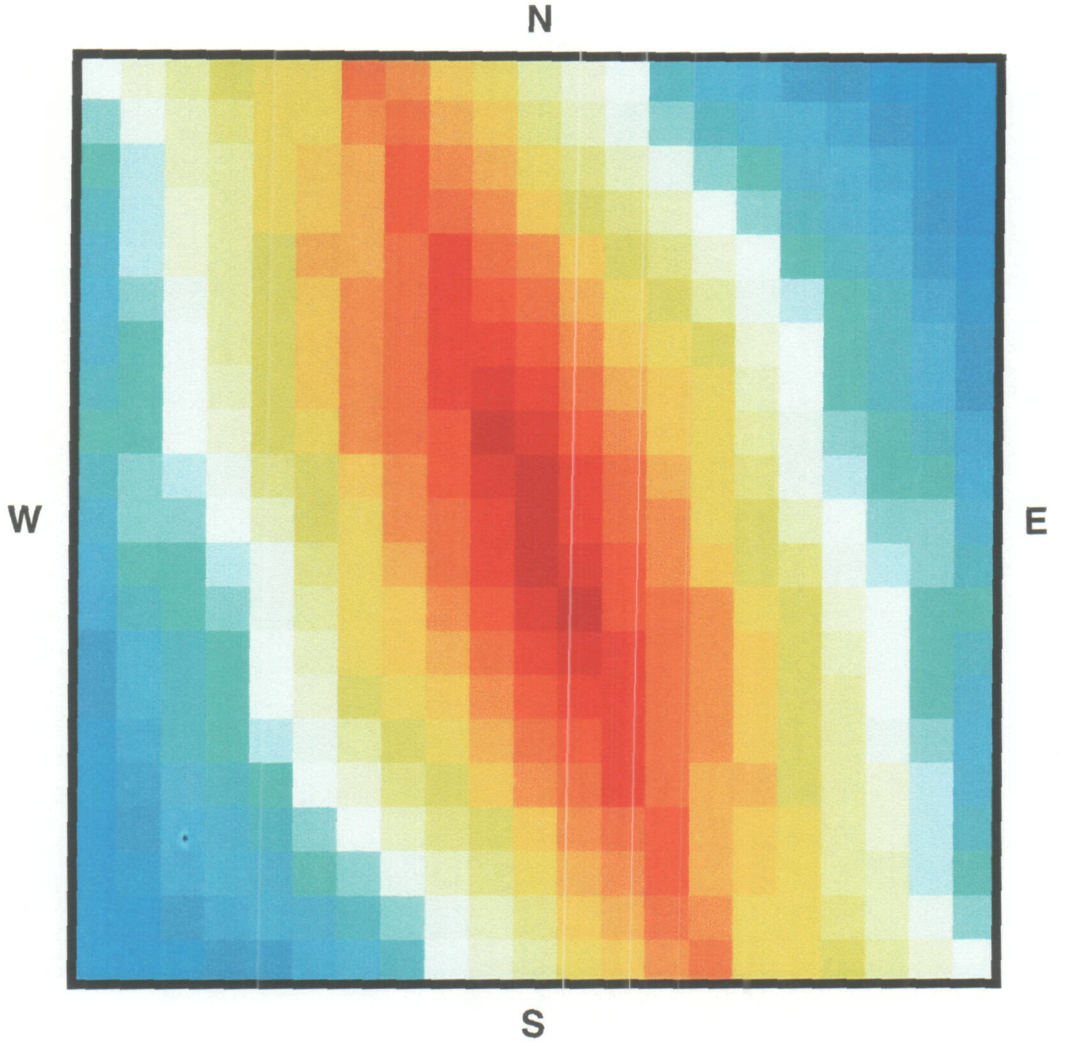

Figure 41. Variogram map of land surface elevation. *Alignment of colors indicates a strong anisotropy in a northwest-southeast direction.*

Variogram Model—Anisotropic

Based on the results of the variogram map, an anisotropic model was fitted to an anisotropic experimental variogram (Figure 42). The anisotropic model consists of two directions perpendicular to one another. The number of data pairs for each lag interval of the anisotropic experimental variogram were too numerous to show on Figure 42.

The lag value and the number of lags used in the isotropic variogram model were also used for the anisotropic variogram model. In addition, nugget, sill, azimuth (i.e., direction of trend), and range values were used as parameters for the anisotropic model (Table 4).

An anisotropic variogram model was used for cross-validation and estimation procedures.

Neighborhood

A circular search neighborhood was selected. The radius of the neighborhood was set at 2,500 m, a distance near where the variograms in the anisotropic variogram model diverge. The minimum number of samples used in the calculation for each neighborhood was one, and the maximum number was ten.

Cross-validation

A base map showing the standardized estimation errors, a histogram of the standardized estimation errors, a scatter diagram of the true data value (Z on the y axis) versus the estimated value (Z^* on the x axis), and a scatter diagram of the standardized estimation error versus the estimated value were used to display the cross-validation results (Figure 43). Based on the distribution of the standardized estimation error, the data were spatially unbiased. The normally distributed histogram of the standardized estimation errors supports the assumption that the elevation data approximated a normal distribution as well as the validity of the variogram model that was used. Based on the scatter diagrams, the data were numerically unbiased.

The cross-validation procedure for land surface elevation resulted in more than 32 nonrobust data points. So few nonrobust data points out of a total of 17,143 imply that the estimates for the land surface elevation were reliable.

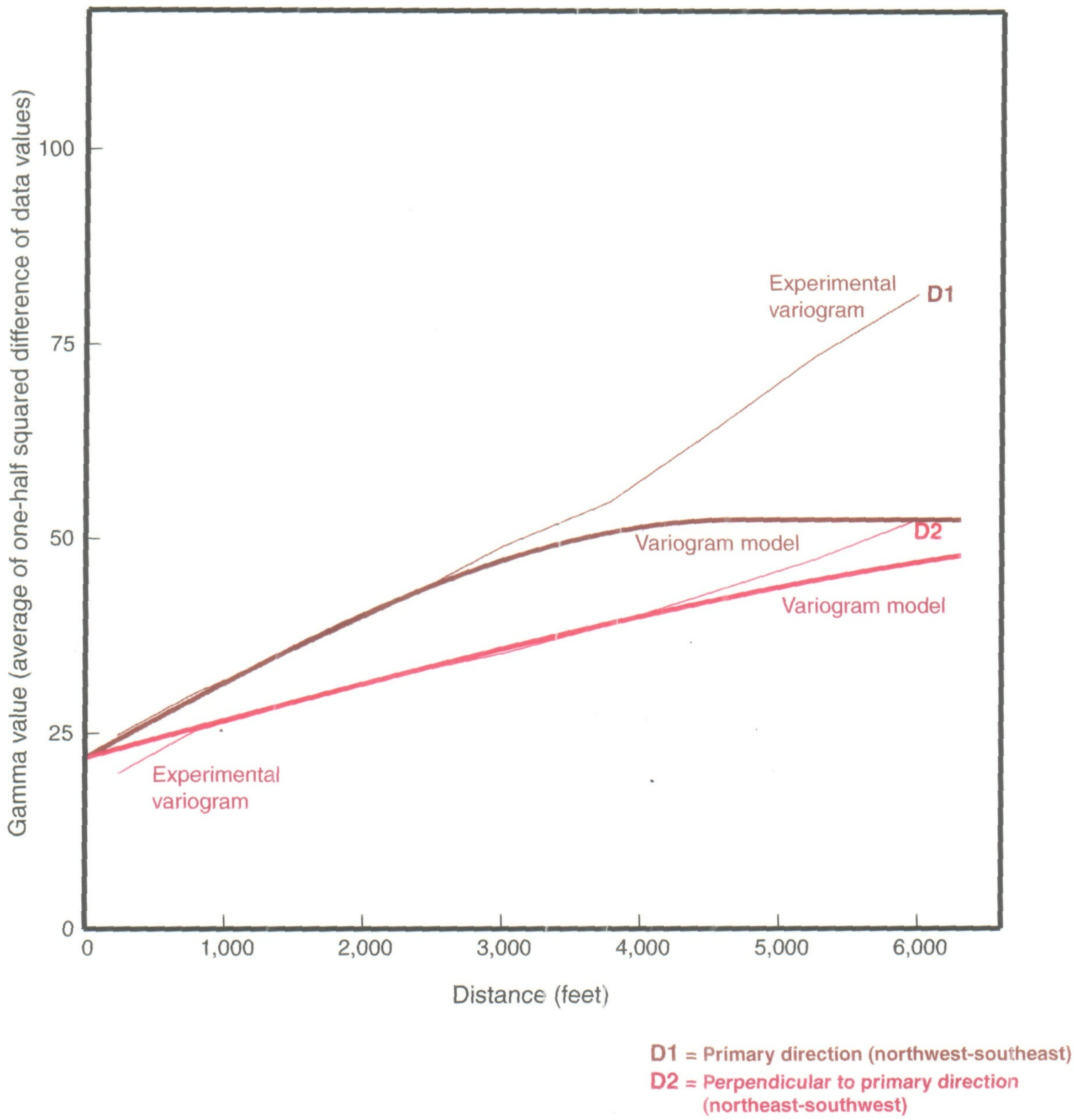

Figure 42. Anisotropic (directional) variogram model of land surface elevation

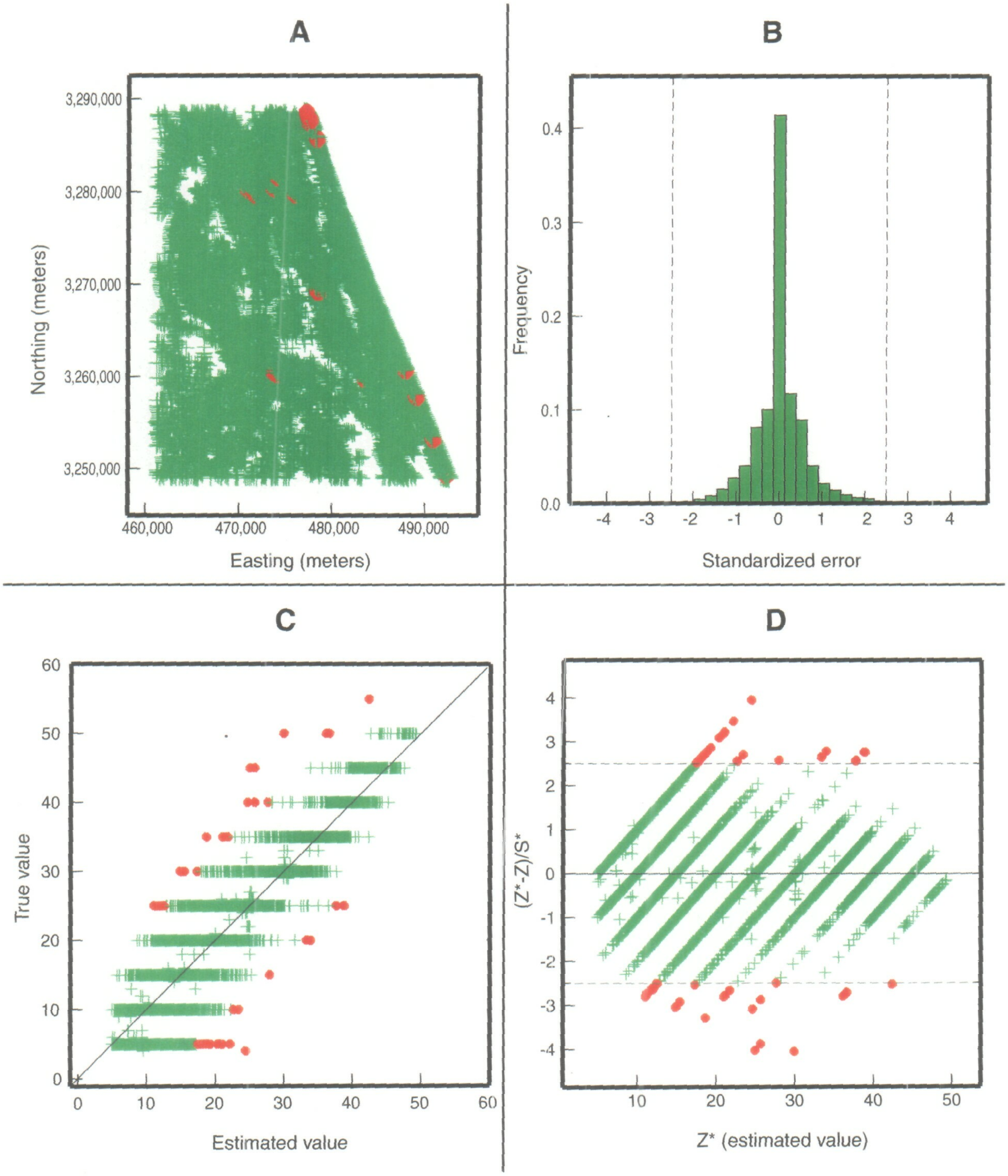

Figure 43. (A) Base map, (B) histogram, and (C, D) scatter diagrams for the cross-validation procedure for land surface elevation. *Red denotes nonrobust data; green denotes data values where standardized error lies between –2.5 and +2.5.*

Table 4. Parameters for the anisotropic variogram model of land surface elevation

Parameter	Numerical Value
Lag value	750 meters
Number of lags	9
Spherical Structure	
Azimuth	−120 degrees (northwest-southeast direction)
Range, principal direction	4,700 meters
Range, secondary direction	9,500 meters
Sill	30.66
Nugget Structure	
Sill	21.85

Estimation

Point kriging was used to estimate land surface elevation on the nodes of the estimation grid. Each grid cell represents a distance of 50 by 50 m on the earth's surface. To encompass the entire Palm Coast study area, the grid had 660 nodes extending in an east-west direction and 794 nodes extending in a north-south direction.

A contour map of land surface elevation was produced using kriging (Figure 44). This map portrays the land surface elevation in the Palm Coast study area. Generally, land surface elevation increases to the west.

A map of the relative standard deviations of the elevation data (Figure 45) depicts the relative accuracy of the estimated values. The estimated values for land surface elevation are least accurate along the coast.

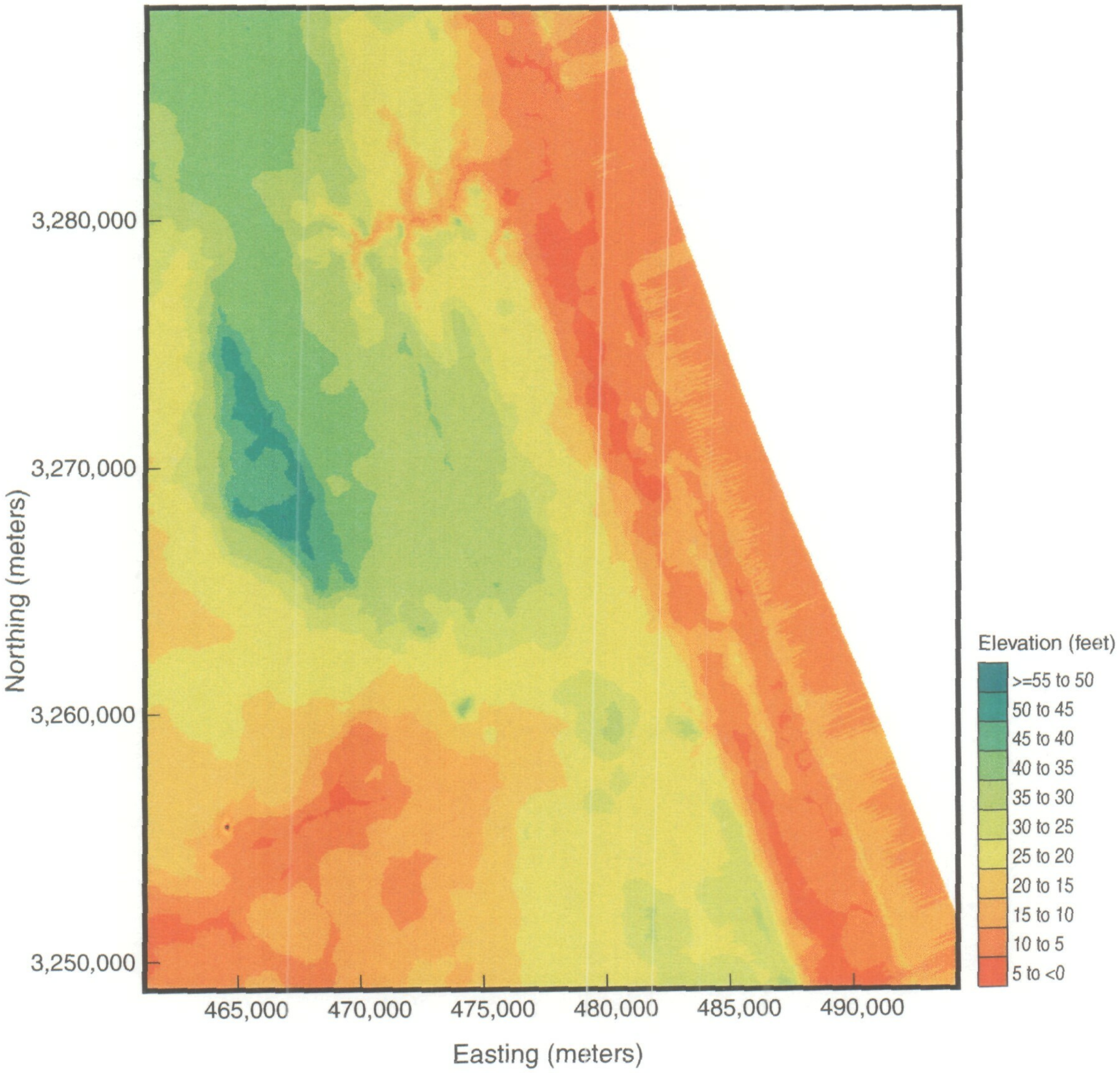

Figure 44. Land surface elevation in the study area

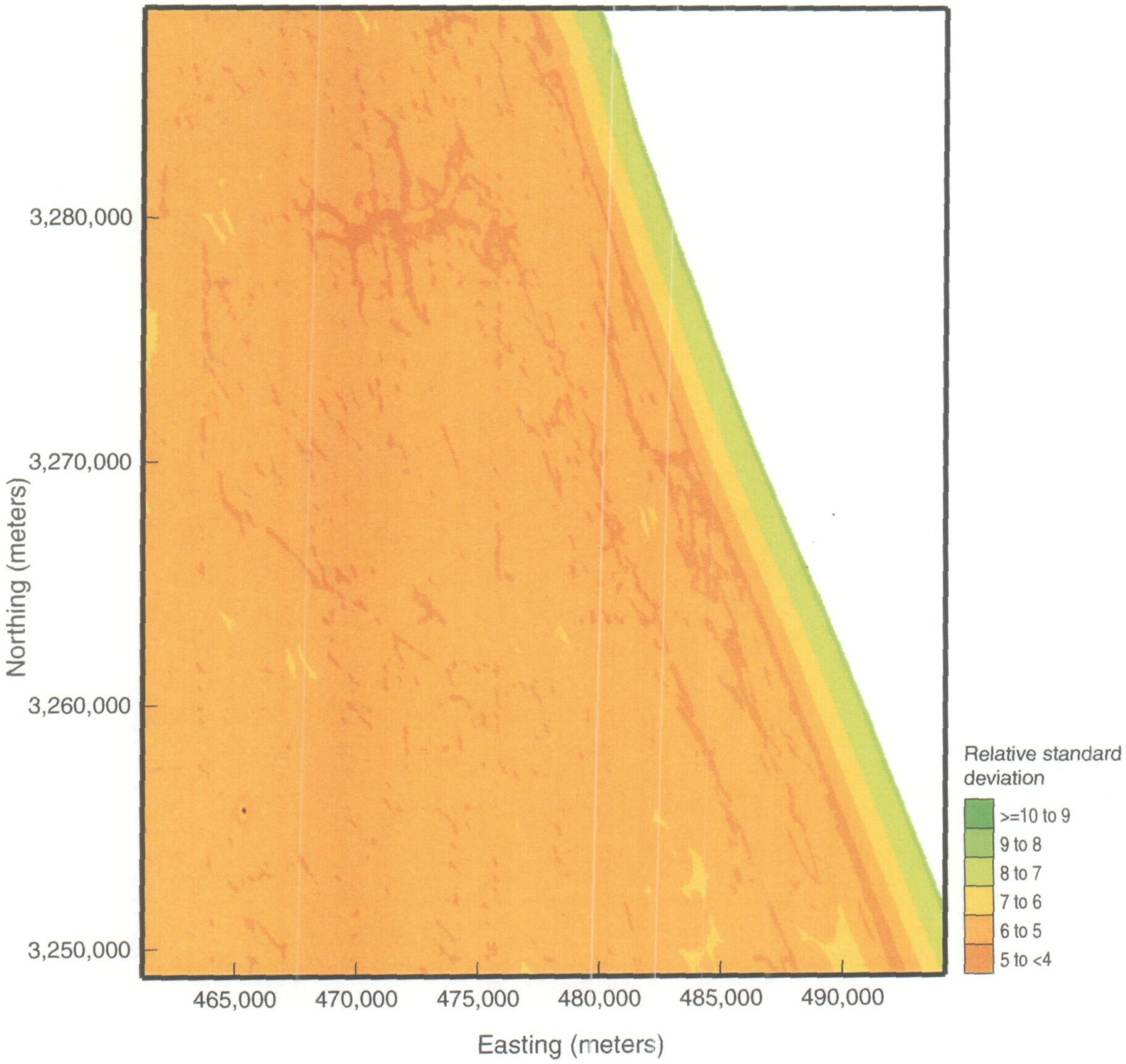

Figure 45. Relative standard deviations of land surface elevation

CONCLUSION

The elevation of the top of the intermediate aquifer, the elevation of the bottom of the intermediate aquifer, the elevation of the top of the confining unit, and the land surface elevation data approximate a normal distribution; each elevation surface was estimated by kriging. The leakance for the confining unit for the intermediate aquifer was multiplied by 10^5, and the natural log of its distribution was simulated. The hydraulic conductivity of the intermediate aquifer was also log-transformed, and the distribution of its natural logarithm was simulated. Output files of these parameters were generated for input into MODFLOW. The proposed MODFLOW model will determine the effects, if any, of groundwater withdrawals on wetlands and the groundwater flow system in the vicinity of Palm Coast, Florida.

REFERENCES

[ASTM] American Society for Testing and Materials. 1994. *Standard guide for content of geostatistical site investigations*. D 5549-94. Philadelphia, Pa.

———. 1996a. *Standard guide for analysis of spatial variation in geostatistical site investigations*. D 5922-96. Philadelphia, Pa.

———. 1996b. *Standard guide for selection of kriging methods in geostatistical site investigations*. D 5523-96. Philadelphia, Pa.

Chu, J., W. Xu, and A.G. Journel. 1994. *Stochastic modeling and geostatistics: Principles, methods, and case studies*. Chapter 16: 3-D implementation of geostatistical analysis—The Amoco case study. J.M. Yarus and R.F. Chambers, eds. Tulsa, Okla.: American Association of Petroleum Geologists.

Englund, E., and A. Sparks. 1988. *GEO-EAS (Geostatistical Environmental Assessment Software) user's guide*. EPA600/4-88/033. Environmental Monitoring Systems Laboratory. Las Vegas, Nev.: U.S. Environmental Protection Agency.

Geovariances. 1997. *ISATIS: The geostatistical key: User's guide*. Avon, France.

Navoy, A.S., and L.A. Bradner. 1987. *Ground-water resources of Flagler County, Florida*. Water-Resources Investigations Report 87-4021. Tallahassee, Fla.: U.S. Geological Survey.

Olea, R.A. 1991. *Geostatistical glossary and multilingual dictionary*. New York: Oxford University Press.

U.S. Environmental Protection Agency. 1990. *Guidance for data usability in risk assessment*. EPA/540/G-90/008. Office of Emergency and Remedial Response. Washington, D.C.

APPENDIX A—GEOHYDROLOGIC DATA IN THE STUDY AREA

Well construction and aquifer properties data for Florida Water Services, July 15, 1999

Well Identification	Well Location		Well Site Elevation* (ft msl)	Elevation, Top of Aquifer (ft msl)	Elevation, Bottom of Aquifer (ft msl)	Production Zone Thickness† (feet)	Elevation, Top of Confining Bed (feet)	Confining Bed Thickness (feet)	Transmissivity (ft^2/day)	Hydraulic Conductivity (ft/day)	Leakance day^{-1}
	Latitude	Longitude									
SW-3	293332	811442	29	-32	-53	21	-22	10	2,000	95.2	4.00E-05
SW-4	293313.3	811503.6	29	-31	-55	24	-26	5	1,957	81.5	4.00E-04
SW-5	293250.1	811504.2	30	-30	-51	21	-18	12	4,709	224.2	4.00E-04
SW-6	293313.9	811524.3	33	-16	-36	20	-1	15	1,330	66.5	4.00E+04
SW-7	293310.8	811547.6	33	-22	-48	26	-12	10	2,030	78.1	4.00E-04
SW-8	293231.4	811459.6	33	-16	-31	15	-6	10	1,000	66.7	4.00E-05
SW-11	292932	811453	25	-37	-47	10	-28	9	283	28.3	2.00E-04
SW-13	293242.6	811433	32	-10	-35	25	-10	0	2,000	80.0	4.00E-05
SW-14	293209.7	811431.6	33	-22	-37	15	-10	12	1,000	66.7	4.00E-05
SW-17	293249.8	811606.2	30	-10	-42	32	0	10	1,340	41.9	2.00E-04
SW-21	292908	811444	25	-35	-70	35	-35	0	1,040	29.7	1.90E-04
SW-24	293017	811415	25	5	-55	60	5	0	8,000	133.3	1.70E-04
SW-25	293037	811420	25	0	-55	55	0	0	8,000	145.5	1.70E-04
SW-27	293133.8	811450.2	30	-15	-55	40	-15	0	2,770	69.3	1.20E-04
SW-28	293210.8	811456.5	35	-25	-65	40	-15	10	2,770	69.3	1.20E-04
SW-29	293214.5	811519.5	30	-25	-50	25	-15	10	2,770	110.8	1.20E-04
SW-30	293236.9	811522.9	30	-30	-50	20	-25	5	1,560	78.0	3.30E-04
SW-31	293153	811455.8	30	-23	-44	21	-18	5	6,411	305.3	2.80E-04
SW-32	293254.2	811533.5	30	-43	-53	10	-40	3	1,560	156.0	3.30E-04
SW-33	293330.5	811600.4	30	-10	-70	60	-10	0	3,570	59.5	4.30E-05
SW-34	293349.4	811609.5	30	-30	-80	50	-20	10	3,570	71.4	4.30E-05
SW-35	293405.9	811617.6	30	-30	-65	35	-20	10	3,570	102.0	4.30E-05
SW-36	293422.7	811625.7	35	-25	-55	30	-13	12	3,570	119.0	4.30E-05
SW-39	293119.6	811302.1	25	-5	-35	30	-2	3	202	6.7	2.00E-04
SW-40	293107	811441	30	-25	-40	15	-25	0	6,072	404.8	2.80E-04
SW-43	293607	811656	35	5	-80	85	5	0	3,570	42.0	4.30E-05
SW-51	293029	811520	25	-32	-42	10	-20	12	1,040	104.0	1.90E-04
SW-52	293022	811317	25	-40	-65	25	-30	10	2,678	107.1	1.90E-04
SW-55	293002.3	811410	25	-25	-35	10	-18	7	785	78.5	2.00E-04
SW-58	293223.9	811559.9	31	-19	-49	30	-9	10	2,500	83.3	3.00E-04
SW-59	293249.8	811607	31	-19	-49	30	-19	0	2,500	83.3	3.00E-04
SW-60	293250.5	811639.9	30	-38	-65	27	-18	20	2,000	74.1	3.0E-04
SW-61	293316.6	811654.2	31	-10	-44	34	0	10	2,000	58.8	3.0E-04
SW-62	293352	811702	31	-29	-49	20	-9	20	2,200	110.0	4.0E-05
SW-65	292914	811347	25	-43	-48	5	-36	7	415	83.0	2.00E-04
SW-74	292833.9	811249.3	30	-20	-30	10	-20	0	793	79.3	1.60E-04
SW-77	292800.2	811127.7	25	-23	-43	20	-17	6	920	46.0	1.60E-04
SW-81	293447.9	811521.2	30	-25	-48	23	-16	9	971	42.2	3.60E-04
SW-82	292637.2	811054.9	25	-25	-35	10	-5	20	1,000	100.0	3.00E-04
SW-83	293114	811434	30	-25	-45	20	-25	0	7,020	351.0	2.8E-04
SW-84	293019	811255	25	-48	-65	17	-38	10	1,175	69.1	1.9E-04
SW-85	293512.6	811644.4	35	-42	-62	20	-31	11	3,751	187.6	1.00E-03

Well Identification	Well Location		Well Site Elevation* (ft msl)	Elevation, Top of Aquifer (ft msl)	Elevation, Bottom of Aquifer (ft msl)	Production Zone Thickness† (feet)	Elevation, Top of Confining Bed (feet)	Confining Bed Thickness (feet)	Transmissivity (ft^2/day)	Hydraulic Conductivity (ft/day)	Leakance day^{-1}
	Latitude	Longitude									
SW-86	293613	811539	30	-35	-45	10	-15	20	557	55.7	3.60E-04
SW-87	293643	811647	25	-38	-48	10	-18	20	1,505	150.5	1.00E-03
SW-89	293820.5	811709.6	20	-42	-52	10	-31	11	1,046	104.6	1.00E-03
SW-90	293631	811808	30	-43	-63	20	17	60	2,790	139.5	1.0E-03
SW-91	293406.5	811743.9	30	-32	-52	20	-32	0	7,638	381.9	1.00E-04
SW-92	293631.7	811807.3	30	-45	-60	15	10	55	3,726	248.4	1.00E-03
SW-93	292735.4	811329.7	20	-53	-63	10	-35	18	229	22.9	1.60E-04
SW-94	292628	811255	25	-40	-48	8	-32	8	1,016	127.0	1.60E-04
SW-95	292732	811329	30	-23	-43	20	-6	17	1,480	74.0	1.6E-04
SW-96	293444	811454	30	-30	-50	20	-22	8	813	40.7	3.6E-04
SW-105	293256.2	811623.8	30	-40	-60	20	-28	12	2,000	100.0	3.0E-04
SW-106	293320.2	811632	31	-44	-59	15	-39	5	2,000	133.3	3.0E-04
SW-107	293400.5	811642.1	33	-7	-51	44	3	10	2,200	50.0	4.0E-05
SW-114	293353.9	811728.6	30	-10	-50	40	0	10	8,356	208.9	1.0E-04
SW-115	293406.3	811743.8	30	-30	-60	30	-20	10	8,356	278.5	1.0E-04
LW-1	293258	811716.2	31	-29	-49	20	1	30	2,000	100.0	3.0E-04
LW-2	293036	811722.7	29	-31	-51	20	-11	20	2,000	100.0	3.0E-04
LW-3	293510	811840	35	-25	-45	20	-5	20	2,000	100.0	3.0E-04
LW-4a‡	293036.2	811715.6	29	-31	-36	5	-11	20	1,000	200.0	3.0E-04
LW-4	293036	811719	35	-25	-45	20	-25	0	2,000	100.0	2.0E-04
LW-5	292948.8	811737.9	30	-30	-49	19	-20	10	800	42.1	3.6E-04
LW-6	292947	811647.2	25	-35	-48	13	-25	10	800	61.5	3.6E-04
LW-6a	292946.9	811653.1	25	-35	-48	13	-25	10	800	61.5	3.6E-04
LW-7	293138.1	811659.2	30	-30	-45	15	-10	20	2,000	133.3	3.00E-04
LW-8	293317	811915.5	25	-10	-60	50	-10	0	4,000	80.0	4.00E-05
LW-10	293323.4	811224.5	25	10	0	10	10	0	2,000	200.0	4.00E-05
LW-11	293313.4	811323.3	20	-20	-50	30	-20	0	3,000	100.0	4.00E-05
LW-12	293312.1	811356.2	25	-5	-15	10	-5	0	1,000	100.0	4.00E-05
LW-13	293316	811240	20	-20	-40	20	-10	10	2,000	100.0	4.00E-05
LW-14	292617	811317	25	-50	-85	35	-40	10	2,000	57.1	2.00E-04
LW-15	292450.9	811221.2	25	-35	-55	20	-30	5	2,000	100.0	3.00E-04
LW-15a	292451.4	811221.7	25	-35	-55	20	-30	5	2,000	100.0	3.00E-04
LW-16	292453.1	811048.3	25	-20	-40	20	-10	10	2,000	100.0	3.00E-04
LW-17	292500	811103	25	-10	-60	50	-10	0	4,000	80.0	4.00E-05
LW-20	293542.4	811911.8	35	-25	-35	10	-15	10	1,000	100.0	4.00E-05
LW-21	292538.3	811307.5	25	-35	-55	20	-15	20	2,000	100.0	3.00E-04
LW-24	292938	811734	32	-18	-53	35	-18	0	3,000	85.7	4.00E-05
LW-25	293048	811649	30	-40	-70	30	-15	25	3,000	100.0	4.00E-05
LW-26	293027	811638	30	-30	-40	10	-20	10	1,000	100.0	4.00E-05
LW-27	293035	811613	30	-30	-49	19	-10	20	800	42.1	3.60E-04
LW-30	292620.1	811341.6	25	-35	-55	20	-15	20	2,000	100.0	3.00E-04
LW-31	292552.7	811311.4	25	-35	-55	20	-15	20	2,000	100.0	3.00E-04
LW-32	292620.5	811240.1	25	-35	-55	20	-15	20	2,000	100.0	3.00E-04

Well Identification	Well Location		Well Site Elevation* (ft msl)	Elevation, Top of Aquifer (ft msl)	Elevation, Bottom of Aquifer (ft msl)	Production Zone Thickness† (feet)	Elevation, Top of Confining Bed (feet)	Confining Bed Thickness (feet)	Transmissivity (ft^2/day)	Hydraulic Conductivity (ft/day)	Leakance day^{-1}
	Latitude	Longitude									
LW-38	293044.4	811521.6	30	-30	-50	20	-10	20	2,000	100.0	4.00E-05
LW-42	292653.8	811416.7	15	-35	-45	10	-25	10	1,000	100.0	4.00E-05
LW-51	292859	811803	25	-35	-48	13	-25	10	800	61.5	3.60E-04
LW-53	293723.4	811601	25	-15	-35	20	-5	10	2,000	100.0	4.00E-05
SJ0039	294300	811407	6	-44	-69	25	-34	10	2,000	80.0	4.00E-05
SJ0128	294000	811527	6	-19	-64	45	-19	0	3,000	66.7	4.00E-05
SJ0151	294300	811417	6	-44	-64	20	-39	5	2,000	100.0	3.00E-04
SJ0602	294213	811944	35	-5	-50	45	-5	0	3,000	66.7	4.00E-05
F-0005	292226	812056	11	-24	-44	20	-24	0	3,000	150.0	4.00E-05
F-0006	292431	812244	16	-54	-74	20	-44	10	2,000	100.0	4.00E-05
F-0007	292512	812303	18	-77	-87	10	-52	25	1,000	100.0	4.00E-05
F-0008	292648	811206	27	-48	-58	10	-28	20	1,000	100.0	4.00E-05
F-0010	292908	812150	24	-71	-86	15	-46	25	1,000	66.7	4.00E-05
F-0011	292908	812154	22	-63	-78	15	-38	25	2,000	133.3	4.00E-05
F-0012	292920	812327	20	-70	-100	30	-50	20	3,000	100.0	4.00E-05
F-0013	292301	811559	16	-39	-54	15	-29	10	1,000	66.7	4.00E-05
F-0014	293313	811357	26	-44	-74	30	-44	0	3,000	100.0	4.00E-05
F-0015	293314	811324	25	-35	-85	50	-35	0	3,000	60.0	4.00E-05
F-0016	293344	811114	9	-41	-91	50	-26	15	4,000	80.0	4.00E-05
F-0017	293402	811110	6	-29	-39	10	-14	15	1,000	100.0	4.00E-05
F-0019	293814	811239	7	-43	-53	10	-33	10	1,000	100.0	4.00E-05
F-0020	293818	811238	7	-8	-23	15	-8	0	1,000	66.7	4.00E-05
F-0021	294002	811252	6	-44	-54	10	-29	15	1,000	100.0	4.00E-05
F-0022	293811	811236	9	-36	-46	10	-21	15	1,000	100.0	4.00E-05
F-0023	293501	811135	4	-41	-61	20	-31	10	2,000	100.0	4.00E-05
F-0044	292750	812211	24	-46	-66	20	-21	25	1,000	50.0	4.00E-05
F-0066	292523	812347	20	-30	-40	10	-5	25	1,000	100.0	4.00E-05
F-0087	292750	811520	21	-44	-59	15	-19	25	1,000	66.7	4.00E-05
F-0101	292538	812202	14	-31	-46	15	-21	10	2,000	133.3	4.00E-05
F-0105	293314	811317	4	-51	-61	10	-26	25	1,000	100.0	4.00E-05
F-0106	293617	811156	10	-40	-55	15	-25	15	1,000	66.7	4.00E-05
F-0107	293628	811158	12	-38	-53	15	-23	15	1,000	66.7	4.00E-05
F-0126	292647	811820	12	-73	-83	10	-48	25	1,000	100.0	4.00E-05
F-0160	293504	811837	35	-40	-50	10	-15	25	1,000	100.0	4.00E-05
F-0161	293256	811720	31	-49	-64	15	-24	25	2,000	133.3	4.00E-05
F-0162A	293320	811225	13	-57	-77	20	-57	0	2,000	100.0	4.00E-05
F-0164	293313	811352	27	-28	-38	10	-18	10	1,000	100.0	4.00E-05
F-0165	293529	811917	33	-72	-82	10	-57	15	1,000	100.0	4.00E-05
F-0182	292737	812202	26	-29	-49	20	-14	15	1,000	50.0	4.00E-05
F-0200	293754	811219	7	-43	-58	15	-28	15	1,000	66.7	4.00E-05
F-0204	293337	812303	26	-34	-44	10	-9	25	1,000	100.0	4.00E-05
F-0206	292850	812250	25	-55	-65	10	-45	10	1,000	100.0	4.00E-05
F-0240	292302	811559	18	-37	-52	15	-27	10	1,000	66.7	4.00E-05

Well Identification	Well Location		Well Site Elevation* (ft msl)	Elevation, Top of Aquifer (ft msl)	Elevation, Bottom of Aquifer (ft msl)	Production Zone Thickness† (feet)	Elevation, Top of Confining Bed (feet)	Confining Bed Thickness (feet)	Transmissivity (ft^2/day)	Hydraulic Conductivity (ft/day)	Leakance day^{-1}
	Latitude	Longitude									
F-0242	293628	811203	13	-37	-52	15	-22	15	1,000	66.7	4.00E-05
F-0294	293344	812324	25	-55	-65	10	-45	10	1,000	100.0	4.00E-05
F-0308	292526	811229	25	-35	-40	5	-20	15	800	160.0	3.00E-05
F-0309	292608	811356	22	-38	-58	20	-38	0	2,000	100.0	4.00E-04
F-0310	292556	811358	22	-43	-63	20	-8	35	2,000	100.0	4.00E-05
F-0311	292536	811310	22	-28	-53	25	-18	10	1,000	40.0	4.00E-05
F-0312	292556	811315	18	-42	-52	10	-32	10	1,000	100.0	4.00E-05
F-0344	292538	811305	24	-26	-36	10	-16	10	1,000	100.0	4.00E-05
F-0345	292602	811415	26	-44	-64	20	-14	30	1,000	50.0	4.00E-05
F-0346	292621	811350	23	-37	-67	30	-37	0	2,000	66.7	4.00E-04
F-0347	292554	811316	25	-35	-65	30	-25	10	2,000	66.7	4.00E-04
F-0348	292622	811238	27	-33	-58	25	-23	10	2,000	80.0	4.00E-04
V-0443	292245	810748	26	-24	-36	10	-24	0	1,000	100.0	4.00E-04
W-194	292905	811115	22	-43	-63	20	-43	0	2,000	100.0	4.00E-04
W-195	292735	811545	18	-37	-57	20	-37	0	2,000	100.0	4.00E-04

Note: ft/day = feet per day
ft^2/day = square feet per day
ft msl = feet, mean sea level

*Approximation.
†Based on production zone interval; production zone taken from geological and geophysical logs.
‡Two wells were designated as LW-4; both are in the central zone. In this table, the first well drilled in 1972 has been re-named LW-4a.

APPENDIX B—ISATIS INPUT FILE FOR THE STUDY AREA

(Well locations are in UTM meters.)

```
ASCII FILE HEADER INTERPRETATION:

# structure = free
#           x_unit = m
#           y_unit = m
# field = 2 , type = alpha , name = Well Name
#       ffff = " " , unit =   , bitlength = -1
#       f_type = Free , f_length = 15 , f_digits = 0
# field = 3 , type = xg , name = East
#       ffff = " " , unit =   , bitlength = 32
#       f_type = Decimal , f_length = 10 , f_digits = 0
# field = 4 , type = yg , name = North
#       ffff = " " , unit =   , bitlength = 32
#       f_type = Decimal , f_length = 10 , f_digits = 0
# field = 5 , type = numeric , name = Elevation
#       ffff = "N/A" , unit = Ft , bitlength = 5
#       f_type = Integer , f_length = 5 , f_digits = 0
# field = 6 , type = numeric , name = IM Top
#       ffff = "N/A" , unit = Ft , bitlength = 5
#       f_type = Integer , f_length = 4 , f_digits = 0
# field = 7 , type = numeric , name = IM Bottom
#       ffff = "N/A" , unit = Ft ,* , bitlength = 5
#       f_type = Free , f_length = 15 , f_digits = 0
# field = 8 , type = numeric , name = Confine Top
#       ffff = "N/A" , unit = Ft , bitlength = 5
#       f_type = Integer , f_length = 4 , f_digits = 0
# field = 9 , type = numeric , name = IM Thickness
#       ffff = "N/A" , unit = Ft ,* , bitlength = 5
#       f_type = Free , f_length = 15 , f_digits = 0
# field = 10 , type = numeric , name = Confine Thickness
#       ffff = "N/A" , unit = Ft , bitlength = 5
#       f_type = Integer , f_length = 4 , f_digits = 0
# field = 11 , type = numeric , name = IM Trans.
#       ffff = "-9999" , unit =   , bitlength = 32
#       f_type = Integer , f_length = 8 , f_digits = 0
# field = 12 , type = numeric , name = Var Leakance
#       ffff = "-9999" , unit =   , bitlength = 32
#       f_type = Decimal , f_length = 10 , f_digits = 8
# field = 13 , type = numeric , name = Confine Leakance
#       ffff = "-9999" , unit =   , bitlength = 32
#       f_type = Decimal , f_length = 10 , f_digits = 6
# field = 14 , type = numeric , name = IM HC
#       ffff = "-" , unit =   , bitlength = 32
#       f_type = Decimal , f_length = 10 , f_digits = 2
#+++++------------+++++++++++++--------------++++-----------+++++++++---------+++++++++---------+++++++++++++++++--------------+++++++++

Number of Header Samples (*) = 0
Number of Samples = 143


PRINTOUT:

++++++++ Directory: data
+++++++++++++ File: wells
++++++++ Selection: None
++++ Distance Unit: m
+++++++++ Variable: East
+++++++++ Variable: North
```

```
+++++++++ Variable: Well Name
+++++++++ Variable: Elevation
+++++++++ Variable: IM Top
+++++++++ Variable: IM Bottom
+++++++++ Variable: Confine Top
+++++++++ Variable: IM Thickness
+++++++++ Variable: Confine Thickness
+++++++++ Variable: Confine Leakance
+++++++++ Variable: IM HC
+++++++++ Variable: IM Trans.

Total number of samples =     143
```

476266	3269755	SW-3	29	-32	-53	-22	21	10	4.000000	95.20	
475684	3269359	SW-4	29	-31	-55	-26	24	5	40.000000	81.50	1957
475666	3268645	SW-5	30	-30	-51	-18	21	12	40.000000	224.20	4709
475127	3269379	SW-6	33	-16	-36	-1	20	15	40.000000	66.50	1330
474500	3269285	SW-7	33	-22	-48	-12	26	10	40.000000	78.10	2030
475789	3268069	SW-8	33	-16	-31	-6	15	10	4.000000	66.70	
480801	3262538	SW-11	25	-37	-47	-28	10	9	20.000000	28.30	283
476505	3268412	SW-13	32	-10	-35	-10	25	0	4.000000	80.00	
476541	3267400	SW-14	33	-22	-37	-10	15	12	4.000000	66.70	
473998	3268640	SW-17	30	-10	-42	0	32	10	20.000000	41.90	1340
476195	3261808	SW-21	25	-35	-70	-35	35	0	19.000000	29.70	1040
476981	3263930	SW-24	25	5	-55	5	60	0	17.000000	133.30	8000
476847	3264546	SW-25	25	0	-55	0	55	0	17.000000	145.50	8000
476038	3266296	SW-27	30	-15	-55	-15	40	0	12.000000	69.30	2770
475871	3267435	SW-28	35	-25	-65	-15	40	10	12.000000	69.30	2770
475252	3267550	SW-29	30	-25	-50	-15	25	10	12.000000	110.80	2770
475162	3268240	SW-30	30	-30	-50	-25	20	5	33.000000	78.00	1560
475889	3266887	SW-31	30	-23	-44	-18	21.	5	28.000000	305.30	6411
474878	3268773	SW-32	30	-43	-53	-40	10	3	33.000000	156.00	1560
474157	3269892	SW-33	30	-10	-70	-10	60	0	4.300000	59.50	3570
473913	3270474	SW-34	30	-30	-80	-20	50	10	4.300000	71.40	3570
473696	3270982	SW-35	30	-30	-65	-20	35	10	4.300000	102.00	3570
473480	3271500	SW-36	35	-25	-55	-13	30	12	4.300000	119.00	3570
478947	3265853	SW-39	25	-5	-35	-2	30	3	20.000000	6.70	202
476284	3265470	SW-40	30	-25	-40	-25	15	0	28.000000	404.80	6072
472672	3274712	SW-43	35	5	-80	5	85	0	4.300000	42.00	3570
475232	3264303	SW-51	25	-32	-42	-20	10	12	19.000000	104.00	1040
478543	3264081	SW-52	25	-40	-65	-30	25	10	19.000000	107.10	2678
477114	3263477	SW-55	25	-25	-35	-18	10	7	20.000000	78.50	785
474165	3267842	SW-58	31	-19	-49	-9	30	10	30.000000	83.30	2500
473976	3268640	SW-59	31	-19	-49	-19	30	0	30.000000	83.30	2500
473091	3268663	SW-60	30	-38	-65	-18	27	20	30.000000	74.10	2000
472708	3269467	SW-61	31	-10	-44	0	34	10	30.000000	58.80	2000
472501	3270557	SW-62	31	-29	-49	-9	20	20	4.000000	110.00	2200
477731	3261990	SW-65	25	-43	-48	-36	5	7	20.000000	83.00	415
479282	3260752	SW-74	30	-20	-30	-20	10	0	16.000000	79.30	793
481478	3259711	SW-77	25	-23	-43	-17	20	6	16.000000	46.00	920
475217	3272272	SW-81	30	-25	-48	-16	23	9	36.000000	42.20	971
482358	3257155	SW-82	25	-25	-35	-5	10	20	30.000000	100.00	
476473	3265686	SW-83	30	-25	-45	-25	20	0	28.000000	351.00	7020
479135	3263987	SW-84	25	-48	-65	-38	17	10	19.000000	69.10	1175
472980	3273037	SW-85	35	-42	-62	-31	20	11	100.000000	187.60	3751
474744	3274892	SW-86	30	-35	-45	-15	10	20	36.000000	55.70	557
472917	3275820	SW-87	25	-38	-48	-18	10	20	100.000000	150.50	1505
472317	3278822	SW-89	20	-42	-52	-31	10	11	100.000000	104.60	1046
470738	3275456	SW-90	30	-43	-63	17	20	60	100.000000	139.50	2790
471374	3271007	SW-91	30	-32	-52	-32	20	0	10.000000	381.90	7638

470756	3275477	SW-92	30	-45	-60	10	15	55	100.000000	248.40	3726
478191	3258954	SW-93	20	-53	-63	-35	10	18	16.000000	22.90	229
479122	3256878	SW-94	25	-40	-48	-32	8	8	16.000000	127.00	1016
478209	3258849	SW-95	30	-23	-43	-6	20	17	16.000000	74.00	1480
475948	3272150	SW-96	30	-30	-50	-22	20	8	36.000000	40.70	813
473525	3268838	SW-105	30	-40	-60	-28	20	12	30.000000	100.00	2000
473306	3269577	SW-106	31	-44	-59	-39	15	5	30.000000	133.30	2000
473037	3270818	SW-107	33	-7	-51	3	44	10	4.000000	50.00	2200
471785	3270618	SW-114	30	-10	-50	0	40	10	10.000000	208.90	8356
471377	3271000	SW-115	30	-30	-60	-20	30	10	10.000000	278.50	8356
472565	3266257	LW-7 ✓	30	-30	-45	-10	15	20	30.000000	133.30	
468904	3269310	LW-8 ✓	25	-10	-60	-10	50	0	4.000000	80.00	
469016	3273786	LW-20 ✓	35	-25	-35	-15	10	10	4.000000	100.00	
474157	3277060	LW-53 ✓	25	-15	-35	-5	20	10	4.000000	100.00	
472114	3268718	LW-1 ✓	31	-29	-49	1	20	30	30.000000	100.00	
471928	3264348	LW-2 ✓	29	-31	-51	-11	20	20	30.000000	100.00	
469870	3272787	LW-3 ✓	35	-25	-45	-5	20	20	30.000000	100.00	
472028	3264348	LW-4 ✓	35	-25	-45	-25	20	0	20.000000	100.00	
472880	3262838	LW-6 ✓	25	-35		-25		10	36.000000	61.50	
472721	3262835	LW-6a ✓	25	-35		-25		10	36.000000	61.50	
471515	3262897	LW-5 ✓	30	-30		-20		10	36.000000	42.10	
479966	3269483	LW-10 ✓	25	10	0	10	10	0	4.000000	200.00	
478383	3269178	LW-11 ✓	20	-20	-50	-20	30	0	4.000000	100.00	
477497	3269140	LW-12 ✓	25	-5	-15	-5	10	0	4.000000	100.00	
479548	3269256	LW-13 ✓	20	-20	-40	-10	20	10	4.000000	100.00	
472867	3262887	LW-51 ✓	25	-35		-25		10	36.000000	61.50	
471619	3262564	LW-24 ✓	32	-18	-53	-18	35	0	4.000000	85.70	
472836	3264715	LW-25 ✓	30	-40	-70	-15	30	25	4.000000	100.00	
473131	3264068	LW-26 ✓	30	-30	-40	-20	10	10	4.000000	100.00	
473805	3264313	LW-27 ✓	30	-30		-10		20	36.000000	42.10	
475189	3264599	LW-38 ✓	30	-30	-50	-10	20	20	4.000000	100.00	
472119	3264354	LW-4a ✓	29	-31	-36	-11	5	20	30.000000	200.00	
478528	3256363	LW-14 ✓	25	-50	-85	-40	35	10	20.000000	57.10	2000
480026	3253710	LW-15 ✓	25	-35	-55	-30	20	5	30.000000	100.00	2000
480013	3253725	LW-15a ✓	25	-35	-55	-30	20	5	30.000000	100.00	2000
482530	3253774	LW-16 ✓	25	-20	-40	-10	20	10	30.000000	100.00	2000
482134	3253987	LW-17 ✓	25	-10	-60	-10	50	0	4.000000	80.00	4000
478782	3255171	LW-21 ✓	25	-35	-55	-15	20	20	30.000000	100.00	2000
477865	3256459	LW-30 ✓	25	-35	-55	-15	20	20	30.000000	100.00	2000
478677	3255614	LW-31 ✓	25	-35	-55	-15	20	20	30.000000	100.00	2000
479522	3256469	LW-32 ✓	25	-35	-55	-15	20	20	30.000000	100.00	2000
476922	3257498	LW-42 ✓	15	-35	-45	-25	10	10	4.000000	100.00	1000
477243	3287235	SJ0039	6	-44	-69	-34	25	10	4.000000	80.00	2000
475082	3281699	SJ0128	6	-19	-64	-19	45	0	4.000000	66.70	3000
476975	3287235	SJ0151	6	-44	-64	-39	20	5	30.000000	100.00	2000
468185	3285810	SJ0602	35	-5	-50	-5	45	0	4.000000	66.70	3000
466140	3249284	F-0005	11	-24	-44	-24	20	0	4.000000	150.00	3000
463241	3253140	F-0006	16	-54	-74	-44	20	10	4.000000	100.00	2000
462734	3254403	F-0007	18	-77	-87	-52	10	25	4.000000	100.00	1000
480442	3257313	F-0008	27	-48	-58	-28	10	20	4.000000	100.00	1000
464723	3261660	F-0010	24	-71	-86	-46	15	25	4.000000	66.70	1000
464616	3261660	F-0011	22	-63	-78	-38	15	25	4.000000	133.30	2000
462112	3262038	F-0012	20	-70	-100	-50	30	20	4.000000	100.00	3000
474150	3250340	F-0013	16	-39	-54	-29	15	10	4.000000	66.70	1000
477476	3269168	F-0014	26	-44	-74	-44	30	0	4.000000	100.00	3000
478364	3269197	F-0015	25	-35	-85	-35	50	0	4.000000	60.00	3000
481864	3270114	F-0016	9	-41	-91	-26	50	15	4.000000	80.00	4000
481972	3270668	F-0017	6	-29	-39	-14	10	15	4.000000	100.00	1000
479592	3278428	F-0019	7	-43	-53	-33	10	10	4.000000	100.00	1000
479619	3278551	F-0020	7	-8	-23	-8	15	0	4.000000	66.70	1000

479248	3281752	F-0021	6	-44	-54	-29	10	15	4.000000	100.00	1000
479672	3278335	F-0022	9	-36	-46	-21	10	15	4.000000	100.00	1000
481303	3272485	F-0023	4	-41	-61	-31	20	10	4.000000	100.00	2000
464150	3259261	F-0044	24	-46	-66	-21	20	25	4.000000	50.00	1000
461549	3254746	F-0066	20	-30	-40	-5	10	25	4.000000	100.00	1000
475220	3259232	F-0087	21	-44	-59	-19	15	25	4.000000	66.70	1000
464380	3255198	F-0101	14	-31	-46	-21	15	10	4.000000	133.30	2000
478552	3269197	F-0105	4	-51	-61	-26	10	25	4.000000	100.00	1000
480742	3274825	F-0106	10	-40	-55	-25	15	15	4.000000	66.70	1000
470367	3257304	F-0126	12	-73	-83	-48	10	25	4.000000	100.00	1000
469950	3272602	F-0160	35	-40	-50	-15	10	25	4.000000	100.00	1000
472012	3268657	F-0161	31	-49	-64	-24	15	25	4.000000	133.30	2000
479952	3269379	F-0162A	13	-57	-77	-57	20	0	4.000000	100.00	2000
477610	3269168	F-0164	27	-28	-38	-18	10	10	4.000000	100.00	1000
468876	3273374	F-0165	33	-72	-82	-57	10	15	4.000000	100.00	1000
480128	3277811	F-0200	7	-43	-58	-28	15	15	4.000000	66.70	1000
462785	3269945	F-0204	26	-34	-44	-9	10	25	4.000000	100.00	1000
463106	3261111	F-0206	25	-55	-65	-45	10	10	4.000000	100.00	1000
474150	3250370	F-0240	18	-37	-52	-27	15	10	4.000000	66.70	1000
480554	3275164	F-0242	13	-37	-52	-22	15	15	4.000000	66.70	1000
462221	3270163	F-0294	25	-55	-65	-45	10	10	4.000000	100.00	1000
479818	3254791	F-0308	25	-35	-40	-20	5	15	3.000000	160.00	800
477477	3256088	F-0309	22	-38	-58	-38	20	0	40.000000	100.00	2000
477422	3255718	F-0310	22	-43	-63	-8	20	35	4.000000	100.00	2000
478714	3255100	F-0311	22	-28	-53	-18	25	10	4.000000	40.00	1000
478580	3255716	F-0312	18	-42	-52	-32	10	10	4.000000	100.00	1000
478849	3255162	F-0344	24	-26	-36	-16	10	10	4.000000	100.00	1000
476964	3255904	F-0345	26	-44	-64	-14	20	30	4.000000	50.00	1000
477639	3256487	F-0346	23	-37	-67	-37	30	0	40.000000	66.70	2000
478553	3255655	F-0347	25	-35	-65	-25	30	10	40.000000	66.70	2000
479579	3256515	F-0348	27	-33	-58	-23	25	10	40.000000	80.00	2000
487384	3249825	V-0443	26	-24	-36	-24	10	0	40.000000	100.00	1000
481823	3261527	W-194	22	-43	-63	-43	20	0	40.000000	100.00	2000
474546	3258771	W-195	18	-37	-57	-37	20	0	40.000000	100.00	2000
480688	3275163	F-0107	12	-38	-53	-23	15	15	4.000000	66.70	1000
464391	3258860	F-0182	26	-29	-49	-14	20	15	4.000000	50.00	1000

+++++++++ END OF PRINTOUT: 143 samples